

QUANTIFICATION OF TRACE LEVELS OF ACTIVE OXYGEN IN PHARMACEUTICAL  
EXCIPIENTS

BY

Stephanie Staub

Submitted to the graduate degree program in Pharmaceutical Chemistry and the Graduate  
Faculty of the University of Kansas in partial fulfillment of the requirements for the degree of  
Master of Science.

---

Chair: Christian Schoneich

---

Co-Chair: Diane Gingrich

---

John Stobaugh

Date Defended: 30 November 2017

The thesis committee for Stephanie Staub  
certifies that this is the approved version of the following thesis:

QUANTIFICATION OF TRACE LEVELS OF ACTIVE OXYGEN IN PHARMACEUTICAL  
EXCIPIENTS

---

Chair: Christian Schoneich

---

Co-Chair: Diane Gingrich

---

John Stobaugh

Date Approved: 30 November 2017

## Abstract

Pharmaceutical drug products contain various excipients in combination with the active pharmaceutical ingredient (API), and those excipients have the potential to have as impurities reactive oxygen species that can react directly with the API and lead to oxidative degradation. Such degradation can impact long-term stability of the drug product, reduce drug product purity, limit shelf life, and increase time to market. Peroxy compounds are a common class of such reactive impurities, but there is an absence in the literature of a method for detection of total peroxide level in pharmaceutical excipients when the identity of the peroxy contaminant is not known. In this thesis, novel modifications were made to the 1966 ASTM E 299-08 method for enhanced and robust detection of active oxygen in pharmaceutical excipients. The modified ASTM E 299-08 method was evaluated using spiked solutions of hydrogen peroxide, a hydroperoxide compound, and a peroxide compound. Liquid and solid excipients were then evaluated for active oxygen levels to demonstrate the utility and breadth of the modified method to cover a wide range of excipients. The polyethylene glycol (PEG) class of compounds was chosen for more in-depth evaluation due to their susceptibility to autoxidation and the existence of various molecular weight grades of PEG compounds. PEG 1000 was chosen along with lestaurtinib (CEP-701) to prepare a novel drug product, which was evaluated on stability for active oxygen and assay impurity levels. The results showed that the modified ASTM E 299-08 method successfully quantified both the total active oxygen levels and the CEP-701 peroxy impurity levels, which agreed with those obtained by an HPLC assay method. The modified ASTM E 299-08 method has important applicability in the pharmaceutical industry as a method that can be used for preliminary screening of excipients and new formulations to predict potential oxidative degradation reactions.

## **Acknowledgements**

I would like to thank my on-site research advisor, Diane Gingrich, for her guidance and support throughout this research project. I am appreciative for the flexibility given to me from Teva Pharmaceuticals to pursue this master's program as well as the encouragement from my director Mehran Yazdanian and vice president Robert McKean. I am grateful for the University of Kansas Pharmaceutical Chemistry Department for offering this distance master's program and am especially thankful for my University of Kansas advisor, Christian Schoneich, for his guidance. I am extremely grateful for the help of several of my colleagues including Brad McIntyre for his help with formulation development, Greg Gilmartin for his help with mass spectra analysis techniques, and Anthony Drager, John Kontir, and Chris Neville for their scientific discussions about the lestaurtinib drug product. I would also like to thank my boyfriend and family for their support and patience while I pursued this degree.

## Table of Contents

<b>Chapter 1. Introduction</b>	
1.1. Pharmaceutical Importance of Excipient Impurities	1
1.2. Comparison of ASTM E 299-08 Method to Competing Methods	2
1.3. The Modified ASTM E 299-08 Method	3
1.4. Pharmaceutical Application of the Modified ASTM E 299-08 Method	4
1.5. References	5
<b>Chapter 2. Modifications to the ASTM E 299-08 Method</b>	
2.1. Introduction	6
2.2. Experimental	8
2.3. Results and Discussion	11
2.4. Conclusions	18
2.5. References	19
<b>Chapter 3. Evaluation of Known Organic Peroxides</b>	
3.1. Introduction	20
3.2. Experimental	22
3.3. Results and Discussion	26
3.4. Conclusions	31
3.5. References	31
<b>Chapter 4. Active Oxygen Detection in Liquid Excipients</b>	
4.1. Introduction	32
4.2. Experimental	33
4.3. Results and Discussion	34
4.4. Conclusions	36
4.5. References	37
<b>Chapter 5. Active Oxygen Detection in Solid Excipients</b>	
5.1. Introduction	38
5.2. Experimental	39
5.3. Results and Discussion	40
5.4. Conclusions	43
5.5. References	43
<b>Chapter 6. Active Oxygen Formation in PEG Excipients</b>	
6.1. Introduction	44
6.2. Experimental	48
6.3. Results and Discussion	49
6.4. Conclusions	54
6.5. References	55

<b>Chapter 7. Evaluation of CEP-701 Drug Product Stability by the Modified ASTM E 299-08 Method</b>	
7.1. Introduction	56
7.2. Experimental	61
7.3. Results and Discussion	66
7.4. Conclusions	84
7.5. References	84
<b>Chapter 8. Final Conclusions and Future Considerations</b>	<b>85</b>
<b>Appendix A.</b>	<b>88</b>
<b>Appendix B.</b>	<b>91</b>
<b>Appendix C.</b>	<b>95</b>
<b>Appendix D.</b>	<b>96</b>

## **CHAPTER 1. Introduction**

### **Purpose of the Research Performed**

The purpose of the research described in this thesis was to develop a sensitive, versatile, reliable, and reproducible method for rapid quantification of trace levels of active oxygen species in pharmaceutical excipients and a model drug product when the identity of the peroxy moiety was either known or unknown.

### **1.1. Pharmaceutical Importance of Excipient Impurities**

Pharmaceutical drug products contain various excipients in combination with the active pharmaceutical ingredient (API), and those excipients have the potential to have as impurities reactive oxygen species that can react with the API and lead to oxidative degradation.<sup>1</sup> Excipients have been found to contain trace amounts of reactive impurities including metal ions, peroxides, low-molecular weight aldehydes, and organic acids.<sup>2</sup> Understanding the impurity profiles of excipients has increased in importance because excipient impurities such as peroxides, even in trace levels, not only have the ability to catalyze API-excipient reactions, but can also catalyze excipient-excipient or impurity-impurity reactions, which can further contribute to the instability of a drug product.<sup>3,4,5</sup> Oxidative degradation of the API can significantly impact the long-term stability of the drug product, which can reduce drug product purity, prolong formulation development, limit shelf life, and increase time to market.<sup>5</sup>

Quantifying the level of peroxides in an excipient before selection for formulation development is especially important when the API is known to be susceptible to oxidative degradation. Screening excipients for peroxide levels prior to use in a formulation is imperative to ensure stability, quality control, and even safety of both the excipient and drug product.<sup>4,6</sup>

Being proactive in characterizing reactive oxygen impurities during excipient selection can enhance the probability of API-excipient compatibility, including evaluation upfront whether the inclusion of an antioxidant will be required, saving valuable development time.<sup>1</sup> However, the identity of the reactive oxygen species in the pharmaceutical excipient may not be known, which makes quantification of the levels in an excipient very difficult, but nonetheless important to predicting the possible reactions that can occur between the excipient impurities and the API.<sup>3</sup> There is limited literature addressing this point and a need exists for a method that can detect the total active oxygen level in a pharmaceutical excipient when the identity and structure of such species are not known.

## **1.2. Comparison of the ASTM E 299-08 Method to Competing Methods**

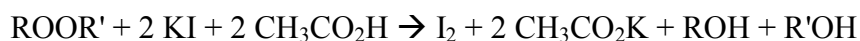
Previously published techniques in the literature evaluated hydrogen peroxide (H<sub>2</sub>O<sub>2</sub>) levels in excipients using a liquid chromatographic method combined with coulometric electrochemical detection (LC-CECD), a liquid chromatographic system with a dual channel amperometric-electrochemical detector (LCEC), and a flow injection (FI) method.<sup>4,6,7</sup> Other techniques evaluated total hydroperoxide content in excipients using version two of the ferrous oxidation-xylenol orange assay method (FOX2) with ultraviolet (UV) detection.<sup>5,8,9,10,11</sup> Ferrous ion methods have been employed to measure peroxide levels, but reviews of the methods in literature have summarized them as less accurate than iodometric methods because they produced 2 to 5 times higher peroxide levels when compared to the same sample measured iodometrically, a well-defined system matrix is needed, and exposure to air must be avoided.<sup>8,12,13</sup> Colorimetric procedures for detection of organic peroxides are also described in the literature, but there are disadvantages within the methods.<sup>14,15</sup> Colorimetric methods have



limited applicability and the utilization of a volumetric procedure does not allow for detection of low peroxide levels, due to high blank values.<sup>14,15,16</sup> In addition, the previous techniques are specific to a known peroxide, measure peroxide levels indirectly, sacrifice sensitivity, include many procedural steps, and are time-consuming.<sup>4,5,6</sup> The American Society for Testing and Materials (ASTM) E 299-08 standard test method was chosen as the basis for the method in this thesis.<sup>17</sup> The ASTM E 299-08 method is an iodometric method that utilizes spectrophotometric analysis, which enhances sensitivity.<sup>16</sup>

### **1.3. The Modified ASTM E 299-08 Method**

A spectrophotometric test method for peroxide quantification, in terms of active oxygen, was developed that utilizes and expands upon the knowledge gained from the ASTM E 299-08 method and iodine redox chemistry.<sup>17,7</sup> Iodometric methods in the literature used acetic acid in the acid solution in order to serve as a medium for the reduction of peroxides by iodide ions.<sup>13,18</sup> The reaction taking place was the reduction of an active oxygen species by the iodide ion, which causes the release of iodine, which can be measured by a spectrophotometer.<sup>18,19</sup> The overall reaction utilized in this method is described below:



where ROOR' is representative of an arbitrary active oxygen compound.<sup>14,20</sup>

The modified method for active oxygen analysis was developed and included procedural improvements to the ASTM E 299-08 method, which was originally approved in 1966, required multiple procedural steps, utilized a custom glass reaction absorption cell for detection of trace active oxygen levels, and specifically focused on active oxygen in organic solvents.<sup>17</sup> The improvements to the ASTM E 299-08 method were developed in order to allow the method to be

more robust, convenient, and flexible. The modified ASTM E 299-08 method reduced the number of steps in the ASTM E 299-08 method and eliminated the need for the special absorption cell without sacrificing the sensitivity and reproducibility of the method. It utilizes iodine standard calibration curves that cover a more specific and lower magnitude range of active oxygen levels, and quantifies the amount of active oxygen (ppm) present in H<sub>2</sub>O<sub>2</sub>-spiked samples accurately.<sup>6,4,7,8,17</sup> The expanded method focuses on rapidly quantifying trace levels of active oxygen in both liquid and solid pharmaceutical excipient lots from different vendors and relates the findings to various classes of excipients.<sup>21,6</sup>

#### **1.4. Pharmaceutical Application of the Modified ASTM E 299-08 Method**

Hydroperoxide compounds are common intermediates in the degradation of fats, oils, and polymers, which are frequently used excipients in pharmaceutical formulations.<sup>22,23</sup> Hydroperoxides are the primary products of autoxidation and thermal oxidation in formulations, which decompose to secondary oxidation products consisting of aldehydes, ketones, alcohols, hydrocarbons, volatile organic acids, and epoxy compounds.<sup>24</sup> Analytical methods in the literature can either determine the total amount of hydroperoxides through primary oxidation products or can determine the amount of hydroperoxide by quantifying the formation of the decomposition products.<sup>22</sup> The negative commonalities between the existing methods are that the peroxide produced must be known, derivatization is used, and chromatographically only the secondary products are quantified.<sup>22,23,24</sup> The modified ASTM E 299-08 method was employed to show its utility to detect both total active oxygen and specific hydroperoxide levels concurrently in a formulation without the downfalls of the existing methods. Different molecular weight grades of polyethylene glycol (PEG) excipients were evaluated and PEG 1000 was

further incorporated into a formulation. The formulation was tracked on stability to show the benefits of the modified ASTM E 299-08 method in a real-life scenario. The ability for the modified ASTM E 299-08 method to detect total peroxide levels, in terms of active oxygen, and the ability to calculate the specific peroxide levels enables quick screening by one sole method.

## 1.5. References

1. Wu, Y.; Levons, J.; Narang, A.; Raghavan, K.; Rao, V. M. *AAPS Pharm. Sci. Tech.* **2011**, *12*, 1248-1263.
2. Hemenway, J. C.; Carvalho, T. C.; Rao, V. M.; Wu, Y.; Levons, J. K.; Narang, A. S.; Paruchuri, S. R.; Stamato, H. J.; Varia, S. A. *J. Pharm. Sci.* **2012**, *101*, 3305-3318.
3. Hovorka, S.; Schoneich, C. *J. Pharma. Sci.* **2001**, *90*, 253-269.
4. Yue, H.; Bu X.; Huang, M.; Young, J.; Raglione, T. *Int. J. Pharm.* **2009**, *375*, 33-40.
5. Wasylaschuk, W. R.; Harmon P. A.; Wagner G.; Harman A. B.; Templeton A.; Xu H.; Reed R. *J. Pharm. Sci.* **2007**, *96*, 106-116.
6. Huang, T.; Garceau, M. E.; Gao, P. *J. Pharm. Biomed. Anal.* **2003**, *31*, 1203-1210.
7. Bloomfield, M.S. *Talanta.* **2004**, *64*, 1175-1182.
8. Gay, C.; Collins, J.; Gebicki, J. M. *Anal. Biochem.* **1999**, *273*, 149-155.
9. Meisner, P.; Gebicki, J. *Acta. Biochim. Pol.* **2009**, *56*, 523-527.
10. Nourooz-Zadeh, J.; Tajaddini-Sarmadi, J.; Wolff, S. *Anal. Biochem.* **1994**, *220*, 403-409.
11. Tarvin, M.; McCord, B.; Mount, K.; Sherlach, K.; Miller, M. *J. Chromatogr., A.* **2010**, *1217*, 7564-7572.
12. Kolthoff, I. M.; Medalia, A. I. *Anal. Chem.* **1951**, *23*, 595-603.
13. Kokatnur, V. R.; Jelling, M. *J. Am. Chem. Soc.* **1941**, *63*, 1432.
14. Banerjee, D. K.; Budke, C. C. *Anal. Chem.* **1964**, *36*, 792-796.
15. Martin, A. J. *Organic Analysis, vol. 4*; Interscience: New York, **1960**.
16. Pobiner, H. *Anal. Chem.* **1961**, *33*, 1423-1426.
17. ASTM E299-08, "Standard Test Method for Trace Amounts of Peroxides in Organic Solvents," ASTM International, West Conshohocken, PA, **2008**, [www.astm.org](http://www.astm.org).
18. Wagner, C. D.; Smith, R. H.; Peters, E. D. *Ibid.* **1947**, *19*, 976-979.
19. Cadle, R. D.; Huff, H. J. *Phys. Colloid Chem.* **1949**, 1191-1195.
20. Wilson, J. N.; Dickinson, R. G. *J. Am. Chem. Soc.* **1937**, *59*, 1358-1361.
21. Rowe, R. C.; Sheskey, P. J.; Cook, W. G.; Quinn, M. E. *Handbook of Pharmaceutical Excipients, 7<sup>th</sup> ed.*; Pharmaceutical Press: London, **2012**.
22. Dobarganes, C.; Velasco, J. *Eur. J. Lipid Sci. Technol.* **2002**, *104*, 420-428.
23. Scheirs, J.; Carlsson, D.J.; Bigger, S. *Polym.-Plast. Technol. Eng.* **1995**, *34*, 97-116.
24. Shahidi, F.; Zhong, Y. Lipid Oxidation: Measurement Methods. In *Bailey's Industrial Oil and Fat Products*, 6<sup>th</sup> ed.; Shahidi, F., Ed. John Wiley & Sons: Hoboken, NJ, **2005**; pp 357-385.

## **CHAPTER 2. Modifications to the ASTM E 299-08 Method**

### **Purpose of the Research Performed**

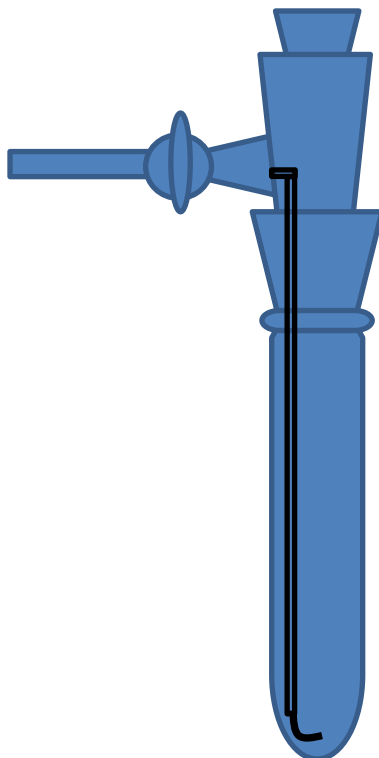
The purpose of the research described in this chapter was to make procedural improvements to the ASTM E 299-08 method and then evaluate the effectiveness of the changes by quantifying the active oxygen levels in solutions spiked with hydrogen peroxide.

### **2.1. Introduction**

The ASTM E 299-08 method, titled Standard Test Method for Trace Amounts of Peroxides in Organic Solvents, was originally approved in 1966 with updated editions in 2002 and 2008. The intended significance for use of the method was defined as a procedure for determining the peroxide or active oxygen level in organic solvents. The need for the general standard was justified by the explanation that dilute solutions of peroxides in organic solvents are used as catalysts and reaction initiators, and can be formed through autoxidation. The formation of peroxides through autoxidation can lead to safety hazards; so quantification of the peroxide levels is important.<sup>1</sup>

The ASTM E 299-08 method claimed that the method can quantify active oxygen in the range from 5 to 80  $\mu\text{g/g}$  (ppm) or higher and is specific to saturated and aromatic hydrocarbons, alcohols, ethers, ketones, esters, olefinic solvents, and some compounds that contain  $\alpha$ ,  $\beta$ , and conjugated unsaturation.<sup>1</sup> The procedural components were modified in order to broaden the scope of the method for incorporation of excipients and to improve efficiency. Dichloromethane replaced chloroform in the 2:1 acid solution mixture of acetic acid: chloroform used for diluting the samples.<sup>1</sup> Dichloromethane has similar functionality to chloroform, but is less toxic and is more commonly used as a solvent. Another modification was the elimination of the special

absorption cell, adapted from ref 1. and represented in **Figure 2.1**, for measurement of low active oxygen levels.<sup>1,2</sup> The cell is a custom piece of glassware that is not commercially available, which decreased the ease of access to the method. To replace the cell, a 20 mL glass GC headspace vial with screw cap septum and a 5.75 inch glass pipette technique was used in order to protect the sample from air during the entire analysis.



**Figure 2.1:** Special Custom Glass Absorption Cell for Low-Active Oxygen Levels Used in ASTM E 299-08 Method<sup>1</sup>

Contrary to the ASTM E 299-08 method, which analyzed peroxides in organic solvents and unsaturates, the objective of this thesis is to measure active oxygen in pharmaceutical excipients.<sup>2,3,4</sup> Pharmaceutical excipients have a wide range of physicochemical properties, which makes the use of a standardization blank important.<sup>6</sup> Methanol was used as the blank solvent because it remains colorless during analysis and is inert in the reaction.<sup>3,4</sup> To show the

accuracy of the modified ASTM E 299-08 method, varying levels of hydrogen peroxide (H<sub>2</sub>O<sub>2</sub>) spikes were evaluated.

## **2.2. Experimental**

An acid solution was prepared by combining 500 mL of glacial acetic acid, 350 mL of dichloromethane, and 30 mL of deionized water and mixing well. A fresh aqueous potassium iodide solution (1 g/mL) was prepared immediately before sample preparation in order to minimize introduction of oxygen from the air. The potassium iodide solution was prepared by accurately weighing and transferring 15 g of potassium iodide (1 g for each sample) to a 50 mL plastic centrifuge tube with printed graduations. The solid was dissolved and diluted to 15 mL (1 mL for each sample) with deionized water, mixed well, and covered with aluminum foil. A gas regulator with a pressure gauge attached to a nitrogen inlet and connected to a small diameter tubing was used to keep a consistent and precise flow of nitrogen through the samples during purging. The potassium iodide solution was purged with nitrogen for about 20 minutes and then capped. Blank sample solutions were prepared by accurately transferring 5 mL of methanol using glass pipettes to 15 mL plastic centrifuge tubes with printed graduations. The methanol blank solutions were diluted to volume with the acid solution and directly transferred to glass 20 mL gas chromatography (GC) headspace vials that had screw cap septa.

A timer was set to 3 minutes and the nitrogen filled tubing was placed directly in to the glass GC headspace vials containing the methanol blank solutions in order to purge the sample. After 2 minutes of purging, 1 mL of aqueous potassium iodide solution was added via a positive displacement pipette and the solutions continued to be purged for an additional 1 minute. After a total of 3 minutes of purging, the solutions were immediately capped as the tubing was removed,

covered with aluminum foil, and kept out of light for 1 hour. It was critical to cap the GC headspace vials immediately to eliminate the possibility of air entering the vials and contributing to the active oxygen levels. After 1 hour protected from light, the samples were removed. Using 5.75 inch glass pipettes, 1 mL aliquots were removed from the samples and transferred to a 1 cm quartz cuvette and analyzed at two different wavelengths. A Beckman Coulter DU 800 spectrophotometer was used to obtain absorbance values at 410 nm and 470 nm using the instrument method in **Table 2.1**.

**Table 2.1:** Instrument Method for Beckman Coulter DU 800 Spectrophotometer

<b>Instrument</b>	Beckman Coulter DU 800 Spectrophotometer
<b>Detection Wavelength</b>	410 nm and 470 nm
<b>Read Mode</b>	Absorbance
<b>Read Average Time</b>	5 seconds

The absorbance units for the methanol blank solutions were low in magnitude:  $\leq 0.0500$  AU at 410 nm and  $\leq 0.0100$  AU at 470 nm. The blank absorbance units were subtracted from the absorbance measurements of the samples to ensure that the calculated active oxygen levels were solely from the samples.

In order to cover a wide range of 0-600  $\mu\text{g}$  of active oxygen, two calibration curves were prepared. The high range active oxygen curve was prepared to cover high magnitude levels from 0 to 600  $\mu\text{g}$  of active oxygen. To produce the high range curve, iodine (0.064 g) was transferred into a 100 mL volumetric flask and diluted to volume with the acid solution to obtain a 0.64 mg iodine/mL stock solution. The stock solution contained 0.64 mg iodine/mL, which was equivalent to 40.0  $\mu\text{g}$  active oxygen/mL.<sup>1</sup> The 40.0  $\mu\text{g}$  active oxygen/mL stock solution was used to spike samples to produce a six point calibration curve. Aliquots of 0, 1.5, 5, 8, 13, and 15 mL of the stock solution were transferred to 15 mL centrifuge tubes and filled to volume with the acid solution. The calibration standards were representative of 0.0, 60.2, 200.6, 321.0, 521.6,

and 601.9  $\mu\text{g}$  of active oxygen. The active oxygen levels of the standards were measured by the modified ASTM E 299-08 method and the absorbance values of each standard were measured at 410 nm and 470 nm.

The low range active oxygen curve was prepared to cover low magnitude levels from 0 to 40  $\mu\text{g}$  of active oxygen, which is the region where the high range calibration curve lacked specificity.<sup>1</sup> To produce the low range curve, iodine (0.064 g) was transferred into a 100 mL volumetric flask and diluted to volume with the acid solution to obtain a 0.64 mg iodine/mL stock solution. The stock solution was further diluted by transferring 10 mL of the 0.64 mg iodine/mL solution into a 100 mL volumetric flask and diluting to volume with the acid solution. The new stock solution contained 0.064 mg iodine/mL, which was equivalent to 4.0  $\mu\text{g}$  of active oxygen/mL.<sup>1</sup> The 4.0  $\mu\text{g}$  of active oxygen/mL stock solution was used to spike samples to produce a six point calibration curve. Aliquots of 0, 1, 3, 5, 8, and 10 mL of the stock solution were transferred to 15 mL centrifuge tubes and filled to volume with the acid solution. The calibration standards were representative of 0.0, 4.1, 12.2, 20.4, 32.6, and 40.7  $\mu\text{g}$  of active oxygen. The active oxygen levels of the standards were measured by the modified ASTM E 299-08 method and the absorbance values of each standard were measured at the 410 nm wavelength.

To show the accuracy of the modified ASTM E 299-08 method, varying levels of hydrogen peroxide ( $\text{H}_2\text{O}_2$ ) spikes were evaluated. A 30% w/w hydrogen peroxide solution was obtained from EMD and diluted with water to obtain a 7.5% hydrogen peroxide solution. Spiked volumes of 1  $\mu\text{L}$ , 3  $\mu\text{L}$ , 5  $\mu\text{L}$ , 8  $\mu\text{L}$ , and 10  $\mu\text{L}$  of the  $\text{H}_2\text{O}_2$  stock solution were added to 15 mL centrifuge tubes. The  $\text{H}_2\text{O}_2$  spikes were then diluted to volume with the acid solution to produce 83.25  $\mu\text{g}$ , 249.75  $\mu\text{g}$ , 416.25  $\mu\text{g}$ , 666.00  $\mu\text{g}$ , and 832.50  $\mu\text{g}$   $\text{H}_2\text{O}_2$  samples. To convert  $\mu\text{g}$  of peroxide to  $\mu\text{g}$  of active oxygen, the following formula was used:



$$\text{Peroxide X } (\mu\text{g}) = \text{active oxygen in sample } (\mu\text{g}) \times F$$

where F is the conversion factor for peroxide X.<sup>5</sup> Conversion factors for peroxides are calculated by dividing the molecular weight of the peroxide by the molecular weight of oxygen (16 g/mol).<sup>5</sup> H<sub>2</sub>O<sub>2</sub> has a molecular weight of 34 g/mol and therefore a conversion factor, F, of 2.125. The calculated theoretical amounts of active oxygen in the H<sub>2</sub>O<sub>2</sub>-spiked samples were 39.16 μg, 117.53 μg, 195.88 μg, 313.41 μg, and 391.76 μg of active oxygen respectively. A summary of the calculated theoretical amounts of H<sub>2</sub>O<sub>2</sub> (μg) and corresponding active oxygen (μg) in the H<sub>2</sub>O<sub>2</sub>-spiked samples is presented in **Table 2.2**. The H<sub>2</sub>O<sub>2</sub>-spiked samples were transferred to 20 mL GC headspace vials and the active oxygen levels were measured by the modified ASTM E 299-08 method.

**Table 2.2:** Calculated Theoretical Amount of Active Oxygen and Corresponding Amount of H<sub>2</sub>O<sub>2</sub> in the H<sub>2</sub>O<sub>2</sub>-Spiked Samples

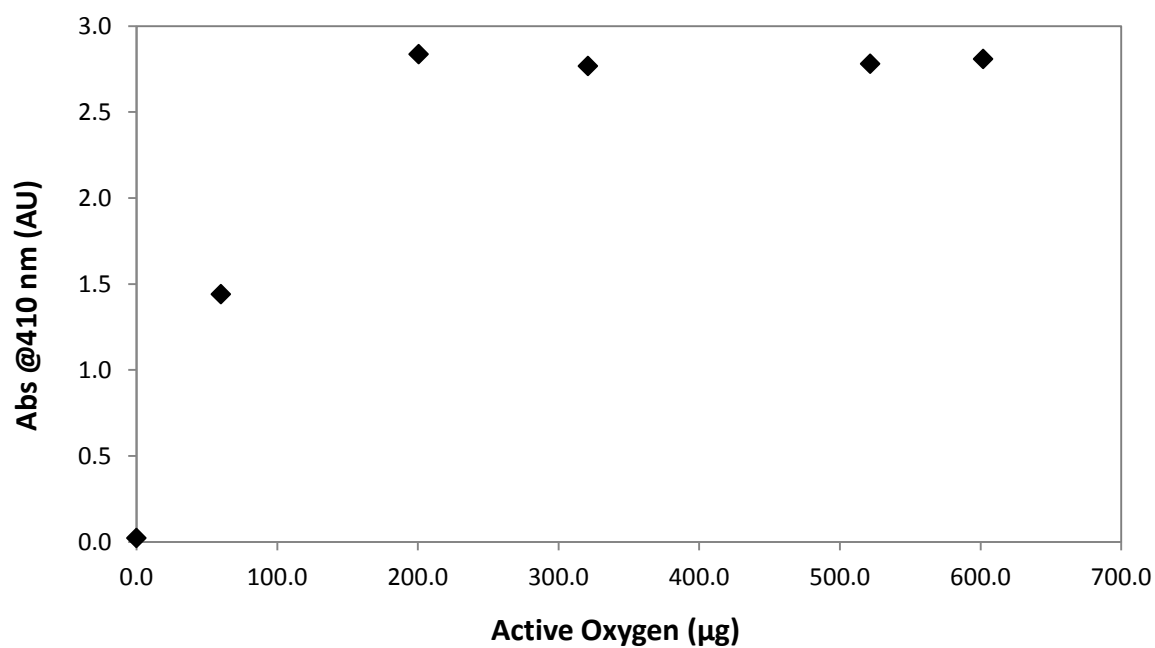
Spiked H <sub>2</sub> O <sub>2</sub> Vol. (μL)	Theoretical Amount of Active Oxygen (μg)	Theoretical Amount of H <sub>2</sub> O <sub>2</sub> (μg)
1	39.16	83.25
3	117.53	249.75
5	195.88	416.25
8	313.41	666.00
10	391.76	832.50

### 2.3. Results and Discussion

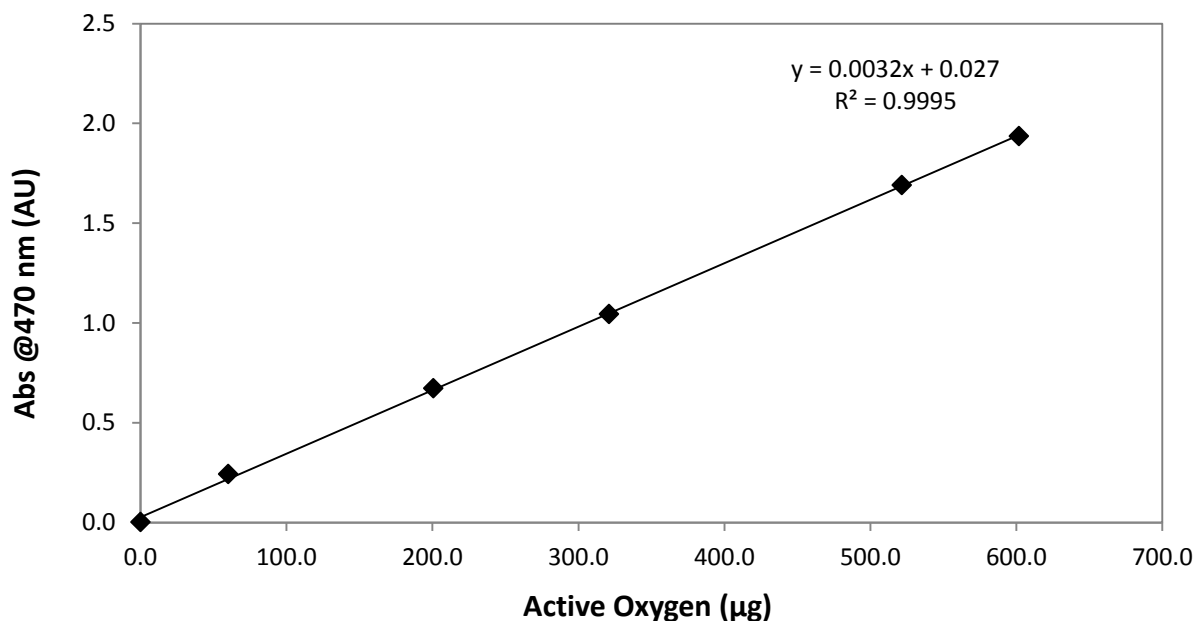
The absorbance values, after methanol blank subtraction, for the high range iodine standards are presented in **Table 2.3** and the calibration curves at the 410 nm and 470 nm wavelengths are presented in **Figure 2.2** and **Figure 2.3**.

**Table 2.3:** Summary Table of Iodine Absorbance Results for the High Range Active Oxygen Calibration Curves

Std.	Vol. Transfer from Stock (mL)	$\mu\text{g}$ iodine/mL	Active Oxygen ( $\mu\text{g}$ )	Abs @ 410 nm (AU)	Abs @ 470 nm (AU)
1	0	0.0	0.0	0.0235	0.0017
2	1.5	63.6	60.2	1.4407	0.2428
3	5	212.0	200.6	2.8369	0.6726
4	8	339.2	321.0	2.7678	1.0437
5	13	551.2	521.6	2.7808	1.6912
6	15	636.0	601.9	2.8079	1.9352



**Figure 2.2:** High Range Active Oxygen Calibration Curve for Iodine Absorbance at the 410 nm Wavelength



**Figure 2.3:** High Range Active Oxygen Calibration Curve for Iodine Absorbance at the 470 nm Wavelength

The calibration curve presented in **Figure 2.2** showed that the absorbance readings at 410 nm reached a maximum at 2.8 AU; hence that wavelength was not suitable for measurement of high active oxygen levels. In contrast, the absorbance readings at 470 nm, presented in **Figure 2.3**, produced a linear curve corresponding to the following equation:

$$y = 0.0032x + 0.027$$

where x is the amount of active oxygen and y is the absorbance measurement at 470 nm. As a quick estimation technique to evaluate the active oxygen levels in the standards, the appearance of the samples after analysis can be utilized. The colorimetric trend observed in the calibration standards that represent the high magnitude active oxygen levels is presented in **Figure 2.4**.



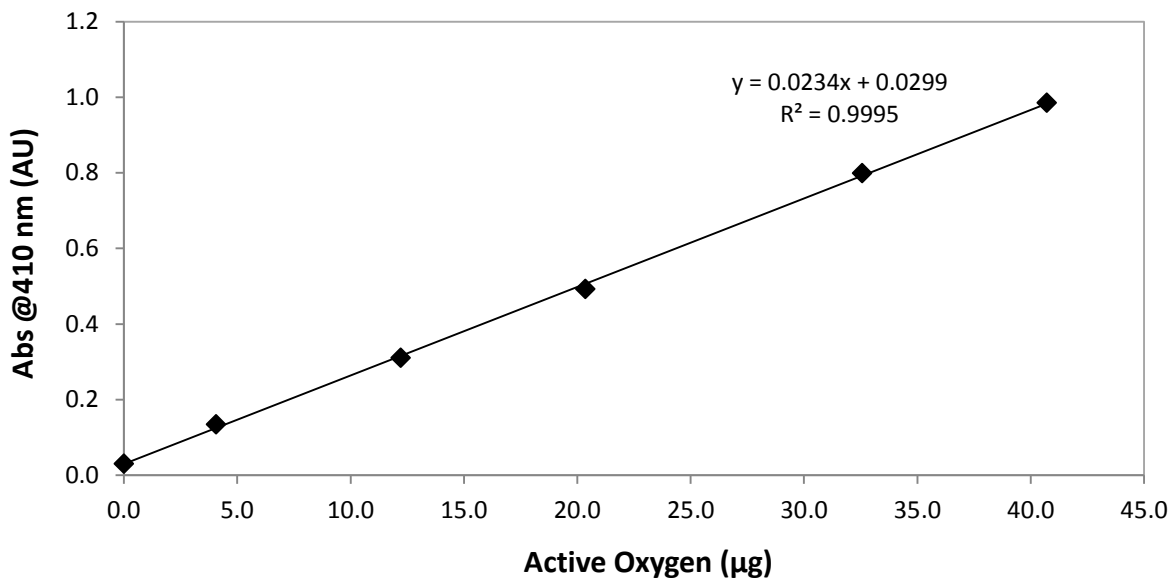
Active Oxygen (µg)	0.0	60.2	200.6	321.0	521.6	601.9
--------------------	-----	------	-------	-------	-------	-------

**Figure 2.4:** Colorimetric Observation of the Iodine Calibration Standards (Following Active Oxygen Analysis)

The absorbance values, after methanol blank subtraction, for the low range iodine standards are presented in **Table 2.4** and the calibration curve at the 410 nm wavelength is presented in **Figure 2.5**.

**Table 2.4:** Summary Table of Iodine Absorbance Results for the Low Range Active Oxygen Calibration Curve

Std	Vol. transfer from stock (mL)	µg iodine/mL	Active Oxygen (µg)	Abs @ 410 nm (AU)
1	0	0.0	0.0	0.0308
2	1	4.3	4.1	0.1344
3	3	12.9	12.2	0.3104
4	5	21.5	20.4	0.4928
5	8	34.4	32.6	0.7985
6	10	43.0	40.7	0.9849



**Figure 2.5:** Low Range Active Oxygen Calibration Curve for Iodine Absorbance at the 410 nm Wavelength

The calibration curve presented in **Figure 2.5** showed that the absorbance readings at 410 nm produced a linear curve corresponding to the following equation:

$$y = 0.0234x + 0.0299$$

where x is the amount of active oxygen and y is the absorbance measurement at 410 nm. The colorimetric trend observed in the calibration standards that represent the low magnitude active oxygen levels is presented in **Figure 2.6**.



Active Oxygen (µg)	0.0	4.1	12.2	20.4	32.6	40.7
--------------------	-----	-----	------	------	------	------

**Figure 2.6:** Colorimetric Observation of the Iodine Calibration Standards (Following Active Oxygen Analysis)

The linear equations produced from the calibration curves can be used for quantitation of unknown levels of active oxygen in sample solutions. Absorbance readings can be measured at both the 410 nm and 470 nm wavelengths and, depending on the magnitude of the absorbance, the appropriate calibration curve can be used.

The absorbance results for the H<sub>2</sub>O<sub>2</sub>-spiked samples at 470 nm were within the limits of the high range calibration curve. The absorbance results at 470 nm, with the methanol blank subtracted, are presented in **Table 2.5** along with the measured amount of active oxygen (µg) and the corresponding amount of H<sub>2</sub>O<sub>2</sub> (µg) in the sample.

**Table 2.5:** Absorbance Measurements, Amount of Active Oxygen and Corresponding Amount of H<sub>2</sub>O<sub>2</sub> in the H<sub>2</sub>O<sub>2</sub>-Spiked Samples

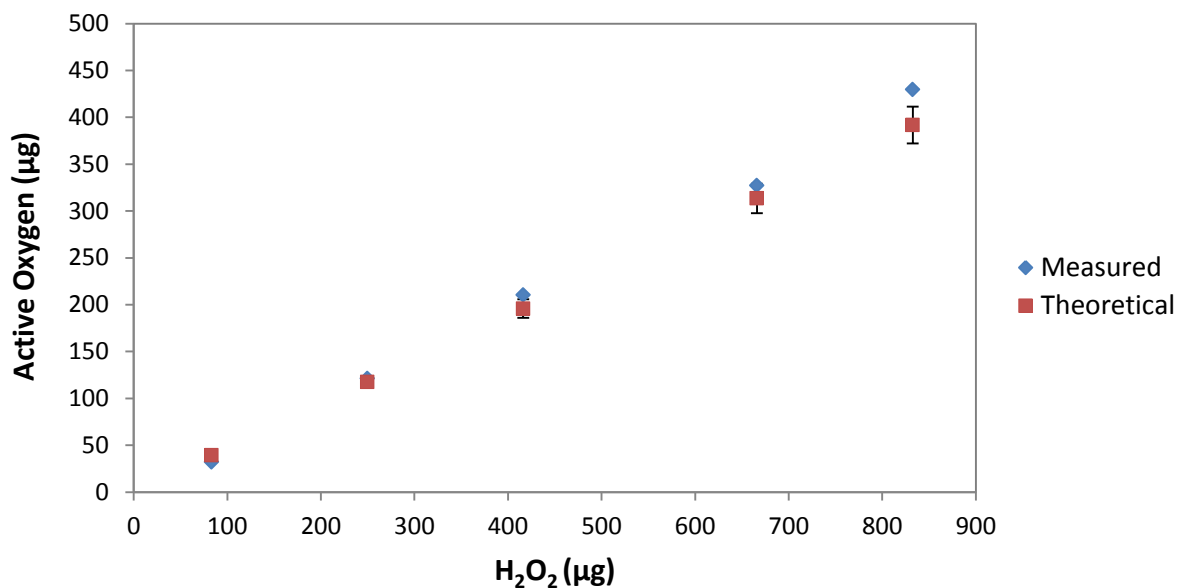
Spiked H <sub>2</sub> O <sub>2</sub> Vol. (μL)	Absorbance @ 470 nm (AU)	Measured Active Oxygen (μg)	Measured H <sub>2</sub> O <sub>2</sub> (μg)
1	0.1304	32.30	68.64
3	0.4148	121.17	257.49
5	0.7001	210.33	446.95
8	1.0759	327.22	695.34
10	1.4015	429.52	912.73

The appearance for the H<sub>2</sub>O<sub>2</sub>-spiked samples following active oxygen analysis is presented in **Figure 2.7**, along with the corresponding measured active oxygen levels (μg). In **Figure 2.8**, the measured active oxygen results are plotted against the calculated theoretical active oxygen levels, from **Table 2.2**, for the H<sub>2</sub>O<sub>2</sub> spiked-samples.



Sample	1 μL Spike	3 μL Spike	5 μL Spike	8 μL Spike	10 μL Spike
Active Oxygen (μg)	32.30	121.17	210.33	327.22	429.52

**Figure 2.7:** Appearance of the H<sub>2</sub>O<sub>2</sub>-Spiked Samples (Following Active Oxygen Analysis)



**Figure 2.8:** Measured Active Oxygen Results and Theoretical Active Oxygen Levels for the H<sub>2</sub>O<sub>2</sub>-Spiked Samples

The measured and theoretical levels of active oxygen in the H<sub>2</sub>O<sub>2</sub>-spiked samples were within 5% error, except for the 10 µL spiked sample. The measured active oxygen levels began to trend higher than the theoretical levels because the method was measuring the total active oxygen produced from H<sub>2</sub>O<sub>2</sub> and all other possible sources. The more concentrated H<sub>2</sub>O<sub>2</sub> sample could have had more heat develop from decomposition, which then raised the temperature of the solution and increased the production of total active oxygen.<sup>7</sup>

## 2.4. Conclusions

The modifications made to the ASTM E 299-08 method added no limitations to the ability to detect active oxygen and varying spiked levels of H<sub>2</sub>O<sub>2</sub> were successfully quantified. The modifications to the ASTM E 299-08 method were improvements that made the method more robust. The glassware and solvents used in the modified method are routinely used in laboratories, which made the method more readily accessible. The successful incorporation of



methanol as the blank will be of importance for dilution purposes when both solid and liquid excipients are evaluated. The iodine calibration curves were also prepared to measure very low levels of active oxygen in samples, which supports the future claim that the modified method can detect trace levels of active oxygen.

## 2.5. References

1. ASTM E299-08, "Standard Test Method for Trace Amounts of Peroxides in Organic Solvents," ASTM International, West Conshohocken, PA, **2008**, [www.astm.org](http://www.astm.org).
2. Banerjee, D. K.; Budke, C. C. *Anal. Chem.* **1964**, *36*, 792-796.
3. Pobiner, H. *Anal. Chem.* **1961**, *33*, 1423-1426.
4. Banerjee, D. K.; Budke, C. C. *Anal. Chem.* **1964**, *36*, 2367-2368.
5. Wilson, J. N.; Dickinson, R. G. *J. Am. Chem. Soc.* **1937**, *59*, 1358-1361.
6. Rowe, R. C.; Sheskey, P. J.; Cook, W. G.; Quinn, M. E. *Handbook of Pharmaceutical Excipients*, 7<sup>th</sup> ed.; Pharmaceutical Press: London, **2012**.
7. Tarvin, M.; McCord, B.; Mount, K.; Sherlach, K.; Miller, M. *J. Chromatogr., A* **2010**, *1217*, 7564-7572.

## CHAPTER 3. Evaluation of Known Organic Peroxides

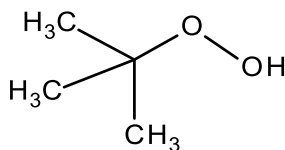
### Purpose of the Research Performed

The purpose of the research described in this chapter was to evaluate the active oxygen levels in spiked samples of hydroperoxide (ROOH) and peroxide (ROOR) compounds, to highlight the versatility of the modified ASTM E 299-08 method for active oxygen analysis of different types of peroxy compounds.

### 3.1. Introduction

Previous methods and techniques in the literature are limited in the range of peroxy compounds they can measure – e.g.,  $H_2O_2$ , hydroperoxides, or a specific known peroxide.<sup>1,2,3</sup> The modified ASTM E 299-08 method is capable of measuring all three types of peroxides at once and is not specific to one over the others. The method's wide scope of peroxy detection is important because excipients can contain multiple impurities, generally unidentified, that together represent the total active oxygen in the excipient.<sup>4</sup> Representative organic peroxide compounds of different structural types were therefore selected for evaluation using the modified ASTM E 299-08 method.

An organic hydroperoxide, *tert*-butyl hydroperoxide (TBHP), presented in **Figure 3.1**, was evaluated as a representative of the ROOH type compounds, with R being a *tert*-butyl group.

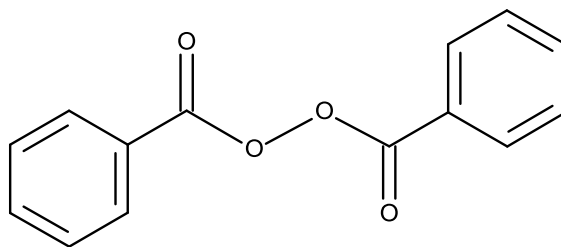


Formula Weight : 90.12  
 Formula :  $C_4H_{10}O_2$

**Figure 3.1:** Structure of *tert*-Butyl Hydroperoxide

Organic hydroperoxides serve as autocatalytic intermediates in oxidation reactions of organic molecules by molecular oxygen.<sup>5</sup> It is important when evaluating excipient stability that the modified active oxygen method can detect organic hydroperoxides if the excipients begin to degrade by oxidation. In addition to being an autocatalytic intermediate, TBHP serves as an initiator along with cumene hydroperoxide, acetyl peroxide, benzoyl peroxide, and methyl amyl ketone peroxide.<sup>6</sup>

A peroxide compound, dibenzoyl peroxide (DBPO), shown in **Figure 3.2**, was evaluated to highlight the claim that the modified method can detect active oxygen levels of the ROOR type compounds when there is no steric hindrance or thermal restrictions. DBPO is representative of the ROOR functionality compounds, with R being a benzoyl group.

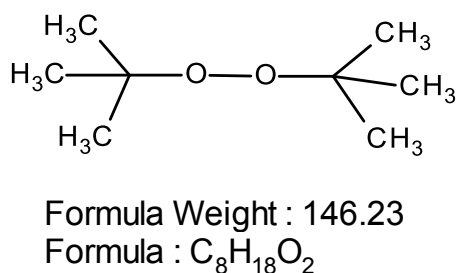


Formula Weight : 242.2  
 Formula :  $C_{14}H_{10}O_4$

**Figure 3.2:** Structure of Dibenzoyl Peroxide

DBPO is a reactive peroxide with a pi-bond system and aromatic rings. The carbon structure is important when considering the reactivity of peroxides, specifically the ease of homolytic thermal dissociation of the peroxides.<sup>5</sup>

Stable di-*tert*-butyl alkyl peroxides are claimed not to react under the analysis conditions of the ASTM E 299-08 method.<sup>6</sup> To verify this claim, di-*tert*-butyl peroxide (DTBP), shown in **Figure 3.3**, was evaluated. DTBP is representative of the ROOR functionality compounds, with R being a *tert*-butyl group.



**Figure 3.3:** Structure of di-*tert*-Butyl Peroxide

DTBP contains two *tert*-butyl groups on either side of oxygen-oxygen bond, which can create steric hindrance making the compound not reactive to potassium iodide under the conditions of the modified ASTM E 299-08 method. A temperature range from 90-130 °C is needed for DTBP to thermally decompose and be reactive.<sup>7</sup> The temperature condition of the modified ASTM E 299-08 method was room temperature, around 25 °C, so it was hypothesized that the spikes of DTBP would not be detected.

### 3.2. Experimental

Solutions with varying levels of TBHP spikes were prepared. An 80% w/w TBHP solution in di-*tert*-butyl peroxide/water (3:2) was obtained from Sigma-Aldrich and diluted with the acid solution to obtain a 180.0 µg TBHP/µL stock solution. Spiked volumes of 1 µL, 3 µL, 5

$\mu\text{L}$ , and 10  $\mu\text{L}$  of the TBHP stock solution were added to 15 mL centrifuge tubes. The TBHP spikes were then diluted to volume with the acid solution to produce 180.0  $\mu\text{g}$ , 540.0  $\mu\text{g}$ , 900.0  $\mu\text{g}$ , and 1800.0  $\mu\text{g}$  TBHP samples. TBHP has a molecular weight of 90.12 g/mol with a conversion factor, F, of 5.6325. The calculated theoretical amounts of active oxygen in the TBHP-spiked samples were 31.96  $\mu\text{g}$ , 95.87  $\mu\text{g}$ , 159.78  $\mu\text{g}$ , and 319.56  $\mu\text{g}$  of active oxygen respectively. A summary of the calculated theoretical amounts of TBHP ( $\mu\text{g}$ ) and corresponding active oxygen ( $\mu\text{g}$ ) in the TBHP-spiked samples is presented in **Table 3.1**. The TBHP-spiked samples were transferred to 20 mL GC headspace vials and the active oxygen levels were measured by the modified ASTM E 299-08 method. Appearance was documented after active oxygen analysis was completed.

**Table 3.1:** Calculated Theoretical Amount of Active Oxygen and Corresponding Amount of TBHP in the TBHP-Spiked Samples

Spiked TBHP Vol. ( $\mu\text{L}$ )	Theoretical Amount of Active Oxygen ( $\mu\text{g}$ )	Theoretical Amount of TBHP ( $\mu\text{g}$ )
1	31.96	180.0
3	95.87	540.0
5	159.78	900.0
10	319.56	1800.0

Solutions with varying levels of DBPO spikes were prepared. A 1% w/w DBPO solution was prepared, by weighing 1 g of DBPO from ACROS Organics into 99 g (126 mL) of acetonitrile. The density of the 1% w/w DBPO solution was measured to be 0.778 g/mL. Spiked volumes of 61.9  $\mu\text{L}$ , 185.8  $\mu\text{L}$ , 309.6  $\mu\text{L}$ , and 619.2  $\mu\text{L}$  of the 7.8  $\mu\text{g}$  DBPO/ $\mu\text{L}$  stock solution were added to 15 mL centrifuge tubes. The spikes were then diluted to volume with the acid solution to produce 483.8  $\mu\text{g}$ , 1451.5  $\mu\text{g}$ , 2419.2  $\mu\text{g}$ , and 4838.4  $\mu\text{g}$  DBPO samples. DBPO has a molecular weight of 242.2 g/mol with a conversion factor, F, of 15.139375. The calculated theoretical amounts of active oxygen in the DBPO-spiked samples were 31.96  $\mu\text{g}$ , 95.88  $\mu\text{g}$ , 159.80  $\mu\text{g}$ , and 319.59  $\mu\text{g}$  of active oxygen respectively. A summary of the calculated

theoretical amounts of DBPO ( $\mu\text{g}$ ) and corresponding active oxygen ( $\mu\text{g}$ ) in the DBPO-spiked samples is presented in **Table 3.2**. The DBPO-spiked samples were transferred to 20 mL GC headspace vials and the active oxygen levels were measured by the modified ASTM E 299-08 method. Appearance was documented after active oxygen analysis was completed.

**Table 3.2:** Calculated Theoretical Amount of Active Oxygen and Corresponding Amount of DBPO in the DBPO-Spiked Samples

Spiked DBPO Vol. ( $\mu\text{L}$ )	Theoretical Amount of Active Oxygen ( $\mu\text{g}$ )	Theoretical Amount of DBPO ( $\mu\text{g}$ )
61.9	31.96	483.8
185.8	95.88	1451.5
309.6	159.80	2419.2
619.2	319.59	4838.4

Solutions with varying levels of DTBP spikes were prepared. A 98% DTBP solution was obtained from Sigma-Aldrich and diluted with acid solution tenfold to obtain a 79.6  $\mu\text{g}$  DTBP/ $\mu\text{L}$  stock solution. Spiked volumes of 1  $\mu\text{L}$ , 3  $\mu\text{L}$ , 5  $\mu\text{L}$ , and 10  $\mu\text{L}$  of the DTBP stock solution were added to 15 mL centrifuge tubes. The spikes were then diluted to volume with the acid solution to produce 79.6  $\mu\text{g}$ , 238.8  $\mu\text{g}$ , 398.0  $\mu\text{g}$ , and 796.0  $\mu\text{g}$  DTBP samples. DTBP has a molecular weight of 146.23 g/mol with a conversion factor, F, of 9.139375. The calculated theoretical amounts of active oxygen in the DTBP-spiked samples were 8.71  $\mu\text{g}$ , 26.13  $\mu\text{g}$ , 43.55  $\mu\text{g}$ , and 87.10  $\mu\text{g}$  of active oxygen respectively. A summary of the calculated theoretical amounts of DTBP ( $\mu\text{g}$ ) and corresponding active oxygen ( $\mu\text{g}$ ) in the DTBP-spiked samples is presented in **Table 3.3**. The DTBP-spiked samples were transferred to 20 mL GC headspace vials and the active oxygen levels were measured by the modified ASTM E 299-08 method.

**Table 3.3:** Calculated Theoretical Amount of Active Oxygen and Corresponding Amount of DTBP in the Low Concentration DTBP-Spiked Samples

Spiked DTBP Vol. ( $\mu\text{L}$ )	Theoretical Amount of Active Oxygen ( $\mu\text{g}$ )	Theoretical Amount of DTBP ( $\mu\text{g}$ )
1	8.71	79.6
3	26.13	238.8
5	43.55	398.0
10	87.10	796.0

To eliminate the possibility of underestimating the concentration during sample preparation four additional DTBP-spiked samples were prepared in higher concentrations than the prior four samples. A 98% DTBP solution was obtained from Sigma-Aldrich and transferred directly to 15 mL centrifuge tubes in spiked volumes of 1  $\mu\text{L}$ , 3  $\mu\text{L}$ , 5  $\mu\text{L}$ , and 10  $\mu\text{L}$ . The spikes were then diluted to volume with the acid solution to produce 796.0  $\mu\text{g}$ , 2388.0  $\mu\text{g}$ , 3980.0  $\mu\text{g}$ , and 7960.0  $\mu\text{g}$  DTBP samples. The calculated theoretical amounts of active oxygen in the DTBP-spiked samples were 87.10  $\mu\text{g}$ , 261.29  $\mu\text{g}$ , 435.48  $\mu\text{g}$ , and 870.96  $\mu\text{g}$  of active oxygen respectively. A summary of the calculated theoretical amounts of DTBP ( $\mu\text{g}$ ) and corresponding active oxygen ( $\mu\text{g}$ ) in the DTBP-spiked samples is presented in **Table 3.4**. The DTBP-spiked samples were transferred to 20 mL GC headspace vials and the active oxygen levels were measured by the modified ASTM E 299-08 method.

**Table 3.4:** Calculated Theoretical Amount of Active Oxygen and Corresponding Amount of DTBP in the High Concentration DTBP-Spiked Samples

Spiked DTBP Vol. ( $\mu\text{L}$ )	Theoretical Amount of Active Oxygen ( $\mu\text{g}$ )	Theoretical Amount of DTBP ( $\mu\text{g}$ )
1	87.10	796.0
3	261.29	2388.0
5	435.48	3980.0
10	870.96	7960.0

### 3.3. Results and Discussion

The absorbance result at the 410 nm wavelength for the 1  $\mu\text{L}$  spiked TBHP sample was within the limits of the low range calibration curve. The absorbance results for the remaining spiked samples at the 470 nm wavelength were within the limits of the high range calibration curve. The absorbance results at 410 nm and 470 nm, with the methanol blank subtracted, are presented in **Table 3.5** along with the measured amount of active oxygen ( $\mu\text{g}$ ) and corresponding measured amount of TBHP ( $\mu\text{g}$ ) in the samples. The appearance for the TBHP-spiked samples following active oxygen analysis is presented in **Figure 3.4**, along with the corresponding measured active oxygen levels ( $\mu\text{g}$ ). In **Figure 3.5**, the measured active oxygen results are plotted against the calculated theoretical active oxygen levels, from **Table 3.1**, for the TBHP-spiked samples.

**Table 3.5:** Absorbance Measurements, Amount of Active Oxygen, and Corresponding Amount of TBHP in the TBHP-Spiked Samples

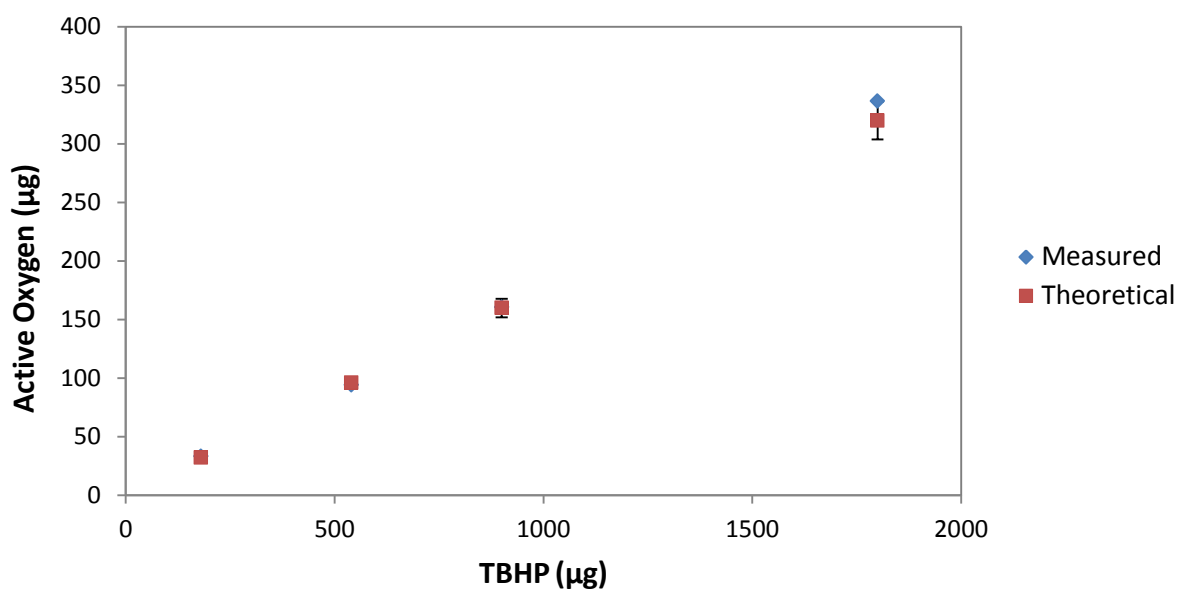
Spiked TBHP Vol. ( $\mu\text{L}$ )	Absorbance @ 470 nm (AU) (410 nm for 1 $\mu\text{L}$ spike)	Measured Active Oxygen ( $\mu\text{g}$ )	Measured TBHP ( $\mu\text{g}$ )
1	0.8058	33.16	186.78
3	0.3281	94.09	529.99
5	0.5405	160.47	903.90
10	1.1035	336.41	1894.93





Sample	1 $\mu\text{L}$ Spike	3 $\mu\text{L}$ Spike	5 $\mu\text{L}$ Spike	10 $\mu\text{L}$ Spike
Active Oxygen ( $\mu\text{g}$ )	33.16	94.09	160.47	336.41

**Figure 3.4:** Appearance of the TBHP-Spiked Samples (Following Active Oxygen Analysis)



**Figure 3.5:** Measured Active Oxygen Results and Theoretical Active Oxygen Levels for the TBHP-Spiked Samples

The measured and theoretical levels of active oxygen for the TBHP-spiked samples were within 5% error. The measured values began to trend higher than the theoretical because the method is measuring total active oxygen in the sample and not just the active oxygen produced solely from TBHP.

The absorbance results at the 470 nm wavelength for the DBPO-spiked samples were within the limits of the high range calibration curve. The absorbance results at the 470 nm wavelength, after methanol blank subtraction, are presented in **Table 3.6** along with the measured amount of active oxygen ( $\mu\text{g}$ ) and corresponding measured amount of DBPO ( $\mu\text{g}$ ) in the samples. The appearance for the DBPO-spiked samples are presented in **Figure 3.6**, along with the corresponding measured active oxygen levels ( $\mu\text{g}$ ). In **Figure 3.7**, the measured active oxygen results are plotted against the calculated theoretical active oxygen levels, from **Table 3.2**, for the DBPO-spiked samples.

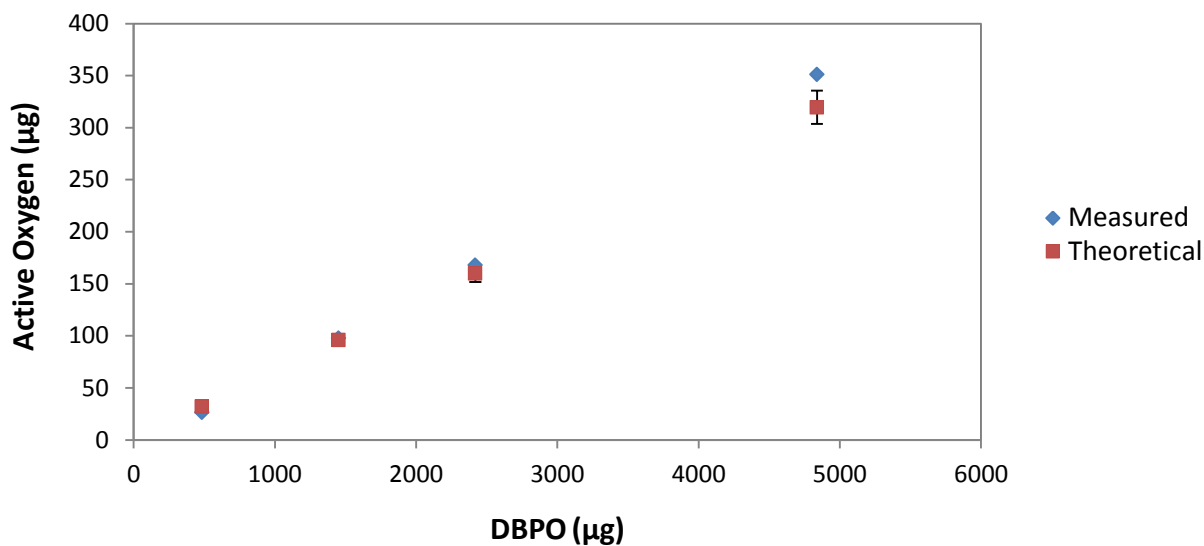
**Table 3.6:** Absorbance Measurements, Amount of Active Oxygen, and Corresponding Amount of DBPO in the DBPO-Spiked Samples

Spiked DBPO Vol. ( $\mu\text{L}$ )	Absorbance @ 470 nm (AU)	Measured Active Oxygen ( $\mu\text{g}$ )	Measured DBPO ( $\mu\text{g}$ )
61.9	0.1114	26.36	399.07
185.8	0.3400	97.80	1480.63
309.6	0.5646	167.98	2543.11
619.2	1.1502	350.98	5313.62



<b>Sample Spike</b>	61.9 $\mu\text{L}$	185.8 $\mu\text{L}$	309.6 $\mu\text{L}$	619.2 $\mu\text{L}$
<b>Active Oxygen (<math>\mu\text{g}</math>)</b>	26.36	97.80	167.98	350.98

**Figure 3.6:** Appearance of the DBPO-Spiked Samples (Following Active Oxygen Analysis)



**Figure 3.7:** Measured Active Oxygen Results and Theoretical Active Oxygen Levels for the DBPO-Spiked Samples

The measured and theoretical levels of active oxygen in the DBPO-spiked samples were within 5% error, except for the 619.2 µL spiked sample. The measured active oxygen levels began to trend higher than the theoretical levels because the method was measuring the total active oxygen produced from DBPO and all other possible sources. The increased amount of DBPO in the sample could have led to more radical-initiated side reactions that produced more total active oxygen.<sup>8</sup>

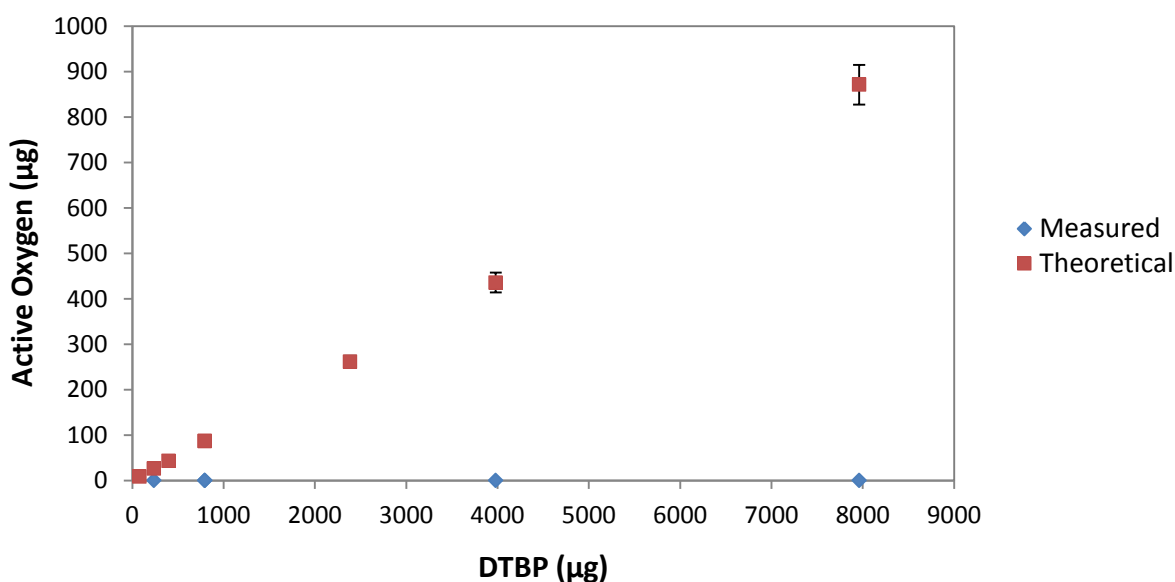
The absorbance results at the 410 nm wavelength for the low and high concentration spiked DTBP samples were within the limits of the low range calibration curve. The absorbance results at the 410 nm wavelength, after methanol blank subtraction, are presented in **Table 3.7** and **Table 3.8** along with the measured amount of active oxygen (µg) and corresponding measured amount of DTBP (µg) in the samples. In **Figure 3.8**, the measured active oxygen results are plotted against the calculated theoretical active oxygen levels, from **Table 3.3** and **Table 3.4**, for the DTBP-spiked samples.

**Table 3.7:** Absorbance Measurements, Amount of Active Oxygen and Corresponding Amount of DTBP in the Low Concentration DTBP-Spiked Samples

Spiked DTBP Vol. (μL)	Absorbance @ 410 nm (AU)	Measured Active Oxygen (μg)	Measured DTBP (μg)
1	0.0282	not detected	0.00
3	0.0364	0.28	2.56
5	0.0284	not detected	0.00
10	0.0304	0.02	0.18

**Table 3.8:** Absorbance Measurements, Amount of Active Oxygen, and Corresponding Amount of DTBP in the High Concentration DTBP-Spiked Samples

Spiked DTBP Vol. (μL)	Absorbance @ 410 nm (AU)	Measured Active Oxygen (μg)	Measured DTBP (μg)
1	0.0380	0.34	3.11
3	0.0298	not detected	0.00
5	0.0364	0.28	2.56
10	0.0407	0.46	4.20



**Figure 3.8:** Measured Active Oxygen Results and Theoretical Active Oxygen Levels for the DTBP-Spiked Samples

The measured active oxygen levels for the high and low concentration DTBP-spiked samples did not agree with the calculated theoretical levels.

### 3.4. Conclusions

Successful detection of active oxygen in the TBHP- and DBPO-spiked samples verified that the modified ASTM E 299-08 method can detect peroxides of the ROOH and ROOR type. The modified active oxygen method could not detect active oxygen in the DTBP-spiked samples. With successful detection of active oxygen in the DBPO- and not the DTBP-spiked samples, the previous hypothesis was confirmed that the bulky R groups in DTBP created steric hindrance and thermal stability and thus was not reactive to the conditions of the method. However, the ability of the modified ASTM E 299-08 method to detect peroxides of different types, gave confidence that the method would be able to detect unknown, unique, and complex peroxides present in liquid and solid excipients.

### 3.5. References

1. Yue, H.; Bu, X.; Huang, M.; Young, J.; Raglione, T. *Int. J. Pharm.* **2009**, *375*, 33-40.
2. Wasylaschuk, W. R.; Harmon, P. A.; Wagner, G.; Harman, A. B.; Templeton, A.; Xu, H.; Reed, R. *J. Pharm. Sci.* **2007**, *96*, 106-116.
3. Huang, T.; Garceau, M. E.; Gao, P. *J. Pharm. Biomed. Anal.* **2003**, *31*, 1203-1210.
4. McGinty, J. W.; Hill, J. A.; La Via, A. L. *J. Pharm. Sci.* **1975**, *64*, 356-357.
5. Thomas, J. R. *J. Am. Chem. Soc.* **1954**, *77*, 246-248.
6. ASTM E299-08, "Standard Test Method for Trace Amounts of Peroxides in Organic Solvents," ASTM International, West Conshohocken, PA, **2008**, [www.astm.org](http://www.astm.org).
7. Shaw, D. H.; Pritchard, H. O. *Can. J. Chem.* **1968**, *46*, 2721-2724.
8. Antolovich, M.; Prenzler, P. D.; Patsalides, E.; McDonald, S.; Robards, K. *Analyst.* **2002**, *127*, 183-198.

## CHAPTER 4. Active Oxygen Detection in Liquid Excipients

### Purpose of the Research Performed

The purpose of the research described in this chapter was to test the applicability of the modified ASTM E 299-08 method to liquid excipients and to assess active oxygen levels in a select set of liquid excipients.

### 4.1. Introduction

One of the main challenges in pharmaceutical development is creating formulations for poorly water-soluble drugs that have slow, incomplete dissolution and low bioavailability. With over 40% of the new drug candidates in the development pipeline having active pharmaceutical ingredients (API) with low aqueous solubility, the need for innovative formulations is critical.<sup>1</sup> Lipid-based drug delivery systems (LBDDS) are one of the innovative formulation techniques utilized to help improve API solubility.<sup>2</sup> Common solubilizing excipients used in commercially available lipid-based formulations were reviewed and examples from the following three classes were selected for evaluation: water-insoluble, triglyceride, and surfactant.<sup>2</sup> The liquid excipients chosen were oleic acid and propylene glycol from the water-insoluble class, tall oil from the triglyceride class, and polysorbate 20, polyethylene glycol 400 (PEG 400), Kolliphor® EL, and polysorbate 80 from the surfactant class. These liquid excipients are commonly used in formulations; so it is beneficial to pharmaceutical scientists to know the active oxygen levels in them.

Liquid excipients with different functionalities were selected to perform a broad screen of the active oxygen levels. The excipients chosen, their excipient functionality, density, and manufacturer details are provided below in **Table 4.1**.<sup>3</sup>

**Table 4.1:** Liquid Excipients Used in Screening of Active Oxygen Levels

Liquid Excipient	Excipient Functionality	Density (g/mL)	Manufacturer
Polyethylene Glycol 400	Coating Agent, lubricant <sup>4,5</sup>	1.126	Sigma-Aldrich
Oleic Acid	Emulsifying agent <sup>6,7</sup>	0.890	Sigma-Aldrich
Kolliphor® EL	Nonionic surfactant, emulsifying agent <sup>8</sup>	1.050	Sigma-Aldrich
Polysorbate 20	Solubilizing agent, nonionic surfactant <sup>9,10</sup>	1.105	Alfa Aesar
Tall Oil	Emulsifier, lubricant <sup>11,12</sup>	0.898	Spectrum
Propylene Glycol	Antimicrobial preservative, solvent <sup>13</sup>	1.036	Spectrum
Polysorbate 80	Nonionic surfactant <sup>14,15</sup>	1.064	Fluka

The density values for each excipient were included in **Table 4.1** because the density values will be used in the conversion of active oxygen from  $\mu\text{g}$  to ppm for each sample.

## 4.2. Experimental

Sample solutions of the liquid excipients were prepared in order to analyze them by the modified ASTM E 299-08 method. The samples were prepared in duplicate to measure the consistency of the modified active oxygen method within the same excipient. A 5 mL volume of each liquid excipient was transferred to 15 mL centrifuge tubes and diluted to volume with the acid solution. The liquid excipients were mixed with the acid solution, transferred to 20 mL GC headspace vials, and then the vials were kept capped pending analysis. Before active oxygen analysis, any liquid excipients that were yellow in appearance also required a color blank to be prepared for that sample (2 mL of the excipient: 4 mL of the acid solution). The color blanks were analyzed by the UV spectrophotometer as is and were not run under the conditions of the modified ASTM E 299-08 method. Subtraction of the sample color blank eliminated any interference in the absorbance measurements due to intrinsic coloration of the liquid excipient

being tested. The excipients that were yellow in appearance and required color blanks were oleic acid, Kolliphor® EL, polysorbate 20, tall oil, and polysorbate 80. The active oxygen levels of the liquid excipients were measured by the modified ASTM E 299-08 method and the absorbance results at the 410 nm and 470 nm wavelengths were recorded. Appearance was documented after active oxygen analysis was completed.

### 4.3. Results and Discussion

The absorbance results for the liquid excipients at the 410 nm and 470 nm wavelengths, after subtraction of the methanol blank and sample color blank if applicable, are presented in

**Table 4.2.**

**Table 4.2:** Absorbance Measurements (n=2) for the Liquid Excipients (Following Active Oxygen Analysis)

Liquid Excipient	Sample #	Absorbance at 410 nm (AU)	Absorbance at 470 nm (AU)
Polyethylene Glycol 400	1	4.2666	1.1682
	2	4.2666	1.1596
Oleic Acid	1	3.8924	0.6985
	2	3.3484	0.4793
Kolliphor® EL	1	3.6350	1.9177
	2	3.4132	1.8630
Polysorbate 20	1	1.3069	0.1514
	2	1.2273	0.1427
Tall Oil	1	1.6944	0.2313
	2	1.3073	0.3948
Propylene Glycol	1	0.0342	0.0209
	2	0.0358	0.0284
Polysorbate 80	1	3.0885	2.0867
	2	3.0885	2.1231

The magnitude of the absorbance values for the liquid excipients, shown in **Table 4.2**, indicated that the active oxygen levels ( $\mu\text{g}$ ) for each liquid excipient were calculated via the high range calibration curve, except for propylene glycol where the active oxygen level was calculated via



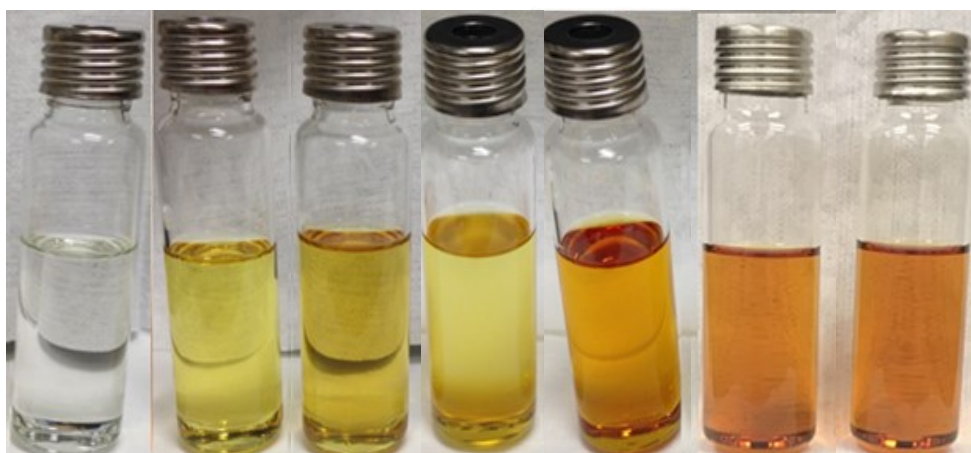
the low range calibration curve. The active oxygen results ( $\mu\text{g}$ ) were calculated from the averaged ( $n=2$ ) absorbance values. To convert the active oxygen levels from  $\mu\text{g}$  to ppm for each excipient, the density of each excipient and the sample volume (5 mL) was used in the following calculation:

$$\text{active oxygen (ppm) of excipient} = \frac{\text{active oxygen } (\mu\text{g}) \text{ of excipient}}{\text{excipient volume (mL)} * \text{density of excipient (g/mL)}}$$

The calculated active oxygen levels in  $\mu\text{g}$  and ppm for each liquid excipient evaluated are presented in **Table 4.3** in rank order from lowest active oxygen level to highest. The corresponding appearance results for the liquid excipient samples are presented in **Figure 4.1**.

**Table 4.3:** Averaged Active Oxygen Levels ( $n=2$ ) for the Liquid Excipients

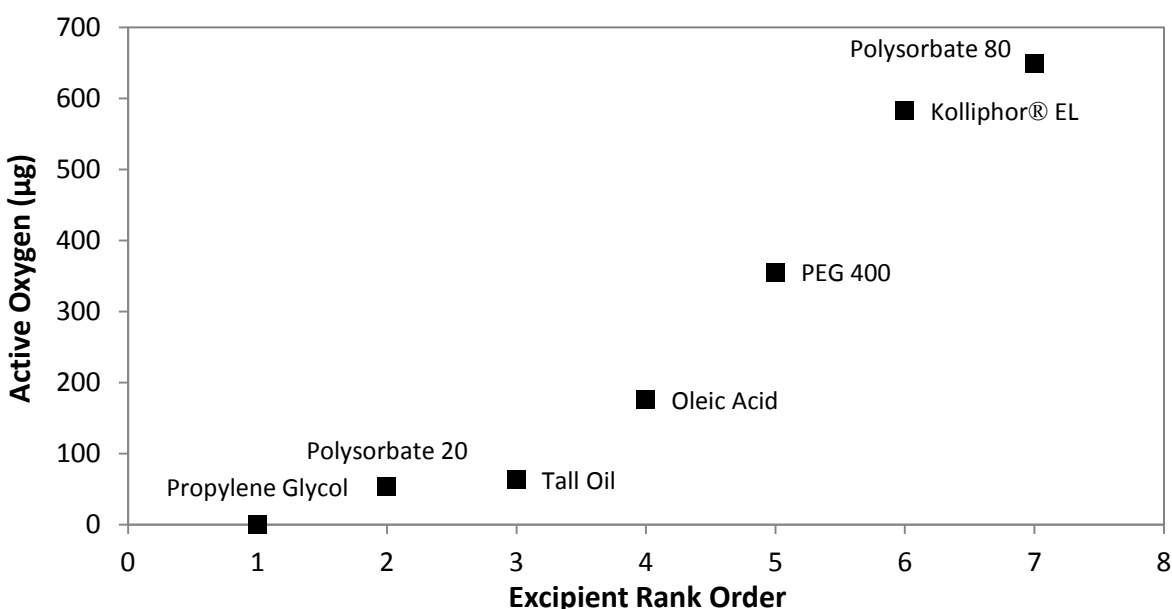
Liquid Excipient	Active Oxygen Level ( $\mu\text{g}$ )	Active Oxygen Level (ppm)
Propylene Glycol	0.22	0.04
Polysorbate 20	52.87	9.61
Tall Oil	62.86	14.00
Oleic Acid	175.59	39.46
Polyethylene Glycol 400	355.28	63.11
Kolliphor® EL	582.30	110.91
Polysorbate 80	649.34	122.06



Sample	Propylene Glycol	Polysorbate 20	Tall Oil	Oleic Acid	PEG 400	Kolliphor® EL	Polysorbate 80
Active Oxygen (ppm)	0.04	9.61	14.00	39.46	63.11	110.91	122.06

**Figure 4.1:** Appearance of the Liquid Excipient Samples (Following Active Oxygen Analysis)

The oleic acid and tall oil samples were not miscible with the 1 mL addition of the aqueous KI solution spike and formed non-homogeneous mixtures that had high background absorbance. The duplicates of the fatty acid samples had differences in absorbance units of 0.22 AU (oleic acid) and 0.16 AU (tall oil), while the other liquid excipients only had a difference in absorbance units of 0.002-0.05 AU. The non-homogeneous appearance of those two fatty acid samples could have led to different absorbance readings depending on the layer of the aliquot that was measured by the spectrophotometer. A comparison plot of the active oxygen levels for each liquid excipient, displayed in **Figure 4.2**, demonstrated the broad range that the modified ASTM E 299-08 method covered.



**Figure 4.2:** Active Oxygen Levels Measured for Each Liquid Excipient

#### 4.4. Conclusions

The modified ASTM E 299-08 method successfully measured the active oxygen levels in several liquid excipients without knowledge of the contributing peroxide. The liquid excipients

possessed widely varying physical characteristics, but the modified method was non-discriminatory and levels in the range of 0.22 µg – 649.34 µg (0.04 ppm – 122.06 ppm) of active oxygen were quantified. The fatty acid excipients showed some limitations for quantification within the duplicate samples because of the incompatibility of the excipient with the aqueous KI solution. A possible solution for this inconsistency would be to dilute the initial liquid excipient sample with methanol to expose less of the excipient to the aqueous KI solution. The dilution would be accounted for in the final calculation and the duplicate results may then have better agreement.

#### 4.5. References

1. Le-Ngoc, Vo C.; Park, C.; Lee, B. *Eur. J. Pharm. Biopharm.* **2013**, *85*, 799-813.
2. Kalepu, S.; Manthina, M.; Padavala, V. *APSB.* **2013**, *3*, 361-372.
3. Rowe, R. C.; Sheskey, P. J.; Cook, W. G.; Quinn, M. E. *Handbook of Pharmaceutical Excipients, 7<sup>th</sup> ed.*; Pharmaceutical Press: London, **2012**.
4. Mohl, S.; Winter, G. *J. Control. Release.* **2004**, *97*, 67-78.
5. Hadia, I. A., et al. *Acta Pharm. Hung.* **1989**, *59*, 137-142.
6. Schroeder, I. Z., et al. *J. Controlled Release.* **2007**, *118*, 196-203.
7. Francoeur, M. L., et al. *Pharm. Res.* **1990**, *7*, 21-627.
8. Carmignani, C., et al. *Drug Dev. Ind. Pharm.* **2002**, *28*, 101-105.
9. Nema, S., et al. *J. Pharm. Sci. Tech.* **1997**, *51*, 166-171.
10. Yalkowski, S. H. *Solubility and Solubilization in Aqueous Media*; Oxford University Press: New York, **1999**, 310-312.
11. Steiner, C. S., Fritz E. *J. Am. Oil. Chem. Soc.* **1959**, *36*, 354-357.
12. Ash, M.; Ash, I. *Handbook of Preservatives*, Synapse Information Resources: New York, **2004**.
13. Williams, A. C.; Barry, B. W. *Adv. Drug Delivery Rev.* **2004**, *56*, 603-618.
14. Zhang, H.; Yao, M.; Morrison, R. A.; Chong, S. *Arch. Pharm. Res.* **2003**, *26*, 768-772.
15. Gulyaev, A. E.; Gelperina, S. E.; Skidan, I. N.; Antropov, A. S.; Kivman, G. Y.; Kreuter, J. *Phar. Res.* **1999**, *16*, 1564-1569.

## CHAPTER 5. Active Oxygen Detection in Solid Excipients

### Purpose of the Research Performed

The purpose of the research described in this chapter was to test the applicability of the modified ASTM E 299-08 method to solid excipients and to assess active oxygen levels in a select set of solid excipients.

### 5.1. Introduction

With the increased presence of API that have poor aqueous solubility, an emerging formulation development technique used to combat this issue in addition to LBDDS, is solid dispersion. Solid dispersion is when one or more API is dispersed in an inert carrier or matrix in the solid-state phase and prepared by solvent, melting, or a combination of the two.<sup>1</sup> Solid dispersions help formulate API compounds that belong to Class II in the Biopharmaceutics Classification System (BCS), which are described as poorly soluble and highly permeable.<sup>1</sup> Excipients used in commercially available solid dispersions were reviewed, and the solid excipients evaluated were from the following carrier types: povidone (PVP), polyethylene glycol (PEG), and poloxamer.<sup>1</sup> The specific solid excipients chosen were polyethylene glycol 1000 (PEG 1000) from the PEG carrier type, polyvinylpyrrolidone 58 (K29-32) from the PVP carrier type, and poloxamer 188 from the poloxamer carrier type. Myrj 52™ was also evaluated because it shares similar characteristics to poloxamer as an emulsifying agent and was also used in solid dispersion formulations.<sup>2,3</sup> These solid excipients are commonly used in formulations; so it is beneficial to pharmaceutical scientists to know the active oxygen levels in them. The solid excipients with different functionalities that were selected are listed in **Table 5.1**, along with their classification, density, and manufacturer.<sup>10</sup>

**Table 5.1:** Solid Excipients Used in Screening of Active Oxygen Levels

Solid Excipient	Excipient Classification	Density (g/mL)	Manufacturer
Polyethylene Glycol 1000	Ointment base, lubricant <sup>4,5</sup>	1.08	Dow
Polyvinylpyrrolidone 58 (K29-32)	Tablet and capsule binder, solubilizing agent <sup>6,7</sup>	1.18	ACROS
Myrj 52™	Emulsifying agent <sup>2</sup>	N/A	S Pharma
Poloxamer 188	Emulsifying agent, nonionic surfactant <sup>8,9</sup>	1.06	Spectrum

The density values for each excipient are included in **Table 5.1**, but during the sample preparation the densities of the final excipient solutions were 1 g/mL. The density values of the excipient solution will be used in the conversion of active oxygen from  $\mu\text{g}$  to ppm for each sample.

## 5.2. Experimental

Sample solutions of the solid excipients were prepared in duplicate to measure the consistency of the modified ASTM E 299-08 method within the same excipient. Ten grams of each solid excipient was transferred into 20 mL scintillation vials and methanol (10 mL) was added to the vials. The sample was mixed until the solid excipient was dissolved and the solution was homogeneous with a density of 1 g/mL. The 1 g/mL methanolic solutions enabled the solid excipients to be evaluated in the same manner as the liquid excipients. The 1 g/mL density is equivalent to the averaged density (1.024 g/mL) for the previous liquid excipients evaluated in *Chapter 4*. Five milliliters of the samples were transferred to 15 mL centrifuge tubes, diluted to volume with the acid solution, and mixed thoroughly. The samples were transferred to 20 mL GC headspace vials and the vials were kept capped pending analysis. Before active oxygen analysis, any excipient solution that was yellow in appearance also required a color blank to be prepared (2 mL of the methanolic solution: 4 mL of the acid

solution). The color blanks were analyzed by the UV spectrophotometer as is and were not run under the conditions of the modified active oxygen method. Subtraction of the sample color blank would eliminate any interference in the absorbance measurements from the intrinsic coloration of the excipient methanolic solution. The solid excipient solution that was yellow in appearance before analysis and required a color blank was the K29-32 methanolic solution. The samples were analyzed using the modified ASTM E 299-08 active oxygen method and the absorbance results were recorded at both the 410 nm and 470 nm wavelengths. Appearance was documented after active oxygen analysis.

### 5.3. Results and Discussion

The absorbance results at the 410 nm and 470 nm wavelengths for the solid excipients, after subtraction of the methanol blank and the sample color blank if applicable, are presented in

**Table 5.2.**

**Table 5.2:** Absorbance Measurements (n=2) for the Solid Excipients (Following Active Oxygen Analysis)

Solid Excipient	Sample #	Absorbance at 410 nm (AU)	Absorbance at 470 nm (AU)
Polyethylene Glycol 1000	1	1.4330	0.1860
	2	1.4742	0.1970
Polyvinylpyrrolidone 58 (K29-32)	1	3.9171	2.6460
	2	3.9229	2.4504
Mytj 52™	1	0.1401	0.0184
	2	0.1167	0.0143
Poloxamer 188	1	0.0770	0.0123
	2	0.0712	0.0293

The higher magnitude absorbance values of PEG 1000 and K29-32, in **Table 5.2**, indicated that the active oxygen levels ( $\mu\text{g}$ ) for these two samples were calculated via the high range calibration curve. The remaining excipients Mytj 52™ and poloxamer 188, in **Table 5.2**, had

lower magnitude absorbance values, for which the low range calibration curve would be used. The active oxygen results ( $\mu\text{g}$ ) are calculated from the averaged absorbance values ( $n=2$ ). To convert the active oxygen levels for each excipient from  $\mu\text{g}$  to ppm, the density of each sample solution (1 g/mL) and the sample volume transferred was used according to the following calculation:

$$\text{active oxygen (ppm) of excipient} = \frac{\text{active oxygen } (\mu\text{g}) \text{ of excipient}}{\text{excipient volume (mL)} * \text{density of excipient (g/mL)}}$$

The calculated active oxygen levels in  $\mu\text{g}$  and ppm for the solid excipients are presented in **Table 5.3** in rank order from lowest active oxygen level to highest. The corresponding appearance of the solid excipient samples, after active oxygen analysis, is presented in **Figure 5.1**.

**Table 5.3:** Averaged Active Oxygen Levels ( $n=2$ ) for the Solid Excipients

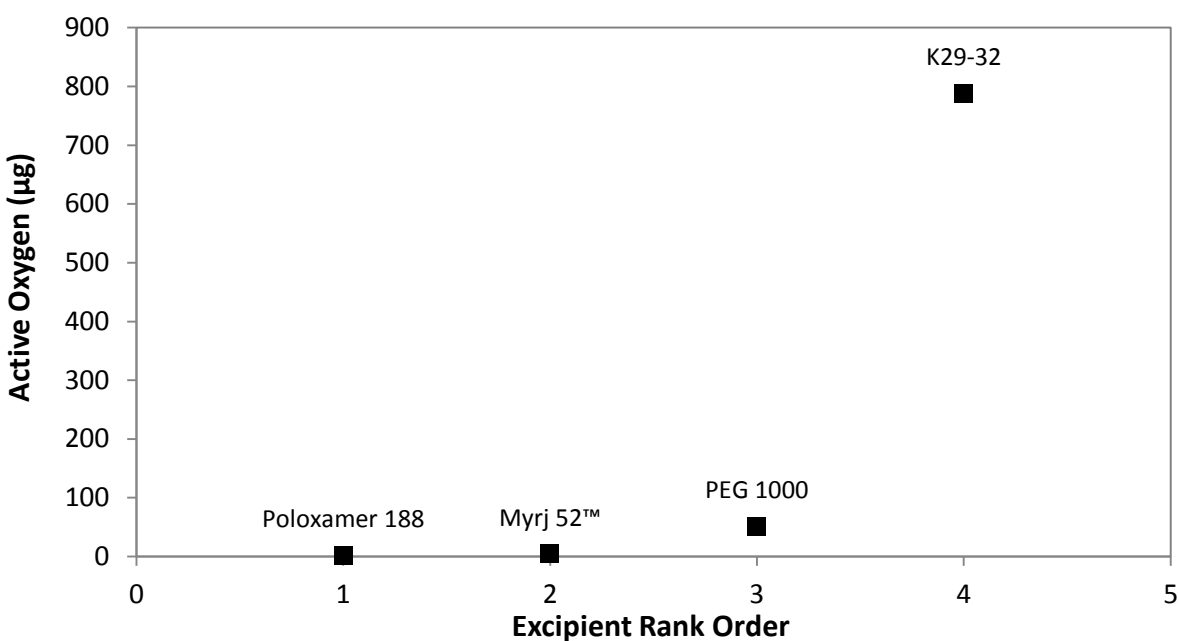
Solid Excipient	Active Oxygen Level ( $\mu\text{g}$ )	Active Oxygen Level (ppm)
Poloxamer 188	1.89	0.38
Myrj 52 <sup>TM</sup>	4.21	1.00
Polyethylene Glycol 1000	51.39	10.26
Polyvinylpyrrolidone 58 (K29-32)	787.88	156.85



Sample	Poloxamer 188	Myrj 52 <sup>TM</sup>	PEG 1000	K29-32
Active Oxygen (ppm)	0.38	1.00	10.26	156.85

**Figure 5.1:** Appearance of the Solid Excipient Samples (Following Active Oxygen Analysis)

The duplicates prepared for the solid excipients poloxamer 188, Myrj 52™, and PEG 1000 had differences in absorbance units of 0.006-0.02 AU. The duplicates prepared for K29-32 had a difference in absorbance units of 0.20 AU. The higher difference in the K29-32 duplicates could be attributed to the fact that two separate samples of K29-32 were prepared on different days because on the first day of analysis there was not enough sample to have a duplicate analysis. It was also observed that the physical characteristic of each solid excipient determined the length of time it took the methanolic solution to be homogeneous. For example, PEG 1000 was a waxy solid and took longer to dissolve in methanol than poloxamer 188, which was a flake and had increased surface area for interaction with methanol. A comparison of the active oxygen levels for these solid excipients, displayed in **Figure 5.2**, demonstrated the broad range that the modified ASTM E 299-08 method covered.



**Figure 5.2:** Active Oxygen Levels Measured for Each Solid Excipient



## 5.4. Conclusions

The modified ASTM E 299-08 method successfully measured the active oxygen levels in several solid excipients, without knowledge of the contributing peroxide. The preparation of methanolic solutions for active oxygen analysis of solid excipients provided a comparable procedural method to the one used for liquid excipients. The solid excipients possessed different physical characteristics, but the modified ASTM E 299-08 method was non-discriminatory and levels in the range of 1.89  $\mu\text{g}$  – 787.88  $\mu\text{g}$  (0.38 ppm – 156.85 ppm) of active oxygen were quantified. Successful quantification of the active oxygen levels in solid excipients verified that the modified ASTM E 299-08 method is applicable for analysis of drug products that are solid dosage forms, such as powders or hot melts.

## 5.5. References

1. Le-Ngoc Vo, C.; Park, C.; Lee, B. *Eur. J. Pharm. Biopharm.* **2013**, *85*, 799-813.
2. Cohn, I., et al. *J. Am. Med. Assoc.* **1963**, *183*, 755-757.
3. Valizadeh, H.; Nokhodchi, A.; Qarakhani, N.; Zakeri-Milani, P.; Azarmi, S.; Hassanzadeh, D.; Lobenberg, R. *Drug Dev. Ind. Pharm.* **2004**, *3*, 303-317.
4. Hadia, I. A., et al. *Acta Pharm. Hung.* **1989**, *59*, 137-142.
5. Kellaway, I. W.; Marriott, C. *J. Pharm. Sci.* **1975**, *64*, 1162-1166.
6. Becker, D., et al. *Drug Dev. Ind. Pharm.* **1997**, *23*, 791-808.
7. Iwata, M.; Udea, H. *Drug Dev. Ind. Pharm.* **1996**, *22*, 1161-1165.
8. Mata, J. P., et al. *J. Colloid Interface Sci.* **2005**, *292*, 548-556.
9. Jebari, M. M., et al. *Polym. Int.* **2006**, *55*, 176-183.
10. Rowe, R. C.; Sheskey, P. J.; Cook, W. G.; Quinn, M. E. *Handbook of Pharmaceutical Excipients*, 7<sup>th</sup> ed.; Pharmaceutical Press: London, **2012**.

## **CHAPTER 6. Active Oxygen Formation in PEG Excipients**

### **Purpose of the Research Performed**

The purpose of the research described in this chapter was to evaluate active oxygen formation in different molecular weight grade polyethylene glycol (PEG) excipients to determine if there were differentiating trends.

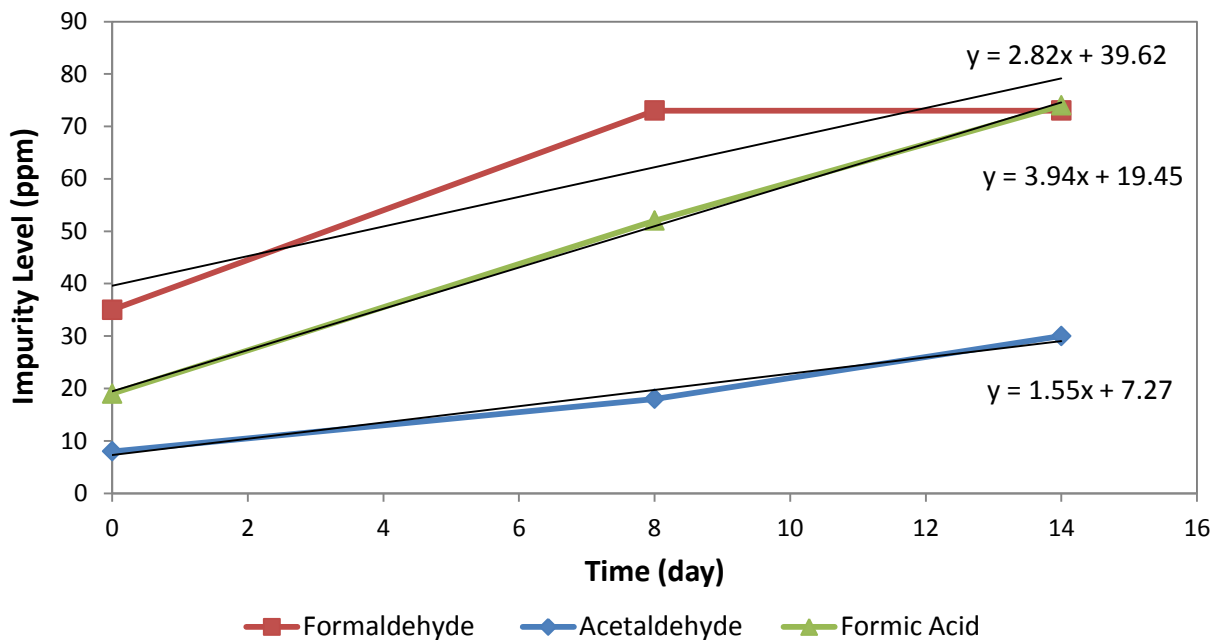
### **6.1. Introduction**

Polyethylene glycol (PEG) excipients were chosen for evaluation because they are known to have trace levels of oxidation products, e.g., peroxides, aldehydes, and organic acids. The impurities in the PEG excipients have been linked to drug-excipient interactions that have led to instability of the drug product formulations due to degradation of the drug.<sup>1</sup> The PEG compounds have been used as lubricants, plasticizers, solvents, softening agents, antiblooming agents, emulsifying agents, and cosmetic bases, but are known to be susceptible to autoxidative degradation when exposed to elevated temperatures in the presence of oxygen and water.<sup>2,3</sup> The main site for oxidation of the PEG compounds is expected to occur at the repeating ether bonds in the chain structures by a peroxidation reaction.<sup>3</sup> The modified ASTM E 299-08 method was suitable to detect the complex peroxides resulting from the PEG compounds because it is non-specific to the peroxides from which the active oxygen is derived.

Two molecular weight grades (PEG 400 and PEG 4000) of PEG were evaluated for active oxygen formation. The PEG excipients contained different physical characteristics – PEG 400 was a liquid and PEG 4000 was a granular solid flake. The average repeating oxyethylene units varied between the PEG grades: 8.7 repeating units for PEG 400 and 90.5 repeating units for PEG 4000.<sup>4,5,6</sup> Lower molecular weight grade PEG compounds are more susceptible to

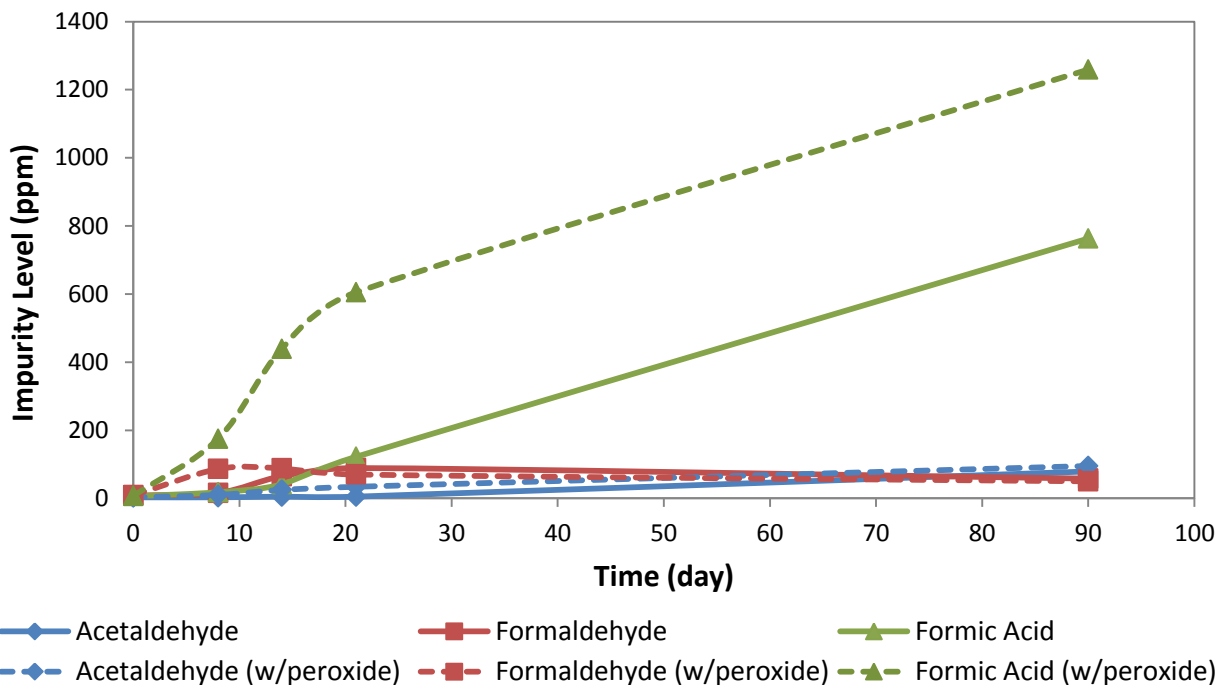
oxidation at low temperatures than higher molecular weight grade PEG compounds.<sup>10</sup> The solid physical nature of the higher molecular weight compounds allow minimal internal surface area available for oxygen interaction and a higher resistance to oxidation. The molecules in the lower molecular weight liquid PEG compounds have exposure to both external surface and internally dissolved oxygen.<sup>9</sup> It has been reported in the literature that at higher temperatures the peroxides in the PEG compounds reach a steady-state concentration before a decrease in concentration.<sup>2</sup> The first-order rate constants for the degradation via autoxidation of the model glycol compound, diethylene glycol, have previously been reported as  $9.0 \times 10^{-5} \text{ sec}^{-1}$  at 75 °C,  $1.6 \times 10^{-5} \text{ sec}^{-1}$  at 55 °C, and  $1.1 \times 10^{-6} \text{ sec}^{-1}$  at 26 °C.<sup>7</sup>

The peroxides in PEG compounds from radical-initiated or autoxidation reactions can lead to formation of other impurities such as aldehydes and organic acids. The formation of formaldehyde, acetaldehyde, and formic acid in PEG 400 has previously been published and the 14-day data set adapted from ref 1. is replotted in **Figure 6.1** for ease of illustration.<sup>1</sup> Formic acid was also included as a PEG impurity because formaldehyde can be converted to formic acid on contact with air.<sup>8</sup> The calculated rate of formation of acetaldehyde, formaldehyde, and formic acid in PEG 400 from the initial level was 1.55 ppm/day for acetaldehyde, 2.82 ppm/day for formaldehyde, and 3.94 ppm/day for formic acid.



**Figure 6.1:** Reactive Impurity Levels in Neat PEG 400 Samples Stored at 50 °C in Glass Vials with Aluminum Crimped Rubber Septum<sup>1</sup>

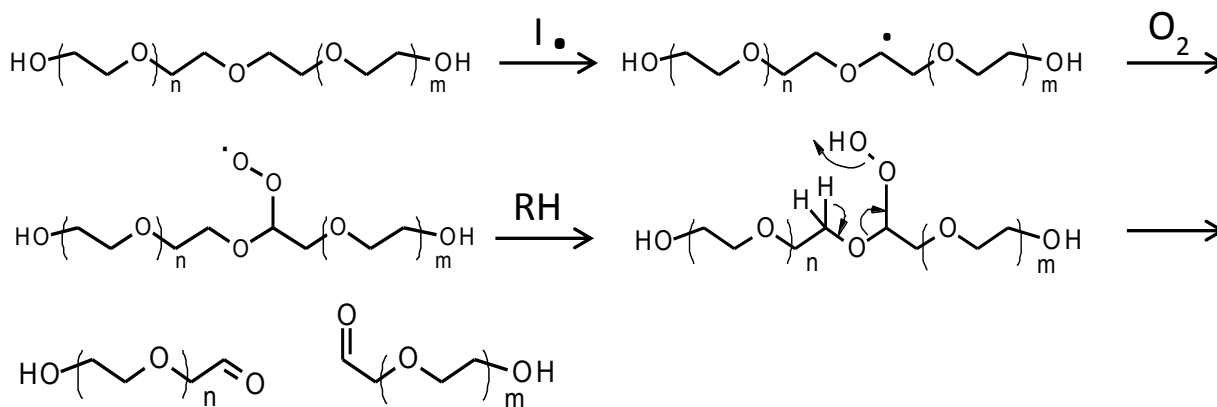
The effect of additive peroxide, such as H<sub>2</sub>O<sub>2</sub>, on the growth of impurity formation in PEG 400 has been previously published and the data adapted from ref 1. is replotted in **Figure 6.2** for ease of illustration.<sup>1</sup> The samples containing H<sub>2</sub>O<sub>2</sub> versus the control samples were reported to have increased formic acid rates and an initial greater increase in formaldehyde.<sup>1</sup>



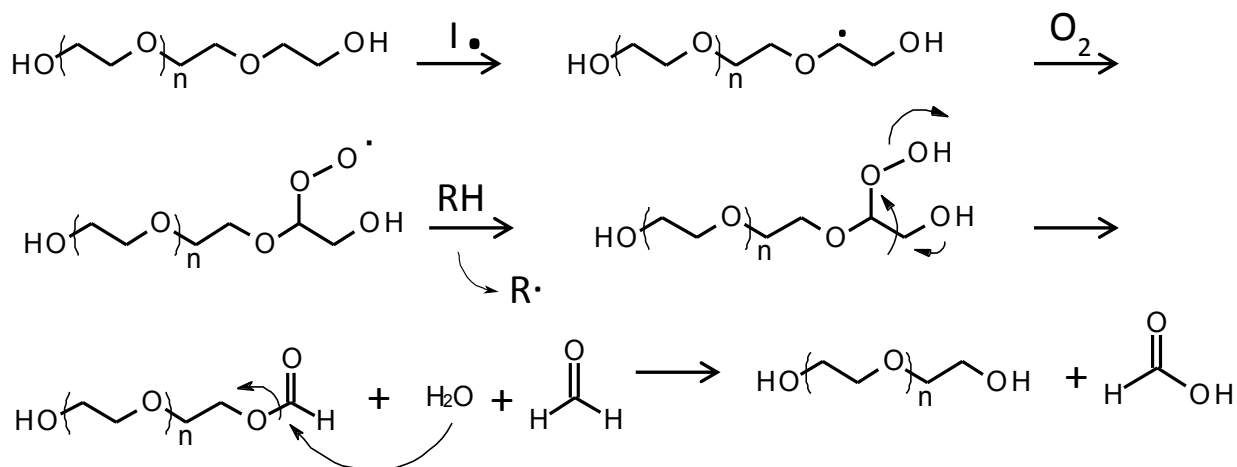
**Figure 6.2:** Reactive Impurity Levels in 1:1 PEG 400: H<sub>2</sub>O Samples With (dashed line) and Without (solid line) Oxidation Inducers Stored at 40 °C in Glass Vials with Aluminum Crimped Rubber Septum<sup>1</sup>

The proposed mechanisms for the oxidative formation of aldehyde, formaldehyde, and formic acid from PEG compounds are adapted and redrawn from ref. 1 and presented in **Figure 6.3** and

**Figure 6.4.**



**Figure 6.3:** Mechanism for the Oxidative Formation of Aldehydes from PEG<sup>1</sup>



**Figure 6.4:** Mechanism for the Oxidative Formation of Formaldehyde and Formic Acid from PEG<sup>1</sup>

The evaluation of the molecular weight grade PEG compounds, PEG 400 and PEG 4000, explored whether or not the active oxygen levels coincided with the impurity trends previously published for PEG 400. The active oxygen evaluation also showed the similarities and differences between the different molecular weight grade PEG compounds.

## 6.2. Experimental

The effect of a nitrogen overlay on active oxygen formation in PEG 400 at room temperature (25 °C) was evaluated. Super Refined PEG 400 from CRODA was chosen because super refined lots historically have the highest purity and should have the lowest initial levels of active oxygen. Two bottles from the same lot were obtained. One bottle was blanketed with nitrogen for 3 minutes after each sample pull and then capped. The second bottle acted as a control and was not blanketed with nitrogen after each sample pull. Sample pulls were taken at initial, 1 week, 2 week, 4 week, and 8 week time points. At each time point, the active oxygen

levels were measured by the modified ASTM E 299-08 method. Appearance of the samples was documented at each time point.

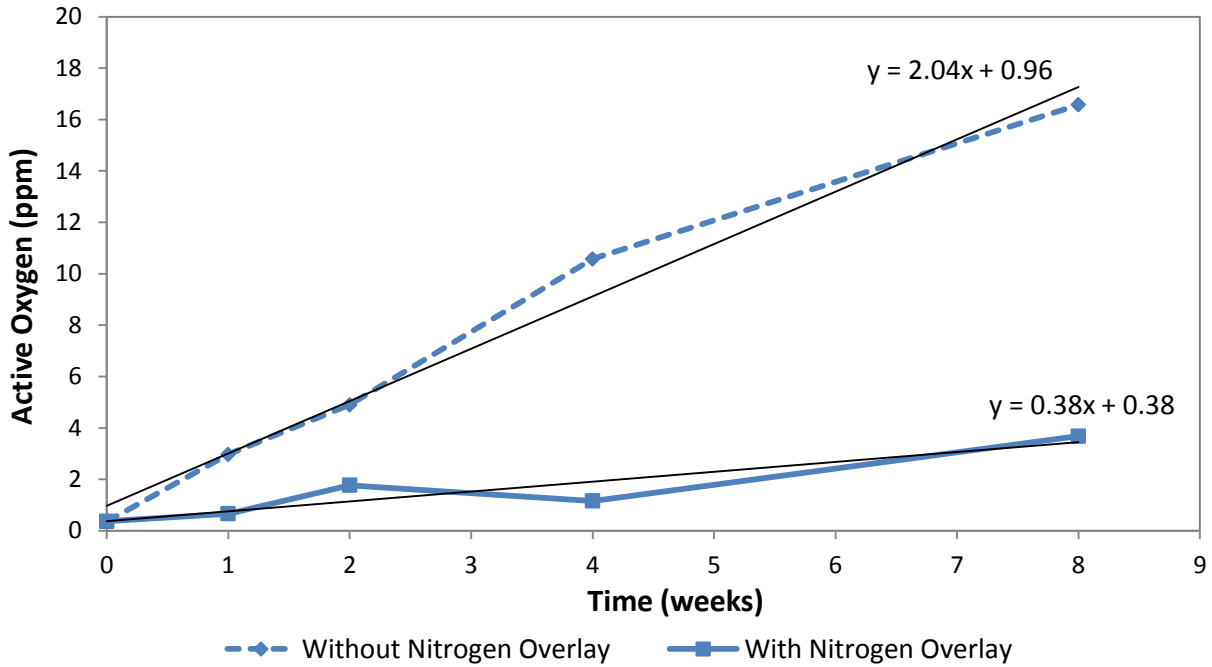
Two molecular weight grades of PEG (PEG 400 and PEG 4000) were prepared for active oxygen analysis. PEG 400, from ACROS Organics, was transferred in 15 mL aliquots to 20 mL scintillation vials. PEG 4000, from ACROS Organics, was transferred and weighed (7 g) into 20 mL scintillation vials. The vials were capped and placed in stability chambers at 25 °C/60% RH and 40 °C/75% RH to be pulled and evaluated for active oxygen formation at initial, 2 days, 7 days, and 14 days. During each sample pull, methanol (7 mL) was added to the warmed (60 °C) solid PEG 4000 sample solutions, to form 1 g/mL methanolic solutions, and the liquid PEG 400 samples were analyzed as is. The active oxygen levels in the PEG stability samples were measured by the modified ASTM E 299-08 method. Appearance of the PEG stability samples was documented after active oxygen analysis was completed.

### **6.3. Results and Discussion**

The averaged active oxygen results for the super refined PEG 400 lot with and without a nitrogen overlay are presented in **Table 6.1**. A plot of the active oxygen levels over time for the PEG 400 lot, with and without a nitrogen overlay, is displayed in **Figure 6.5**. Appearance of the samples after active oxygen analysis is provided in **Figure 6.6**.











**Table 6.1:** Averaged (n=2) Active Oxygen Results (ppm) for Super Refined PEG 400 With and Without Nitrogen Overlays

Sample	Initial	1 week	2 week	4 week	8 week
Bottle without N <sub>2</sub> Overlay	0.36	2.97	4.90	10.58	16.57
Bottle with N <sub>2</sub> Overlay	0.37	0.66	1.77	1.16	3.68



**Figure 6.5:** Active Oxygen Levels over Time for Super Refined PEG 400 With and Without a Nitrogen Overlay



Super Refined PEG 400		
Time (week)	w/o N <sub>2</sub> Overlay	w/ N <sub>2</sub> Overlay
initial		
1		
2		
4		
8		

**Figure 6.6:** Appearance of the Super Refined PEG 400 Samples With and Without a Nitrogen Overlay (Following Active Oxygen Analysis)

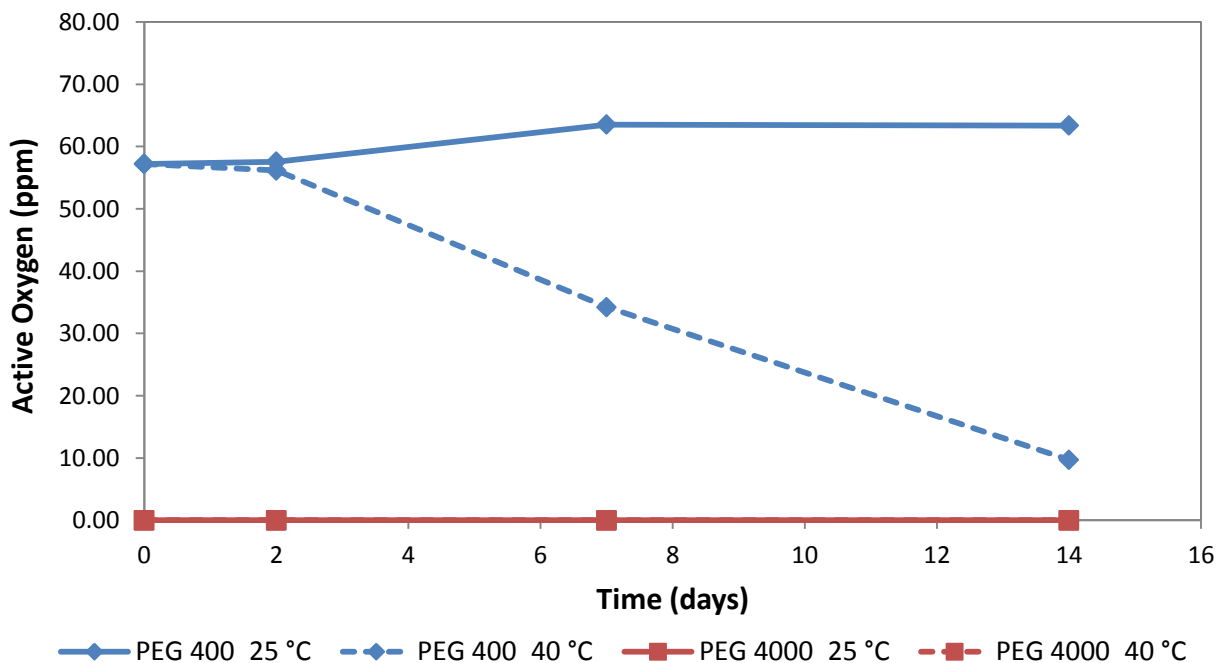
Super refined PEG 400 showed a drastic jump in active oxygen levels when a nitrogen overlay was absent between sample pulls. The rate of the active oxygen increase in the sample

was 2.04 ppm/week. When the same lot was exposed to a nitrogen overlay between sample pulls the rate of active oxygen formation was decreased to 0.38 ppm/week.

















The active oxygen results for PEG 400 and PEG 4000 on stability are presented below in **Table 6.2**. The corresponding plotted data and appearance are shown in **Figure 6.7** and **Figure 6.8**.

**Table 6.2:** Active Oxygen Levels in PEG Compounds

PEG Sample	Active Oxygen Levels (ppm)			
	PEG 400		PEG 4000	
Temperature	25 °C	40 °C	25 °C	40 °C
Time (day)				
0	57.20	57.20	nd	nd
2	57.56	56.15	nd	nd
7	63.53	34.22	nd	nd
14	63.38	9.70	nd	nd
<b>Key</b>	<i>nd – not detected</i>			



**Figure 6.7:** Active Oxygen Levels in PEG Compounds

Time (day)	25 °C		40 °C	
	PEG 400	PEG 4000	PEG 400	PEG 4000
initial				
2				
7				
14				

**Figure 6.8:** Appearance of PEG Compounds (Following Active Oxygen Analysis)

The PEG 400 stability results, in **Figure 6.7**, showed a stable active oxygen level at 25 °C/60% RH over 14 days and a steady state at 40 °C/75% RH between 0-2 days before a decrease in active oxygen. The decay rate in active oxygen for PEG 400 was  $4.5 \times 10^{-5} \text{ sec}^{-1}$  at 40 °C/75% RH after 14 days. PEG 4000 had no detectable active oxygen levels at 25 °C/60% RH and 40 °C/75%RH. The decay rate at 40 °C/75% RH for PEG 400 was three times greater than the published first-order rate constant decay value of diethylene glycol at 55 °C ( $1.6 \times 10^{-5} \text{ sec}^{-1}$ ).<sup>7</sup>

The decrease in active oxygen for PEG 400 at 40 °C/75%RH was 3.57 ppm/day which was similar to the formation rate of formic acid (3.94 ppm/day) published in the literature.<sup>1</sup> The similarity of the rates between the decrease of active oxygen and the formation of formic acid supported the hypothesis that peroxides initiate the formation of formic acid in PEG 400. The result demonstrated that when peroxides are present in PEG 400, formic acid will increase to a greater extent than when peroxides are absent.

#### **6.4. Conclusions**

The analysis of PEG 400 with and without a nitrogen overlay demonstrated that nitrogen incorporated into the storage of excipients can help reduce the rate of oxidative degradation reactions. The PEG 400 sample without a nitrogen overlay had a 5.4 times faster formation rate of active oxygen compared to the sample that had a nitrogen overlay. PEG 400 had a higher magnitude active oxygen decay rate than diethylene glycol, which confirmed that the repeating oxyethylene units in PEG 400 led to higher susceptibility to autoxidation. PEG 400 was more susceptible to autoxidation than PEG 4000 because it was a liquid and a lower molecular weight. A liquid composition has more contact with internal and external oxygen than solids, which have contact with oxygen predominantly on the external surface.<sup>9</sup> The susceptibility to oxidation for a compound also decreases with increase in molecular weight.<sup>10</sup> The modified ASTM E 299-08 method successfully demonstrated the ability to account for peroxides that led to the decay rate of PEG purity and showed the differences in active oxygen levels between the dissimilar molecular weight grade PEG compounds.

## 6.5. References

1. Hemenway, J. C.; Carvalho, T. C.; Rao, V. M.; Wu, Y.; Levons, J. K.; Narang, A. S.; Paruchuri, S. R.; Stamato, H. J.; Varia, S. A. *J. Pharm. Sci.* **2012**, *101*, 3305-3318.
2. Lloyd, W. G. *J. Chem. Eng. Data.* **1961**, *6*, 541-547.
3. Glastrup, J. *Polym. Degrad. Stab.* **1996**, *52*, 217-222.
4. Tech sheet PEG 400 from DOW
5. Tech sheet PEG 1000 from DOW
6. Tech sheet PEG 4000 from DOW
7. Lloyd, W. G. *J. Am. Chem. Soc.* **1956**, *78*, 72-75.
8. del Barrio, M.-A.; Hu, J.; Zhou, P.; Cauchon, N. *J. Pharm. Biomed. Anal.* **2006**, *41*, 738-743.
9. Shanley, E.S. Organic Peroxides: Evaluation and Management of Hazards. In *Organic Peroxides*, Swern, D., Ed.; Wiley Interscience Publishers: New York, 1972; Vol 3.
10. Jackson, H.L.; McCormack, W.B.; Rondestvedt, C.S.; Smeltz, K.C.; Viele, I.E. *J. Chem. Educ.* **1970**, *47*, A175.

## **CHAPTER 7. Evaluation of CEP-701 Drug Product Stability by the Modified ASTM E 299-08 Method**

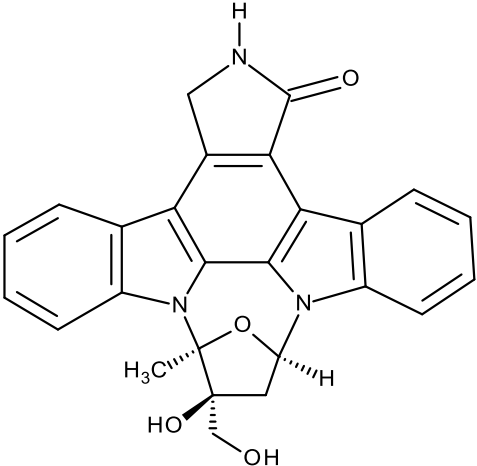
### **Purpose of the Research Performed**

The purpose of the research described in this chapter was to evaluate the active oxygen formation in a model drug product whose formulation contained lestaurtinib (CEP-701), PEG 1000, Myrj 52™, and water. The goal was to quantify the active oxygen contribution from PEG 1000, which led to the degradation of lestaurtinib (CEP-701).

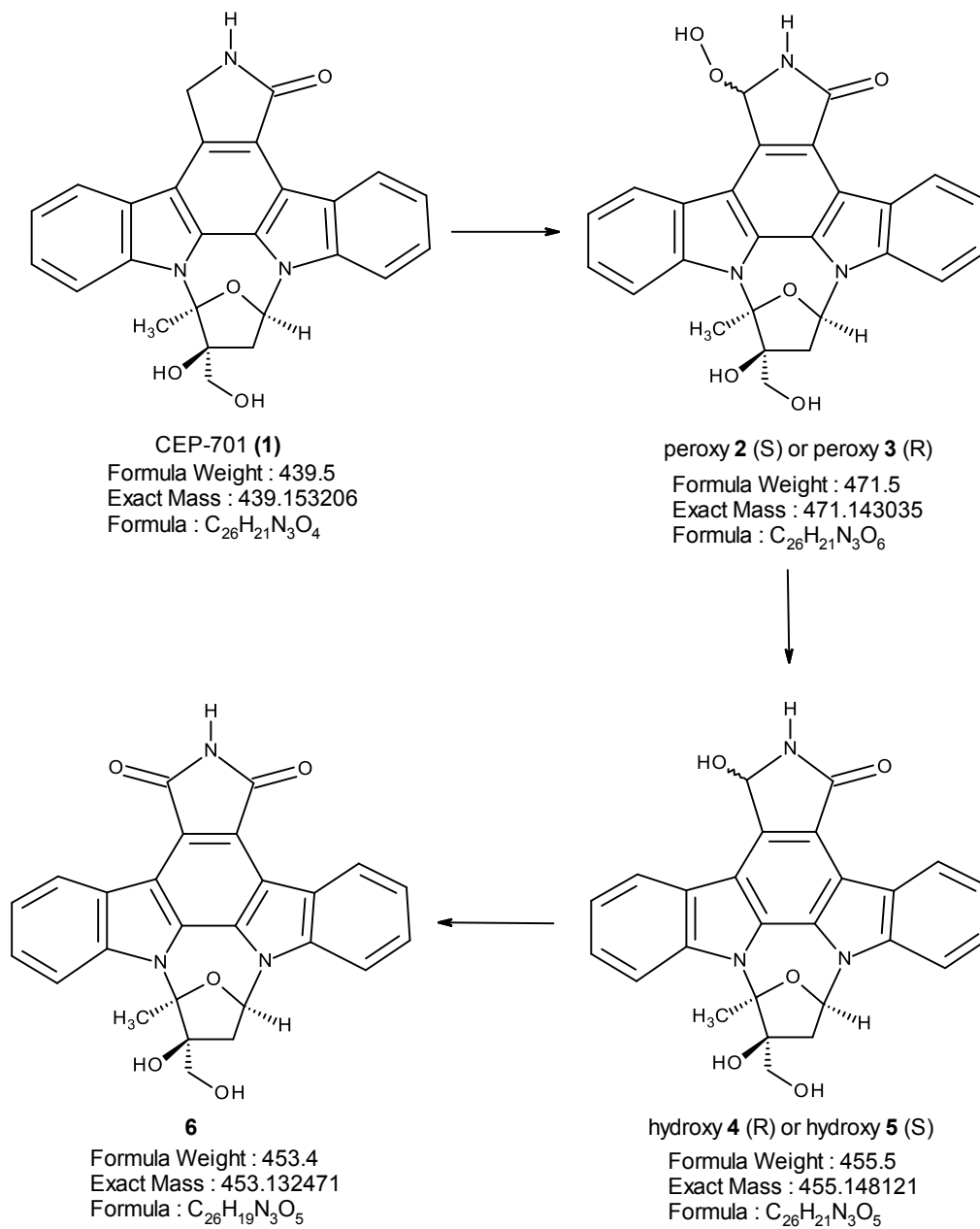
### **7.1. Introduction**

A model drug product formulation was prepared containing the drug substance lestaurtinib, which is also known as CEP-701. CEP-701 was developed by Cephalon (Frazer, PA, USA) and was incorporated in a formulation that contained PEG 1000 as one of the excipients. CEP-701 is a fms-like tyrosine kinase 3 (FLT3) inhibitor studied for targeted therapy in the treatment of acute myelogenous leukemia (AML), where FLT3 mutations are present.<sup>1</sup> Fms is a proto-oncogene that is similar to the receptor for a macrophage colony-stimulating factor.<sup>1</sup> Around 30% of AML patients have FLT3 mutations and the five-year survival rate for AML is about 26%.<sup>5</sup> The chemical structure and some properties of CEP-701 are presented in **Table 7.1.**<sup>1</sup>

**Table 7.1:** Drug Summary of Lestaurtinib (CEP-701)<sup>1</sup>

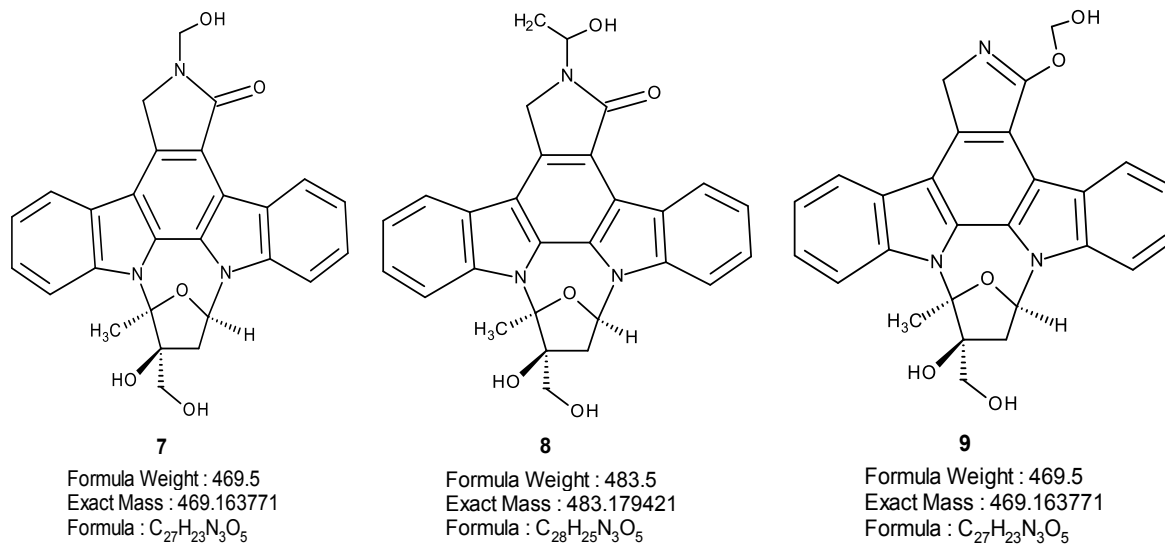
<b>Drug Name</b>	lestaurtinib , CEP-701
<b>Phase</b>	Phase III
<b>Indications</b>	acute myelogenous leukemia (AML)
<b>Pharmacology description</b>	fms-like tyrosine kinase 3 inhibitor
<b>Route of administration</b>	Alimentary, by mouth
<b>Chemical structure</b>	

The CEP-701 structure contains sites susceptible to oxidative degradation and hydroperoxide formation by peroxides and impurities found in PEG 1000. The reaction scheme for oxidative degradation of CEP-701 is presented in **Figure 7.1**. The related impurities to PEG 1000, specifically formic acid and its esters, can react with the nitrogen or oxygen of the amide functional group in CEP-701.<sup>2</sup> The CEP-701 impurities related to formaldehyde and acetaldehyde addition to the 2-pyrrolidone ring are displayed in **Figure 7.2**. The structures for compounds **7 – 9**, have historically been isolated and characterized by Cephalon via nuclear magnetic resonance (NMR) spectroscopy and mass spectrometry.



**Figure 7.1:** Reaction Scheme for Oxidative Degradation of CEP-701





**Figure 7.2:** Structures of CEP-701 Impurity Compounds from Formaldehyde (**7**, **9**) and Acetaldehyde (**8**) Addition

The model formulation contained CEP-701, PEG 1000, polyoxyl (40) stearate (Myrj 52™), and water. At each time point the stability samples were evaluated for active oxygen levels, assay, purity, and appearance. A side-by-side evaluation with both the modified ASTM E 299-08 method and the HPLC assay method was intended to quantitatively show active oxygen formation as well as the formation of CEP-701 degradative impurities. In addition to the drug product, a placebo and individual PEG 1000 and Myrj 52™ samples were evaluated on stability for active oxygen levels and appearance. Analysis of the placebo and the excipients explored whether the active oxygen levels could be accounted for as being derived from PEG 1000 alone or if the combination of excipients led to the active oxygen level of the drug product.

The CEP-701 drug product stability samples were evaluated under three different vial conditions: capped, capped with nitrogen overlay, and uncapped. The observation was previously reported in *Chapter 6* that nitrogen reduces the rate of active oxygen formation in PEG excipients. The capped with nitrogen overlay vial condition for the drug product should

exhibit the same behavior and reduce the rate of active oxygen formation in the samples.

Capped versus uncapped vials were evaluated to see if the amount of oxygen available in the sample impacted the rate of active oxygen formation in the drug product. The capped storage condition was oxygen-limiting, while the uncapped storage condition had no limits on oxygen exposure. The excipient and placebo samples were only evaluated under the capped vial condition because it was representative of commercial drug product storage.

The CEP-701 drug product stability samples were evaluated under four different temperature conditions: 5 °C, 25 °C/60% RH, 30 °C/65% RH, and 40 °C/75% RH. According to the FDA Guidance for Industry Q1A(R2), Stability Testing of New Drug Substances and Products, the recommended storage temperatures for a drug product are: long-term storage at 25 °C/60% RH or 30 °C/65% RH, intermediate storage at 30 °C/65% RH, and accelerated storage at 40 °C/75% RH.<sup>3</sup> The long-term storage is recommended for 12 months and the intermediate and accelerated storage is recommended for 6 months. The recommendations for drug products intended for storage in a refrigerator are: long-term storage at 5 °C for 12 months and accelerated storage at 25 °C/60% RH for 6 months.<sup>3</sup> The CEP-701 drug product stability samples were treated as samples that required long-term storage at both refrigerated (5 °C) and 30 °C/65 % RH. The corresponding accelerated conditions used were 25 °C/60% RH and 40 °C/75% RH. The melting point range of PEG 1000 was 37-40 °C, which indicated that storage at 40 °C/75% RH may have been too aggressive and melting of PEG 1000 could have manipulated the active oxygen levels.<sup>4</sup> To be proactive in case the 40 °C/75% RH condition was too aggressive, the samples at 25 °C/60% RH were held for 12 months as a backup to the 30 °C/65% RH long-term storage condition. If the 25 °C/60% RH condition became the long-term condition then the 30 °C/65% RH condition, would become the accelerated condition. To

cover each temperature condition, the CEP-701 drug product was placed on stability following the stability study plan presented in **Table 7.2**.

**Table 7.2:** Stability Study Plan for the CEP-701 Drug Product

Condition	Initial	1 Month	2 Month	3 Month	6 Month	9 Month	12 Month
5 °C	X, Y, Z	X, Y, Z	X, Y, Z	X, Y, Z	X, Y, Z	(X, Y, Z)	X, Y, Z
25 °C/60% RH	X, Y, Z	X, Y, Z	X, Y, Z	X, Y, Z	X, Y, Z	(X, Y, Z)	(X, Y, Z)
30 °C/65% RH	X, Y, Z	X, Y, Z	X, Y, Z	X, Y, Z	X, Y, Z	(X, Y, Z)	X, Y, Z
40 °C/75% RH	X, Y, Z	X, Y, Z	X, Y, Z	X, Y, Z	(X, Y, Z)	(X, Y, Z)	(X, Y, Z)
<b>Key</b>	<i>X - Capped, Y – Uncapped, Z – Capped w/N<sub>2</sub> Overlay, ( ) – Optional Pull</i>						

The stability study plan for the drug product placebo and the individual excipients is presented in **Table 7.3**. The placebo was evaluated at all four temperatures (5 °C, 25 °C/60% RH, 30 °C/65% RH, and 40 °C/75% RH) and the individual excipients were evaluated at 5 °C, 30 °C/65% RH, and 40 °C/75% RH.

**Table 7.3:** Stability Study Plan for the Drug Product Placebo and Excipients

Condition	Initial	1 Month	2 Month	3 Month	6 Month	9 Month	12 Month
5 °C	P, E	P, E	P, E	P, E	P, E	(P, E)	(P, E)
25 °C/60% RH	P	P	P	P	P	(P)	(P)
30 °C/65% RH	P, E	P, E	P, E	P, E	P, E	(P, E)	(P, E)
40 °C/75% RH	P, E	P, E	P, E	P, E	(P, E)	(P, E)	(P, E)
<b>Key</b>	<i>P - Placebo, E – Excipients, ( ) – Optional Pull</i>						

## 7.2. Experimental

The model formulation contained CEP-701, PEG 1000, Myrj 52™, and water. Due to the susceptibility of CEP-701 drug substance to degradation by light, the formulation process was performed under yellow light. Prior to formulation, the CEP-701 drug substance was sieved to achieve a 125 µm particle size for improved dissolution in order to minimize exposure to heat and light. A 610 g batch of drug product was prepared at a 50 mg/g (55 mg/mL) CEP-701 concentration. Due to the high viscosity of the warmed (60-65 °C) drug product, a 10 mL

positive displacement pipette was used to transfer sample aliquots (7 mL) to 28 (20 mL) glass scintillation vials. As the viscous solution cooled, a waxy solid was formed. The vials were filled and capped, with sets of 7 vials placed in stability chambers at 2-8 °C, 25 °C/60% RH, 30 °C/65% RH, and 40 °C/75% RH. The filling process was repeated for the uncapped vial condition with the cap left off of the vial. The filling process was repeated for the nitrogen overlay vial condition, with the vials being exposed to a nitrogen atmosphere within a glove box prior to being capped and stored.

The samples were removed from the stability chambers at each time point and appearance was documented. At room temperature, the CEP-701 drug product was a solid; so the novel active oxygen procedure for a solid excipient, presented in *Chapter 5*, was followed for each stability sample. Due to the density of the warmed drug product solution being 1.1 g/mL at 60-65 °C, 7 mL of drug product in the vial equaled 7.7 g. The drug product samples were warmed to 60 °C and 7.7 mL methanol was added to achieve 1 g/mL methanolic solutions. Due to the drug product appearance being yellow in color, color blank samples had to be prepared prior to active oxygen analysis (2 mL methanolic sample solution: 4 mL acid solution). At the 9-month and 12-month time points, the samples and the corresponding color blanks for all three vial conditions held at 40 °C/75% RH, after being placed in the dark for 1 hour, had to be diluted (2 mL sample : 4 mL methanol) prior to UV analysis because of their dark yellow appearance. The active oxygen levels in the drug product stability samples were measured by the modified ASTM E 299-08 method. Appearance was documented after active oxygen analysis.

The CEP-701 drug product methanolic solutions at each time point and in each stability condition were diluted and used for the assay and impurity analysis. Aliquots (240 µL) of the CEP-701 drug product methanolic solutions were transferred via a positive displacement pipette

to 25 mL volumetric flasks. The flasks were then filled to volume with methanol to achieve a 0.25 mg/mL concentration. Sample aliquots were removed from the flasks and transferred to HPLC vials for analysis by the HPLC assay method presented in **Table 7.4**. The assay analysis of the drug product was conducted with a performance verified Agilent 1100 series High Performance Liquid Chromatography (HPLC) system. The HPLC system included a quaternary SL pump, degasser, high performance autosampler SL with thermostat, thermostatted column compartment with a 2-valve column switcher, and a DAD SL detector.

**Table 7.4:** HPLC Method Parameters for Assay Analysis of the CEP-701 Drug Product

<b>Column</b>	Alltech, Alltima C18, 150 x 4.6 mm ID, 3 µm packing		
<b>Column Temperature</b>	40 °C		
<b>Autosampler Temperature</b>	Ambient		
<b>UV Detection</b>	227 nm		
<b>Injection Volume</b>	10 µL		
<b>Mobile Phase A</b>	0.1% Methanesulfonic Acid (aq)		
<b>Mobile Phase B</b>	100% Acetonitrile		
<b>Run Time</b>	20 min		
<b>Flow Rate</b>	0.8 mL/min		
<b>Gradient</b>	<i>Time (min)</i>	<i>%A</i>	<i>%B</i>
	0.0	60	40
	12.0	45	55
	15.0	45	55
	15.1	60	40
	20.0	60	40

At the 9-month time point, the uncapped vial sample at 40 °C/75% RH was chosen for analysis by LC-MS because the sample had the highest impurity total. An aliquot was removed from the 0.25 mg/mL assay solution for the 9 month sample and transferred to an HPLC vial for analysis by LC-MS following the method presented in **Table 7.5**. LC-MS analysis was conducted with a Waters Acquity UPLC and Waters Synapt G2 QTOF high resolution mass spectrometer.

**Table 7.5:** LC-MS Method Parameters for Impurity Analysis of the CEP-701 Drug Product

<b>Column</b>	Alltech, Alltima C18, 150 x 4.6 mm ID, 3 µm packing		
<b>Column Temperature</b>	40 °C		
<b>Autosampler Temperature</b>	Ambient		
<b>Injection Volume</b>	10 µL		
<b>Mobile Phase A</b>	0.1% Formic Acid (aq)		
<b>Mobile Phase B</b>	0.1% Formic Acid in Acetonitrile		
<b>Run Time</b>	20 min		
<b>Flow Rate</b>	0.8 mL/min		
<b>Gradient</b>	<i>Time (min)</i>	<i>%A</i>	<i>%B</i>
	0.0	60	40
	12.0	45	55
	15.0	45	55
	15.1	60	40
	20.0	60	40
<b>Detection</b>	MS: Electrospray source in positive ion mode and leucine enkephalin lockmass. Compounds were also detected with an in-line PDA detector scanning from 210-450 nm.		

At the 12-month time point, an additional capped vial sample held at 30 °C/65% RH was prepared for analysis by both the modified active oxygen method and the HPLC method. After the sample preparation for HPLC assay analysis, the same solution was used (5 mL) for analysis by the active oxygen method. Additionally, after active oxygen analysis of a separately prepared sample, the remaining solution was then diluted (770 µL active oxygen sample: 25 mL methanol) for HPLC analysis. Analysis of the same prepared sample solutions by both methods enabled a check to be performed to verify that the methods were both measuring the same composition of the starting sample.

The drug product placebo and both the PEG 1000 and Myrj 52™ individual excipients were prepared for stability evaluation. The same lots of PEG 1000 and Myrj 52™ that were used for the CEP-701 drug product were also used for the placebo and excipient stability studies. The drug product formulation procedure, shown above, was followed to make the placebo, but the CEP-701 drug substance was not included. A 240 g batch was prepared and aliquots (7 mL) of

the warmed (60-65 °C) placebo solution were transferred to 28 (20 mL) glass scintillation vials using a 10 mL positive displacement pipette. The vials were capped and placed in stability chambers at 5 °C, 25 °C/60% RH, 30 °C/65% RH, and 40 °C/75% RH.

PEG 1000 was warmed (60 °C) to a liquid solution and aliquots of 6.9 mL (7.6 g) were transferred to 21 (20 mL) glass scintillation vials using a positive displacement pipette. The scintillation vials were capped and sets of 7 vials were placed in stability chambers at 5 °C, 30 °C/65% RH, and 40 °C/75% RH. Myrj 52™ (7 g) was transferred to 21 (20 mL) glass scintillation vials and each vial was capped. Sets of 7 scintillation vials, filled with Myrj 52™, were placed in stability chambers at 5 °C, 30 °C/65% RH, and 40 °C/75% RH.

At each time point, the placebo and excipient stability samples were removed from the chambers and appearance was documented. The drug product placebo and excipients were solids, so the novel active oxygen procedure for a solid excipient, presented in *Chapter 5*, was followed. Due to the density of the warmed placebo solution being 1.1 g/mL at 60-65 °C, 7 mL of placebo in the vial equaled 7.7 g. Methanol (7.7 mL) was added to the warmed (60 °C) placebo samples to achieve 1 g/mL methanolic solutions. Methanol was added to the warmed (60 °C) PEG 1000 and Myrj 52™ samples (7.6 mL and 7.0 mL, respectively) to obtain 1 g/mL methanolic solutions. Due to the yellow appearance of the Myrj 52™ methanolic solutions, color blanks had to be prepared for active oxygen analysis (2 mL Myrj 52™ methanolic solution: 4 mL acid solution). The active oxygen levels of the placebo and excipient samples were measured by the modified ASTM E 299-08 method. Appearance was documented after each active oxygen analysis.

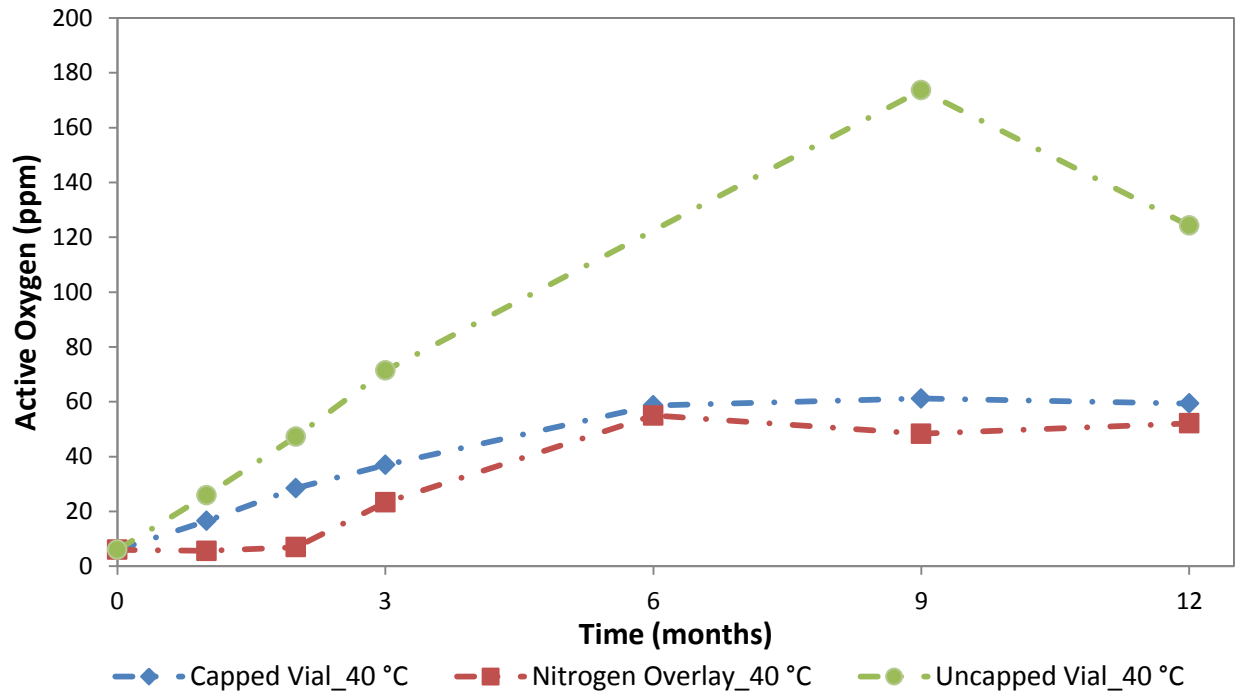
### 7.3. Results and Discussion

The active oxygen, assay, and impurity results for the CEP-701 drug product, with corresponding plotted data and appearance, are presented in **Table 7.6 – Table 7.8** and **Figure 7.3 – Figure 7.10**. Summary tables for the percent impurity results for the CEP-701 drug product are provided in **Table A.1 – Table A.3** in *Appendix A*. The LC-MS results for the impurity compounds are referenced in **Figure B.1 – Figure B.4** in *Appendix B*. An example HPLC chromatogram for the 9-month stability CEP-701 drug product sample at 40 °C/75% RH (uncapped vial condition) is presented in **Figure C.1** in *Appendix C*. The 25 °C/60% RH condition was evaluated as a back-up to the 30 °C/65% RH condition and was only analyzed until the 6-month time point, which is indicated by black cells for the 9-month and 12-month time points in the following tables and figures.

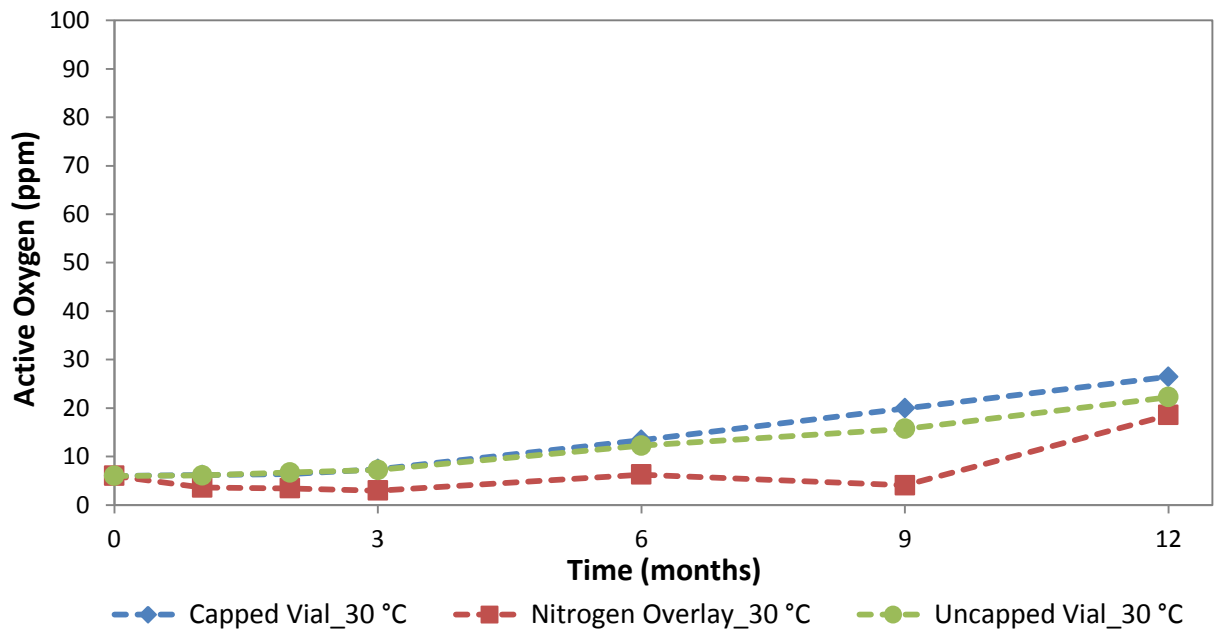
**Table 7.6:** Active Oxygen Levels for the CEP-701 Drug Product

		Active Oxygen Levels (ppm)											
Storage Condition		Capped Vial				Nitrogen Overlay (w/cap)				Uncapped Vial			
Temp.(°C)	Time(mo.)	5	25	30	40	5	25	30	40	5	25	30	40
0			6.0	6.5	6.0	6.0	6.0	6.5	6.0	6.0	6.0	6.5	6.0
1		5.1	6.6	6.2	16.5	4.7	5.9	3.6	5.6	5.3	6.7	6.1	25.9
2		5.0	7.2	6.4	28.5	4.3	5.6	3.4	6.9	4.8	7.0	6.7	47.3
3		4.7	7.7	7.4	37.0	4.4	6.3	3.0	23.3	4.7	7.3	7.2	71.4
6		3.9	12.2	13.4	58.7	3.6	7.0	6.3	55.0	3.9	12.4	12.2	18.8
9		3.7		19.9	61.1	3.5		4.1	48.3	3.7		15.7	173.7
12		3.4		26.4	59.4	3.2		18.5	52.1	3.4		22.2	124.3

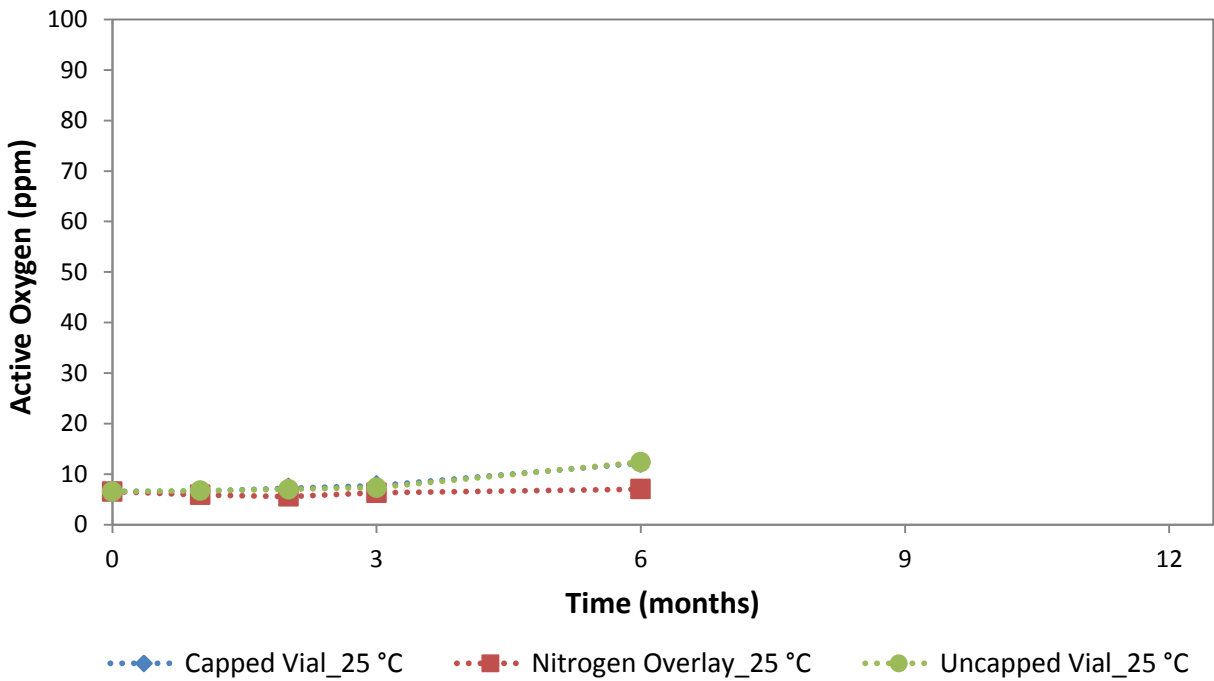




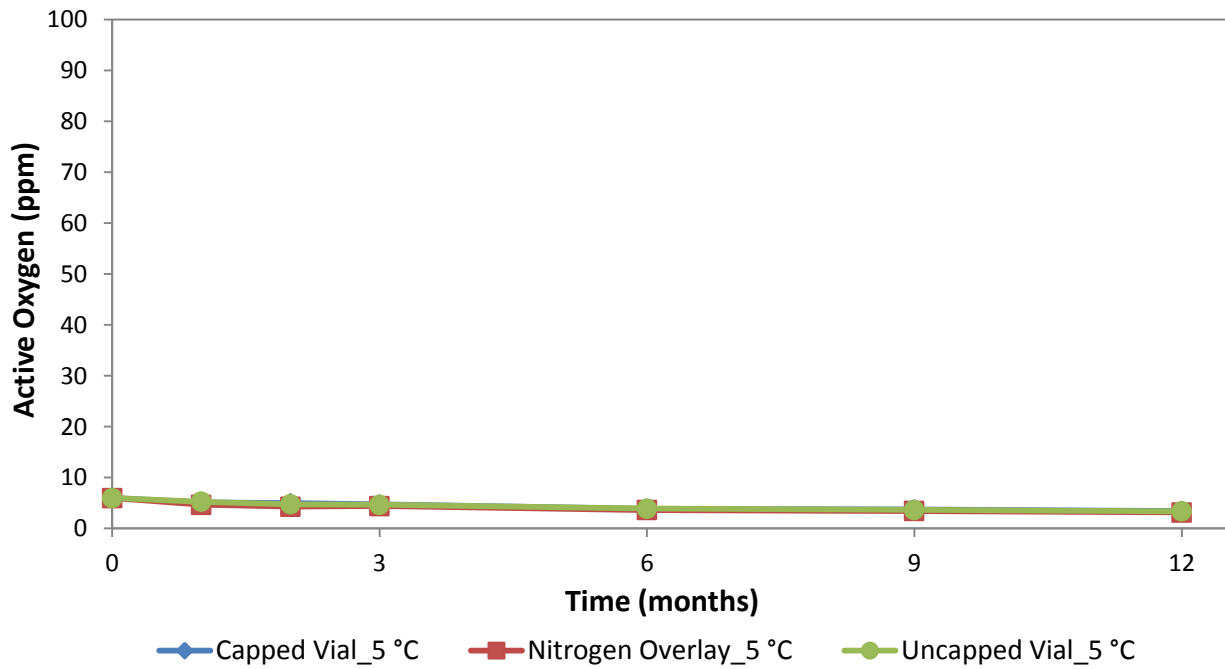
**Figure 7.3:** Active Oxygen Levels for the CEP-701 Drug Product at 40 °C/75% RH








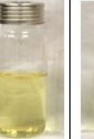


























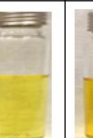























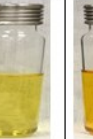








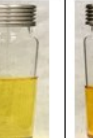









**Figure 7.4:** Active Oxygen Levels for the CEP-701 Drug Product at 30 °C/65% RH



**Figure 7.5:** Active Oxygen Levels for the CEP-701 Drug Product at 25 °C/60% RH



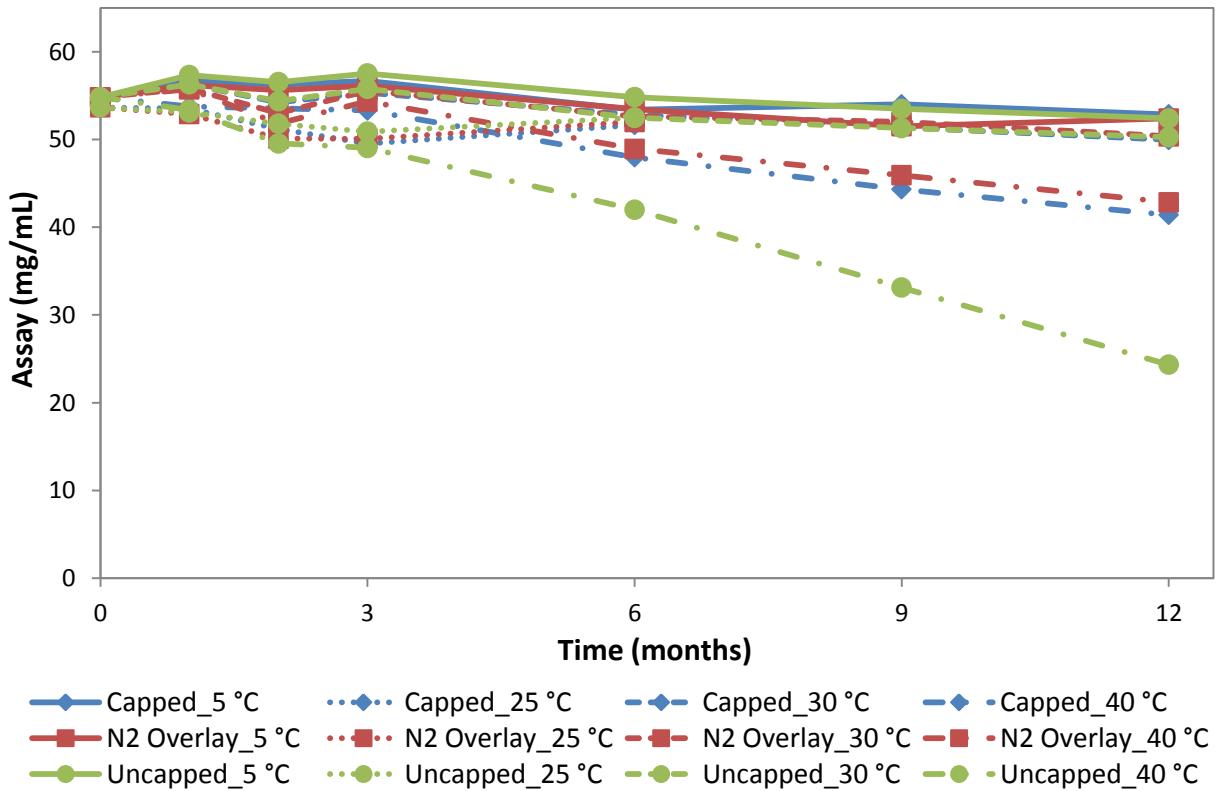
**Figure 7.6:** Active Oxygen Levels for the CEP-701 Drug Product at 5 °C

Time (month)	5 °C			25 °C			30 °C			40 °C		
	Capped	N <sub>2</sub> Overlay	Uncapped	Capped	N <sub>2</sub> Overlay	Uncapped	Capped	N <sub>2</sub> Overlay	Uncapped	Capped	N <sub>2</sub> Overlay	Uncapped
Initial												
1												
2												
3												
6												
9												
12												

**Figure 7.7:** Appearance of the CEP-701 Drug Product (Following Active Oxygen Analysis)

**Table 7.7:** Assay Levels for the CEP-701 Drug Product

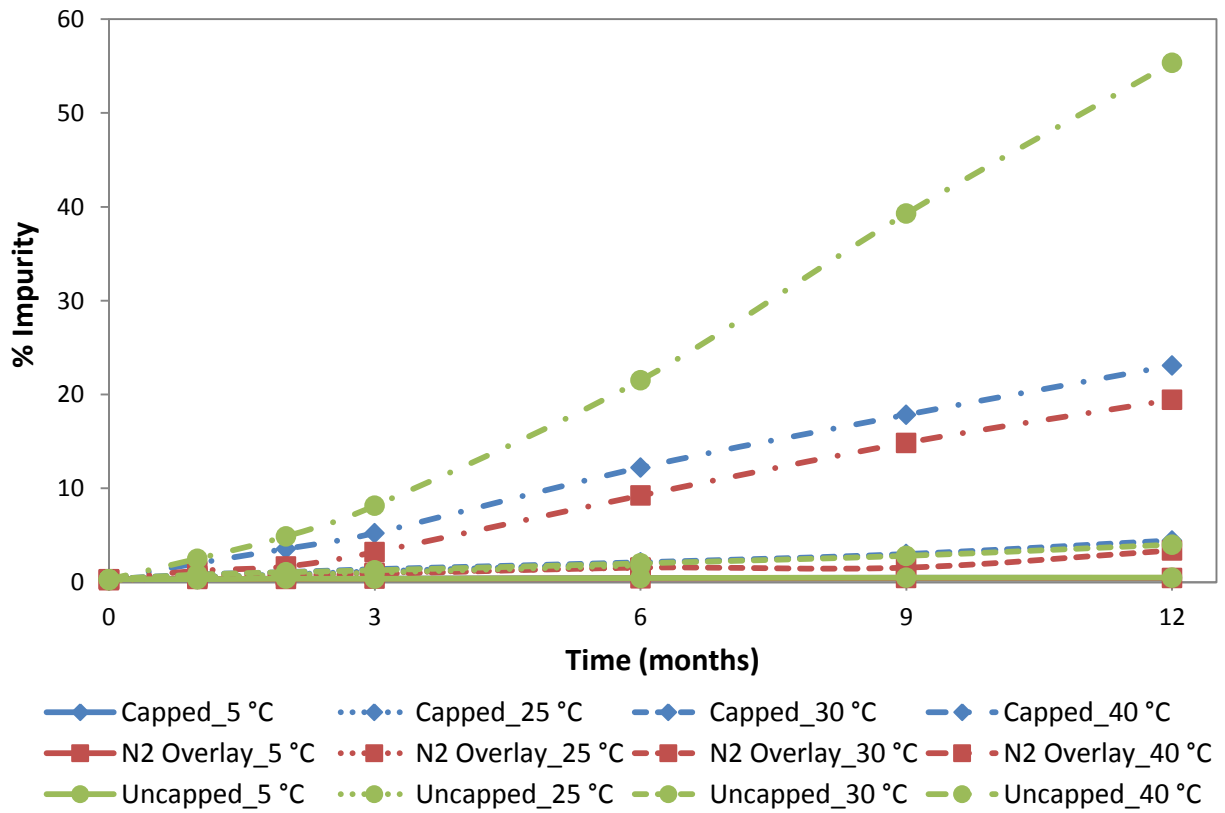
Storage Condition	Assay (mg/mL)											
	Capped Vial				Nitrogen Overlay (w/cap)				Uncapped Vial			
	Temp. (°C)	5	25	30	40	5	25	30	40	5	25	30
Time (mo.)	5	25	30	40	5	25	30	40	5	25	30	40
0	54.8	53.7	54.8	54.8	54.8	53.7	54.8	54.8	54.8	53.7	54.8	54.8
1	56.7	53.5	56.3	53.8	56.2	52.9	55.8	55.7	57.3	53.1	56.3	53.4
2	56.2	51.2	54.2	53.5	55.6	50.1	53.0	51.8	56.5	51.8	54.4	49.6
3	56.7	49.5	55.3	53.3	56.1	50.1	55.6	54.3	57.5	50.9	55.8	49.1
6	53.4	51.7	52.8	48.0	53.5	52.0	52.6	48.9	54.8	52.5	52.5	42.0
9	54.0		51.4	44.3	51.5		52.0	45.9	53.5		51.3	33.1
12	52.9		50.0	41.4	52.4		50.4	42.8	52.4		50.3	24.3



**Figure 7.8:** Assay Levels for the CEP-701 Drug Product

**Table 7.8:** Total Percent Impurity Levels for the CEP-701 Drug Product

		Total Percent Impurity (CEP-701 Related Compounds)											
Storage Condition		Capped Vial				Nitrogen Overlay (w/cap)				Uncapped Vial			
Temp. (°C)	Time (mo.)	5	25	30	40	5	25	30	40	5	25	30	40
0			0.31	0.19	0.31	0.31	0.31	0.19	0.31	0.31	0.31	0.19	0.31
1		0.32	0.54	0.83	2.02	0.33	0.47	0.65	1.21	0.32	0.52	0.81	2.50
2		0.37	0.82	1.07	3.56	0.34	0.67	0.78	1.67	0.37	0.78	1.06	4.89
3		0.37	1.16	1.39	5.23	0.36	0.99	0.87	3.20	0.36	1.01	1.27	8.14
6		0.43	1.96	2.12	12.21	0.40	1.55	1.55	9.23	0.44	1.79	2.00	21.52
9		0.47		3.00	17.84	0.44		1.55	14.85	0.48		2.81	39.27
12		0.45		4.45	23.09	0.46		3.38	19.44	0.49		4.00	55.34



**Figure 7.9:** Total Percent Impurity Levels for the CEP-701 Drug Product

Time (month)	5 °C			25 °C			30 °C			40 °C		
	Capped	N <sub>2</sub> Overlay	Uncapped	Capped	N <sub>2</sub> Overlay	Uncapped	Capped	N <sub>2</sub> Overlay	Uncapped	Capped	N <sub>2</sub> Overlay	Uncapped
Initial												
1												
2												
3												
6												
9												
12												

**Figure 7.10:** Appearance of the CEP-701 Drug Product (After Removal from Stability Chambers)

The active oxygen stability results and appearance for the drug product placebo are presented in **Table 7.9** and **Figure 7.11**.

**Table 7.9:** Active Oxygen Levels for the Drug Product Placebo

	Active Oxygen Levels (ppm)			
Sample	Placebo			
Storage Condition	Capped Vial			
Temp. (°C)	5	25	30	40
Time (mo.)				
0	8.13	8.13	8.13	8.13
1	7.65	8.73	6.90	18.08
2	7.44	9.88	6.79	0.23
3	8.01	10.87	7.01	4.40
6	6.76	7.59	8.64	9.55

Time (month)	Stability Vials				Following Active Oxygen Analysis			
	5 °C	25 °C	30 °C	40 °C	5 °C	25 °C	30 °C	40 °C
Initial								
1								
2								
3								
6								

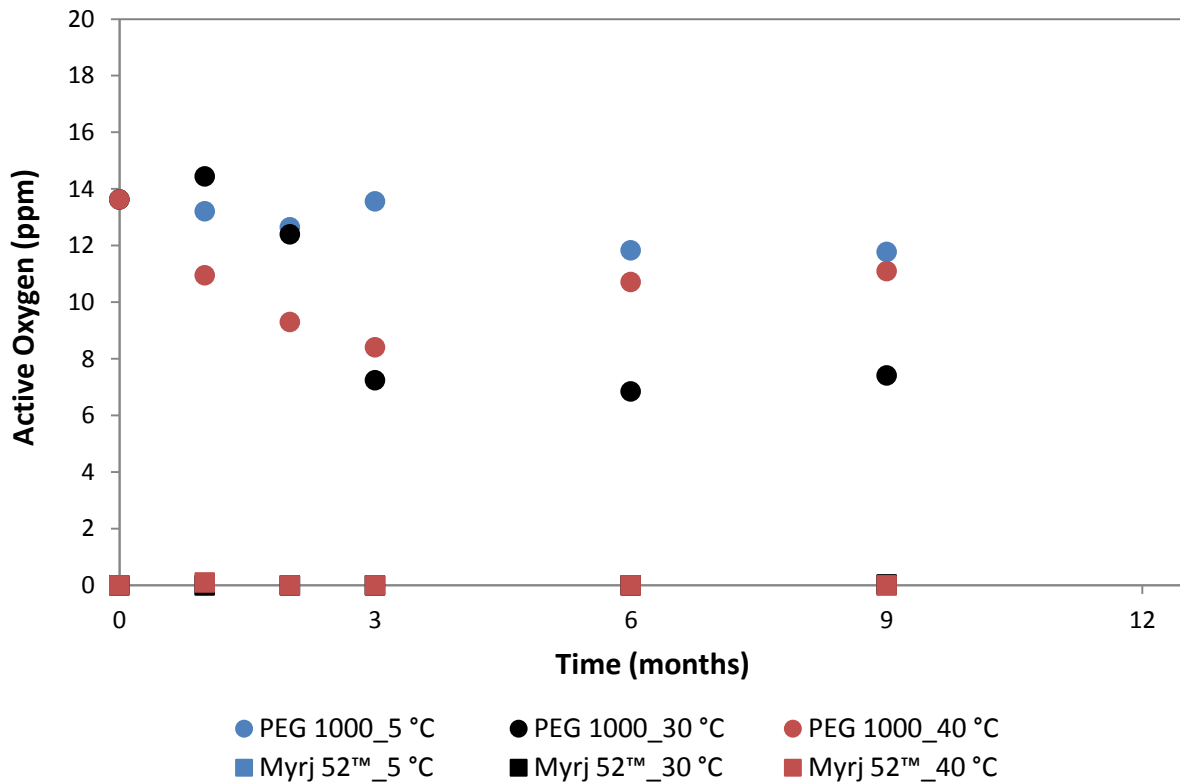
**Figure 7.11:** Appearance of the Drug Product Placebo (Before and Following Active Oxygen Analysis)







































The active oxygen stability results for the drug product excipients, with corresponding plotted data and appearance are presented in **Table 7.10** and **Figure 7.12 – Figure 7.13**.

**Table 7.10:** Active Oxygen Levels for the Drug Product Excipients

Excipient	Active Oxygen Levels (ppm)					
	PEG 1000			Myrj 52™		
Storage Condition	Capped Vial			Capped Vial		
Temp. (°C)	5	30	40	5	30	40
Time (mo.)						
0	13.63	13.63	13.63	nd	nd	nd
1	13.21	14.44	10.95	nd	nd	0.10
2	12.64	12.39	9.30	nd	nd	nd
3	13.56	7.24	8.40	nd	nd	nd
6	11.83	6.85	10.71	nd	nd	nd
9	11.77	7.41	11.09	nd	0.03	0.00
<b>Key</b>	<i>nd – not detected</i>					



**Figure 7.12:** Active Oxygen Levels for the Drug Product Excipients

Time (month)	PEG 1000 (Capped vial)			Myrj 52™ (Capped Vial)		
	5 °C	30 °C	40 °C	5 °C	30 °C	40 °C
Initial						
1						
2						
3						
6						
9						

**Figure 7.13:** Appearance of the Drug Product Excipients (Following Active Oxygen Analysis)

Trends were observed following completion of the 12-month stability study for the CEP-701 drug product. A plot of the active oxygen results, presented in **Figure 7.3**, showed that the samples held at 40 °C/75% RH for all three vial conditions had the greatest increase in active oxygen. The 9-month data point for the uncapped vial at 40 °C/75% RH had an active oxygen level of 173.68 ppm, which confirmed that the result at 6 months was out of trend. Dilution of the 9-month sample at 40 °C/75% RH prior to UV analysis brought the active oxygen level within the linear range of the calibration curve. The reported italicized data point at 6 months for the uncapped vial at 40 °C/75% RH (18.8 ppm), in **Table 7.6**, was likely underestimated because dilution prior to UV analysis was not performed. This data point was removed from the overall plot in **Figure 7.3** containing active oxygen levels at 40 °C/75% RH for that reason. The samples held at 25 °C/60% RH and 30 °C/65% RH for all three vial conditions, presented in **Figure 7.4** and **Figure 7.5**, had intermediate levels of active oxygen between the levels at 40 °C/75% RH and 5 °C (**Figure 7.6**). The active oxygen levels for the capped and uncapped vials at 30 °C/65% RH increased between 3 and 12 months on stability, while the levels for the nitrogen overlay vials increased between 9 and 12 months. The active oxygen levels for the samples held at 5 °C for all three vial conditions, presented in **Figure 7.6**, were the lowest in magnitude and remained stable. The nitrogen overlay vial condition had the lowest active oxygen level for each temperature condition. The total percent impurity levels for the CEP-701-related impurity compounds, presented in **Table 7.8** and **Figure 7.9**, followed the same trends as the active oxygen levels. The samples held at 40 °C/75% RH for all three vial conditions had the highest total impurity levels, followed by the 25 °C/60% RH and 30 °C/65% RH results, and then the 5 °C results, which were stable. As the total impurity levels increased, the assay levels decreased accordingly as displayed in **Table 7.7** and **Figure 7.8**.

The impurity peaks in the CEP-701 stability samples were of large magnitude at the 9-month time point, which enabled LC-MS analysis to be performed to verify the identity of the impurities. The ultimate goal was to verify the peroxy-related CEP-701 impurities, in **Figure 7.1**, in order to see if the modified active oxygen method successfully quantified the peroxy impurities. The peroxy-related CEP-701 impurity compounds are diastereomers labeled as compounds **2** and **3**. The additional oxidative degradants for CEP-701 are hydroxy compounds **4** and **5** and impurity compound **6**.

The LC-MS results for the 9-month, uncapped vial sample, at 40 °C/75%RH are presented in **Figure B.1 – Figure B.5** in *Appendix B* and show identification of impurity compounds **2-9**. The extracted ion chromatograms (EIC) were obtained for the known mass of each CEP-701 oxidative impurity along with the UV diode array chromatogram. As shown in **Figure B.1** in *Appendix B*, strong signals were present for CEP-701 (**1**) ( $t_R = 9.23$  min) and compound **6** ( $t_R = 13.42$  min). The peroxy compounds **2** and **3** had quantifiable signals at  $t_R = 5.86$  min and  $t_R = 8.16$  min and the hydroxy compounds **4** and **5** had signals at  $t_R = 5.04$  min and  $t_R = 6.95$  min.

In addition to the known CEP-701 oxidative degradants, three additional impurity peaks were prevalent and grew over time in the HPLC assay analysis. The impurity peaks had retention times equal to 7.80 min, 10.08 min, and 12.55 min in the LC-MS chromatograms. The extracted mass spectrum for the peak with  $t_R = 7.80$  min, shown in **Figure B.2** in *Appendix B*, produced a major fragment ion  $[M+H]^+ = 470$ , which equaled  $m/z$  469. An extracted ion chromatogram, presented in **Figure B.1** in *Appendix B*, was obtained for  $[M+H]^+ = 470$  and two peaks were found at  $t_R = 7.82$  min and 10.07 min. The extracted mass spectrum for the peak with  $t_R = 12.55$  min, shown in **Figure B.3** in *Appendix B*, produced a major fragment ion

$[M+H]^+ = 466$ , which equaled  $m/z$  465. An extracted ion chromatogram, presented in **Figure B.4** in *Appendix B*, was obtained for  $[M+H]^+ = 466$  and a peak was found at  $t_R = 12.54$  min.

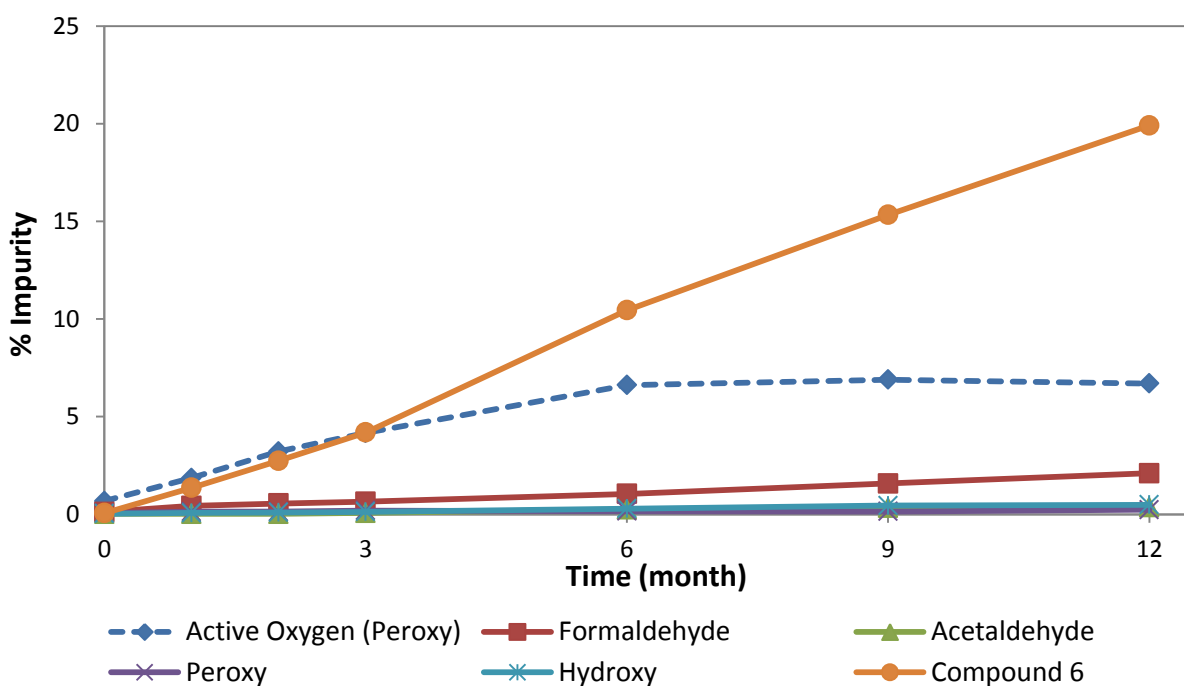
To identify the structures of the unknown impurities at retention times 7.80 min, 10.08 min, and 12.55 min, formaldehyde and acetaldehyde addition were considered. Formaldehyde and acetaldehyde are prevalent in PEG 1000 and can interact with the nitrogen of the 2-pyrrolidone ring in the CEP-701 structure.<sup>6</sup> Formaldehyde and acetaldehyde addition to CEP-701 would produce the structures presented in **Figure 7.2** and are identified as compound **7** ( $m/z$  469), compound **8** ( $m/z$  483), and compound **9** ( $m/z$  469) respectively. Compound **7** is formaldehyde addition to the nitrogen of the 2-pyrrolidone ring and was therefore identified as the unknown peak at  $t_R = 7.80$  min and the enol form, compound **9** (formaldehyde addition to the oxygen), was identified as the unknown peak at  $t_R = 10.08$  min. Compound **8** was identified as the unknown peak at  $t_R = 12.55$  min, with  $[M-H_2O+H]^+ = 466$  as the major fragment identified for the compound. A corrected mass spectrum is presented in **Figure B.3** in *Appendix B*, with the fragments relabeled with the knowledge of  $[M+H]^+ = 484$ .

The relative retention times for the peaks in the LC-MS chromatograms were compared to those in the HPLC chromatograms to properly identify and track the CEP-701 impurities. The 9-month HPLC chromatogram for the uncapped vial at 40 °C/75% RH is presented in **Figure C.1**, in *Appendix C*, with the CEP-701 impurity peaks properly labeled. To correlate the active oxygen levels in  $\mu\text{g}$  or ppm to the percent impurity levels, the active oxygen levels were converted to assay terms (mg/mL). The following conversion equation was used:

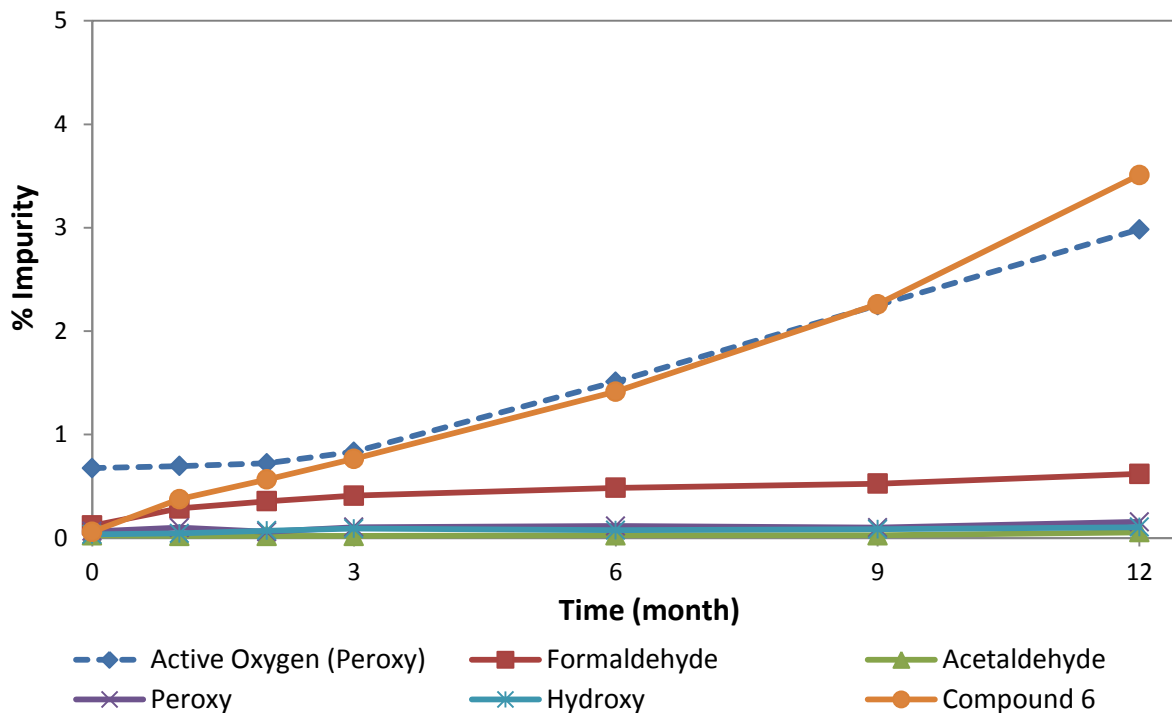
$$\frac{[(\text{Active oxygen level } (\mu\text{g}) \times F) / (5 \text{ mL} \times 1000 \mu\text{L}/1 \text{ mL})]}{\text{Initial Diluted Assay Claim (mg/mL)}} \times 100\% = \% \text{ Impurity}$$

where F is the active oxygen conversion factor for the CEP-701 peroxy impurities **2** and **3**. The peroxy compounds **2** and **3** have a molecular weight of 471.14 g/mol and therefore a conversion

factor, F, of 29.44625 (see the equation for F calculation in *Chapter 2*). The active oxygen levels for the capped vials at 40 °C/75% RH and 30 °C/65% RH were converted to peroxy percent impurity values. The capped vial condition was used so comparisons could be made to the placebo stability study that also used the capped vial condition. The active oxygen results for the nitrogen overlay and uncapped vial conditions at 30 °C/65% RH and 40 °C/75% RH were also converted to peroxy percent impurity values and are presented in **Figures D.1- D.4** in *Appendix D*. The peroxy percent impurity values calculated by the active oxygen method (dotted line) were plotted against the assay percent impurity levels of the peroxy, hydroxy, formaldehyde, acetaldehyde, and compound 6 related CEP-701 compounds in **Figure 7.14** and **Figure 7.15**.



**Figure 7.14:** Comparison of CEP-701-Related Active Oxygen (Peroxy), Formaldehyde, Acetaldehyde, Peroxy, Hydroxy, and Compound 6 Impurities in the Capped Vial at 40 °C/75% RH Sample



**Figure 7.15:** Comparison of CEP-701-Related Active Oxygen (Peroxy), Formaldehyde, Acetaldehyde, Peroxy, Hydroxy, and Compound 6 Impurities in the Capped Vial at 30 °C/65% RH Sample

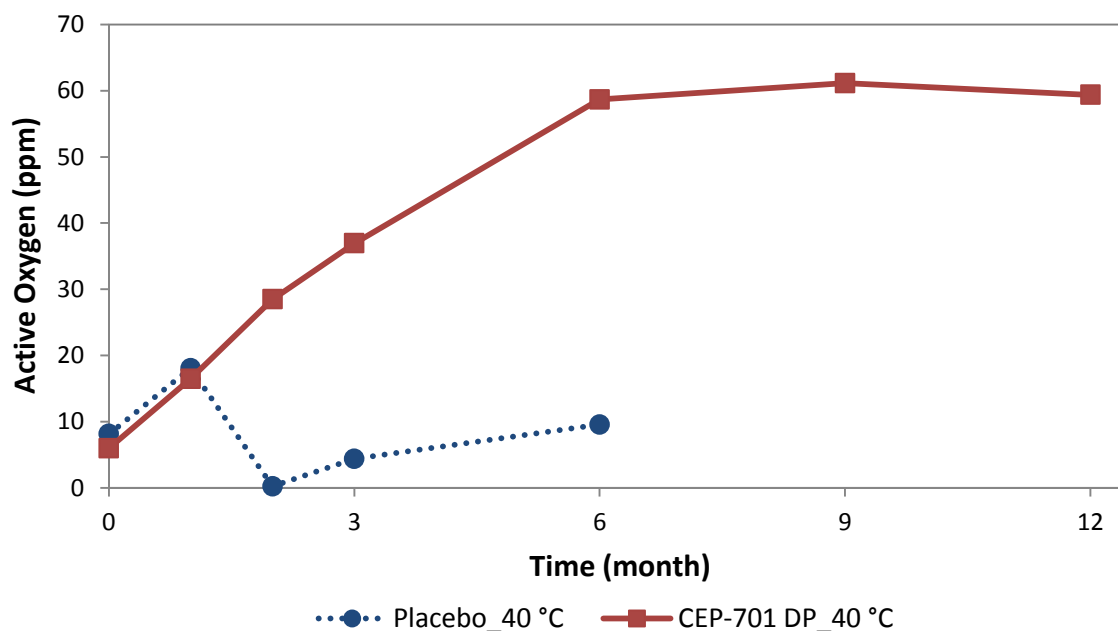
The peroxy compounds **2** and **3** were short-lived in the HPLC analyzed stability samples and were converted to the hydroxy compounds **4** and **5**, and then to compound **6**. The instability of the peroxy compounds can be attributed to the presence of silica gel in the column, which can have surface interaction and catalyze peroxide decomposition.<sup>7,8</sup> The catalyzed decomposition and conversion of the peroxy and hydroxy compounds by the conditions of the HPLC method explained why compound **6** was the largest impurity peak detected by the assay method. The comparison between the percent impurity levels, in **Figure 7.15**, for the 30 °C/65% RH condition showed that the active oxygen method successfully quantified the peroxy impurities and that the levels coincided with the HPLC assay impurity totals for compound **6**. The coinciding rates showed that the formation rate of the CEP-701 peroxy impurity was equal to the decomposition rate to compound **6**. As verification, analysis by the orthogonal methods showed

that the assay value for the sample after active oxygen analysis was 51.38 mg/mL (3.62% impurity for compound **6**), which corresponded to the actual assay determined value of 50.29 mg/mL (3.62% impurity for compound **6**). Likewise, the active oxygen level for the sample prepared for HPLC analysis had an absorbance of 0.0236 AU at the 410 nm wavelength, which corresponded to the actual active oxygen determined absorbance value of 0.0174 AU. The comparison between the impurity levels in **Figure 7.14**, for the 40 °C/75% RH condition, showed that the active oxygen levels coincided with the HPLC assay impurity totals for compound **6** within the first 3 months. In the first three months at the accelerated temperature condition, the formation rate of the CEP-701 peroxy impurity was equal to the decomposition rate to compound **6** and between 3 and 12 months, the peroxy decomposition was faster than the rate of formation. The continued formation rate of compound **6** was present as the active oxygen calculated CEP-701 peroxy levels reached steady state. The modified ASTM E 299-08 method was therefore more sensitive than the HPLC assay method in detection of the peroxy levels in the CEP-701 stability samples because the results related directly to the amount of peroxy present.

The individual excipient stability study showed some trends were evident throughout the 9 months of the study. The 9-month data for the excipient stability study at 30°C/65%RH and 40 °C/75% RH, presented in **Figure 7.12**, showed that over time the active oxygen levels for PEG 1000 decreased to steady-state levels and that the levels remained non-detectable for Myrj 52™. The active oxygen-forming moieties in PEG 1000 produced the initial levels, but over time degraded or converted into PEG impurities whose detection was not specific to the active oxygen method. PEG 1000 was therefore shown to be the main contributor of the active oxygen levels present in the placebo.



As PEG 1000 degraded on stability, PEG impurities and related radicals were formed. The increased presence of the formaldehyde impurity from PEG caused the CEP-701 degradants related to formaldehyde addition to form. The comparison between the formation of CEP-701 formaldehyde compounds 7 and 9 and the rate of active oxygen formation in the drug product can be viewed in **Figure 7.14** and **Figure 7.15**. The active oxygen levels for the CEP-701 drug product at 40 °C/75% RH are plotted against the active oxygen levels for the placebo in **Figure 7.16**. The active oxygen levels observed in the placebo at 40 °C/75% RH within the first 6 months correlated with the peroxy impurity and active oxygen results observed for the CEP-701 drug product. The rates of active oxygen formation within the first month for the placebo (9.95 ppm/month) and drug product (10.50 ppm/month) were similar. After the first month, the excipients in the placebo decreased in active oxygen (6.84 ppm/month) and produced more radicals. The radical initiated oxidative degradation of the drug product consequently increased to the same rate (7.48 ppm active oxygen/month).



**Figure 7.16:** Active Oxygen Levels for the CEP-701 Drug Product and Placebo at 40 °C/75% RH (Capped Vial Condition)

## 7.4. Conclusions

The oxidative degradation of the CEP-701 drug product was successfully quantified orthogonally by the modified ASTM E 299-08 method and the HPLC assay method. The modified active oxygen method was able to quantify the total levels of active oxygen as well as the primary peroxy impurity produced in the drug product. The HPLC assay method confirmed the accuracy of the results produced by the modified active oxygen method. The modified ASTM E 299-08 method was suitable for sensitive detection of active oxygen levels in excipients, placebos, and drug products without derivatization or manipulation of the sample. The modified active oxygen method showed that it can be used as a preliminary test for screening new formulations, to predict the possible reaction mechanisms that can occur between the excipient's reactive impurities and the drug substance, before performing a full stability study. Being proactive in screening an excipient in formulation development can necessitate the change to a different excipient or inclusion of an antioxidant early in the process, which saves valuable development time and enhances drug substance and excipient compatibility.

## 7.5. References

1. Shabbir, M.; Stuart, R. *Expert Opin. Investig. Drugs*. **2010**, *19*, 427-436.
2. del Barrio, M.-A.; Hu, J.; Zhou, P.; Cauchon, N. *J. Pharm. Biomed. Anal.* **2006**, *41*, 738-743.
3. FDA Guidance for Industry, Q1A(R2) Stability Testing of New Drug Substances and Products. **2003**, Revision 2.
4. *Carbowax™ Polyethylene Glycol (PEG) 1000*; SDS No. 00132377 [Online]; The Dow Chemical Company: Midland, MI, Aug 13, 2015. <http://www.dow.com/enus/elibrary#q=00132377> (accessed Aug 8, 2016).
5. Ma, X.; Zhou, J.; Wang, C.; Carter-Cooper, B.; Yang, F.; Larocque, E.; Fine, J.; Tsuji, G.; Chopra, G.; Lapidus, R. G.; Sintim, H. O. *ACS Med. Chem. Lett.* **2017**, *8*, 492-497.
6. Hemenway, J. C.; Carvalho, T. C.; Rao, V. M.; Wu, Y.; Levons, J. K.; Narang, A. S.; Paruchuri, S. R.; Stamato, H. J.; Varia, S. A. *J. Pharm. Sci.* **2012**, *101*, 3305-3318.
7. Zaklika, K. A.; Burns, P. A.; Schaap, A.P. *J. Am. Chem. Soc.* **1978**, *100*, 318-320.
8. Turner, J. A.; Herz, W. *J. Org. Chem.* **1977**, *42*, 2006-2008.

## CHAPTER 8. Final Conclusions and Future Considerations

The modifications made to the ASTM E 299-08 method described in this thesis reduced the procedural steps of the 1966 original method, eliminated the need for a special absorption cell without sacrificing sensitivity or reproducibility, and increased the lower magnitude range of the calibration curves. The method successfully quantified spiked amounts of hydrogen peroxide (HOOH), *tert*-butyl hydroperoxide (ROOH), and dibenzoyl peroxide (ROOR), thus demonstrating the method's non-discriminatory response for peroxide detection. The modified ASTM E 299-08 method was advantageous over other techniques because it was not specific to just one form of a peroxide compound and could also measure total active oxygen as well.

The versatility in the types of peroxide detected by this method enabled complex pharmaceutical excipients to be evaluated. The modified ASTM E 299-08 method detected active oxygen levels in liquid excipients, in the range of 0.04 ppm – 122.06 ppm, from varying chemical classes including water-insoluble, triglyceride, and surfactant. A novel procedure was implemented in the sample preparation of solid excipients to enable a comparative analysis to liquid excipients. The modified method detected active oxygen levels in solid excipients, in the range of 0.38 ppm – 156.85 ppm, from the carrier types: povidone, polyethylene glycol, and poloxamer. The incorporation of the above types of excipients in formulations is growing to combat the increase in poorly water-soluble API in the development pipeline, which makes knowledge of the active oxygen content important.

The polyethylene glycol (PEG) class of excipients was further studied by the modified ASTM E 299-08 method since it had molecular weight grades that are liquid (PEG 400) and solid (PEG 4000). The impact of the physical composition of the PEG compounds on the rate of active oxygen formation was also evaluated. The observation was that the PEG compounds

susceptible to autoxidation experienced a steady-state active oxygen level before first-order decay at the accelerated 40 °C/75% RH condition. PEG 400, a liquid, had more contact with oxygen both internally and externally than PEG 4000, a solid, which had only external contact. As a result, PEG 400 had quantifiable active oxygen levels and an active oxygen decay rate of  $4.5 \times 10^{-5} \text{ sec}^{-1}$ . PEG 4000 was a higher molecular weight compound and a solid so therefore was not susceptible to autoxidation under the conditions studied.

The PEG 1000 compound was formulated in a drug product to evaluate the impact that an excipient, which was susceptible to autoxidation and contained active oxygen components, had on the drug substance stability. A model drug product was chosen, which contained CEP-701 API and PEG 1000 as one of the excipients. The drug product, placebo, and individual excipients were placed on stability at a range of storage and accelerated temperature conditions within different vial conditions. The active oxygen levels were evaluated by the modified ASTM E 299-08 method and an orthogonal HPLC assay method was used to evaluate the assay and impurity levels. The modified ASTM E 299-08 method successfully quantified the CEP-701 peroxy-related impurity and the levels matched those obtained by the HPLC assay method for the final oxidative impurity product.

The modified active oxygen method is suitable for trace level detection of active oxygen in excipients, placebos, and drug products without derivatization or manipulation of the sample. The modified active oxygen method can be used as a preliminary screen for new formulations to predict the potential degradation reactions that can occur. In the case of the demonstrated model drug product, a targeted therapy drug for AML where patients only have a 26% percent five-year survival rate, screening the formulation by the modified active oxygen method would have been imperative in the development phase to eliminate downstream drug product instability. The

modified ASTM E 299-08 method would have shown that an antioxidant was needed from the onset without direct knowledge of the impurity peroxide, which would have saved development time and enhanced drug product stability, potentially enabling a life-improving drug to reach the market more quickly than would otherwise have been the case.

The novel modified ASTM E 299-08 method developed is a sensitive, versatile, reliable, and reproducible method that has significant application in the pharmaceutical industry. To further explore the application of the modified ASTM E 299-08 method, additional drug product formulations should be evaluated. The drug product formulations should consist of various compositions common to pharmaceuticals such as liquids, suspensions, and tablets. The drug products should be placed on stability and evaluated for active oxygen and potential peroxide impurities by the modified ASTM E 299-08 method. The incorporation of antioxidants in the drug products should also be explored and the active oxygen levels quantified, to show the additional benefits of the modified ASTM E 299-08 method in pharmaceutical development.





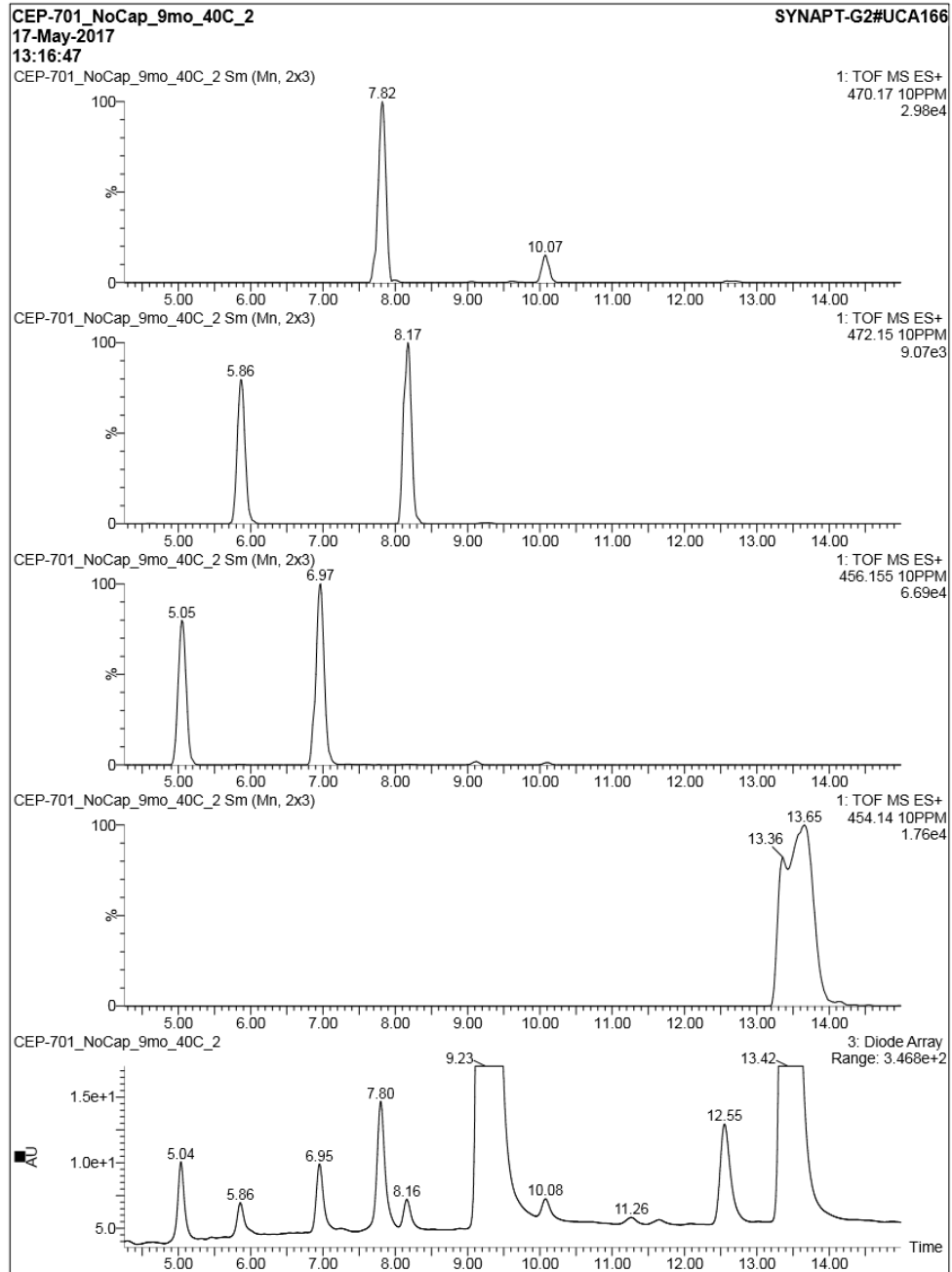
**Table A.3:** Summary of % Impurity Levels in the CEP-701 Drug Product on Stability with an Uncapped Vial Condition

lot# 3753-3818-279 (Uncapped Vial)	time (mo.)	Temperature : 5 °C												Temperature : 25 °C						Temperature : 30°C						Temperature : 40°C																										
		Temperature : 5 °C												Temperature : 25 °C						Temperature : 30°C						Temperature : 40°C																										
		1	2	3	6	9	12	initial	1	2	3	6	12	1	2	3	6	9	12	1	2	3	6	9	12	1	2	3	6	9	12																					
	tR (min)																																																			
Unknown A	4.58	0.53	0.02	0.01	0.01	0.02	0.01	nd	0.01	nd	0.01	nd	0.01	0.01	0.01	0.01	nd	nd	0.01	0.01	0.01	nd	nd	nd	0.01	0.01	0.01	nd	nd	nd	nd	nd	nd	nd	nd	nd	0.02	0.02	nd													
hydroxy 4 (m/z 455)	4.76	0.55	0.03	0.03	0.03	0.03	0.03	0.04	0.04	0.04	0.04	0.03	0.05	0.07	0.09	0.10	0.10	0.08	0.04	0.04	0.04	0.05	0.06	0.07	0.05	0.08	0.12	0.28	0.60	0.67																						
Unknown B	4.95	0.57	0.09	0.10	0.08	0.09	0.10	0.09	0.09	0.07	0.09	0.10	0.10	0.08	0.08	0.07	0.07	0.05	0.05	0.06	0.08	0.07	0.07	0.05	0.05	0.06	0.07	0.07	0.08	0.06	0.02	nd																				
Unknown C	5.22	0.60	0.03	0.03	0.03	0.03	0.03	0.03	0.03	0.03	0.03	0.03	0.02	0.03	0.03	0.03	0.02	0.02	0.02	0.02	0.02	0.02	0.02	0.01	0.02	0.02	0.02	0.02	0.01	nd																						
peroxy 2 (m/z 471)	5.58	0.64	0.04	0.01	0.02	0.02	0.02	0.02	0.01	0.02	0.04	0.03	0.04	0.06	0.04	0.06	0.08	0.05	0.07	0.06	0.04	0.06	0.08	0.05	0.07	0.17	0.18	0.24	0.33	0.32	0.29																					
hydroxy 5 (m/z 455)	6.66	0.77	0.01	0.01	0.01	0.01	0.02	0.01	0.01	0.02	0.02	0.01	0.02	0.01	0.02	0.02	0.01	0.02	0.02	0.04	0.04	0.04	0.03	0.04	0.05	0.05	0.05	0.24	0.45	0.53																						
Unknown D	6.69	0.77	0.01	0.01	0.01	0.01	0.01	nd	nd	nd	0.01	nd	nd	0.01	0.02	0.03	0.03	0.04	0.04	0.01	0.02	0.03	0.03	0.04	0.04	nd	nd	nd	nd	nd	nd																					
Unknown E	7.16	0.82	0.02	0.02	0.02	0.02	0.02	0.02	0.02	0.02	0.02	0.02	0.02	0.02	0.02	0.02	0.02	0.02	0.02	0.02	0.02	0.02	0.03	0.02	0.03	0.02	0.03	0.02	0.01	0.04																						
7 (m/z 469)	7.48	0.86	0.07	0.09	0.12	0.12	0.13	0.14	0.15	0.02	0.12	0.20	0.26	0.33	0.24	0.30	0.33	0.36	0.41	0.43	0.24	0.30	0.33	0.36	0.41	0.43	0.32	0.41	0.52	0.90	1.50	2.07																				
peroxy 3 (m/z 471)	7.86	0.91	0.03	0.02	0.02	0.02	0.01	0.01	0.02	0.03	0.03	0.03	0.05	0.03	0.03	0.04	0.05	0.04	0.06	0.03	0.03	0.04	0.05	0.04	0.06	0.11	0.18	0.25	0.35	0.40	0.41																					
Unknown F	8.13	0.94	0.01	nd	0.01	0.01	0.01	nd	0.01	0.01	nd	nd	nd	nd	0.01	0.01	0.01	nd	nd	nd	0.01	0.01	0.01	nd	nd	nd	0.02	0.01	nd	nd	nd																					
CEP-701 (I) (m/z 439)	8.68	1.00	99.70	99.68	99.64	99.64	99.57	99.52	99.52	99.82	99.49	99.22	99.00	98.21	99.20	98.94	98.74	98.00	97.20	96.01	97.50	95.12	91.86	78.48	60.74	44.67																										
9 (m/z 469)	9.93	1.14	0.05	0.04	0.04	0.02	0.06	0.06	0.05	0.06	0.05	0.03	0.05	0.03	0.05	0.03	0.03	0.05	0.06	0.05	0.04	0.08	0.02	0.05	0.12	0.11																										
8 (m/z 483)	11.55	1.33	0.03	0.03	0.02	0.02	0.02	0.02	0.02	0.02	0.02	0.02	0.02	0.02	0.02	0.02	0.02	0.02	0.04	0.02	0.02	0.02	0.02	0.03	0.04	0.02	0.03	0.12	0.45	1.18	2.19																					
6 (m/z 453)	12.86	1.48	0.06	0.08	0.12	0.13	0.16	0.20	0.20	0.02	0.24	0.42	0.58	1.26	0.37	0.58	0.73	1.36	2.14	3.26	1.76	3.90	6.84	18.93	34.71	49.10																										
Unknown G	14.04	1.62	0.01	0.01	0.01	0.01	0.01	0.01	0.01	nd	0.01	0.01	nd	0.01	0.01	0.01	0.01	nd	0.01	0.01	0.01	0.01	0.01	nd	0.01	0.01	0.01	0.03	nd	nd	nd																					
Unknown H	14.11	1.62	0.02	0.02	0.02	0.02	0.02	0.01	0.02	nd	nd	0.01	nd	nd	0.02	0.02	0.02	0.01	0.02	0.02	0.02	0.01	0.03	0.01	0.02	0.02	0.02	0.01	0.03	0.01	nd	nd																				
Unknown I	14.67	1.69	nd	0.02	0.02	0.02	0.02	0.02	0.03	0.01	nd	0.01	0.02	0.02	0.02	0.03	0.03	0.04	0.03	0.03	0.04	0.04	0.04	0.04	0.10	0.17																										
<b>Total Impurities</b>			<b>0.31</b>	<b>0.32</b>	<b>0.37</b>	<b>0.36</b>	<b>0.44</b>	<b>0.48</b>	<b>0.49</b>	<b>0.19</b>	<b>0.52</b>	<b>0.78</b>	<b>1.01</b>	<b>1.79</b>	<b>0.81</b>	<b>1.06</b>	<b>1.27</b>	<b>2.00</b>	<b>2.81</b>	<b>4.00</b>	<b>2.50</b>	<b>4.89</b>	<b>8.14</b>	<b>21.52</b>	<b>39.27</b>	<b>55.34</b>																										

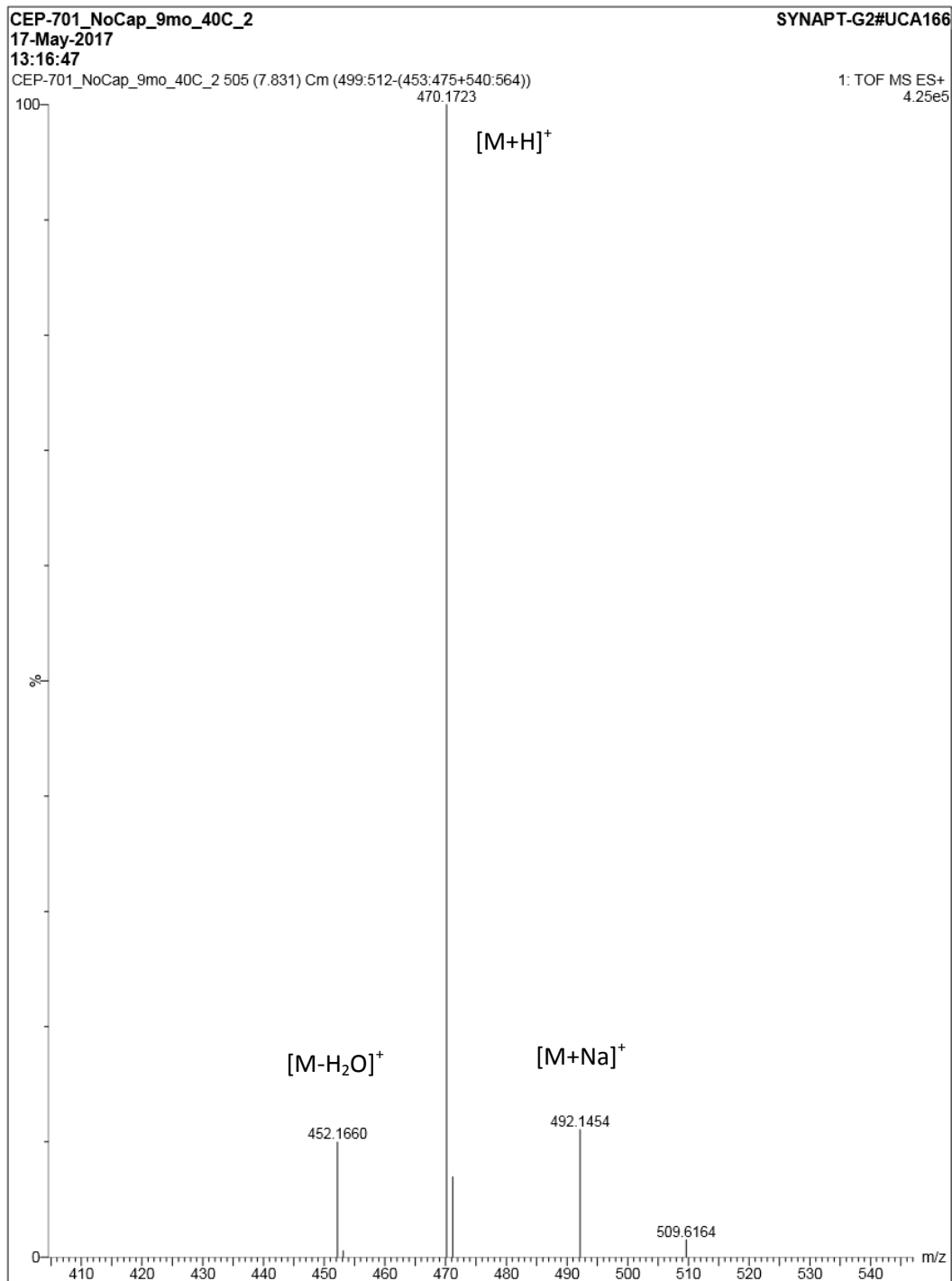
nd = not detected



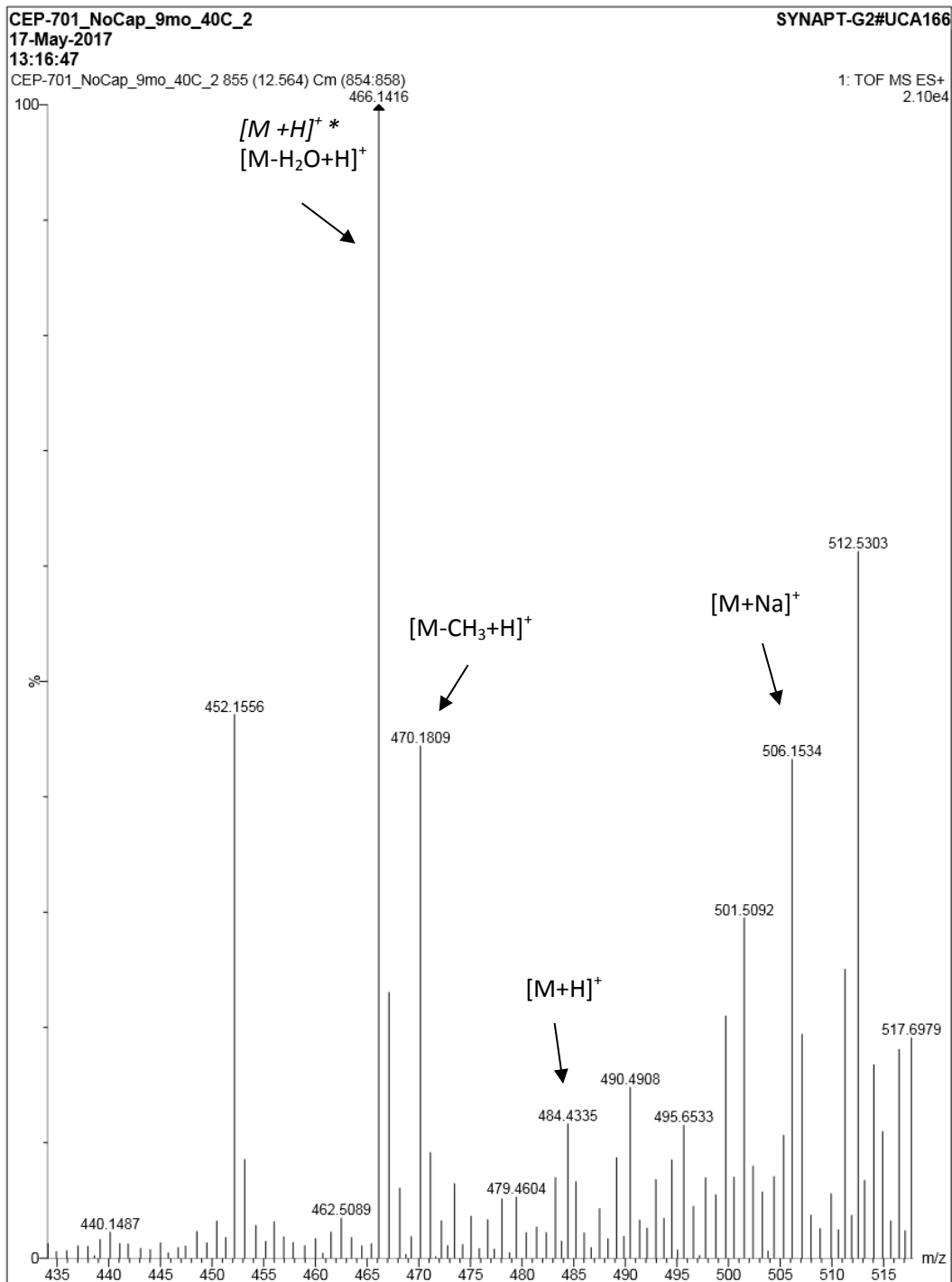
## Appendix B.



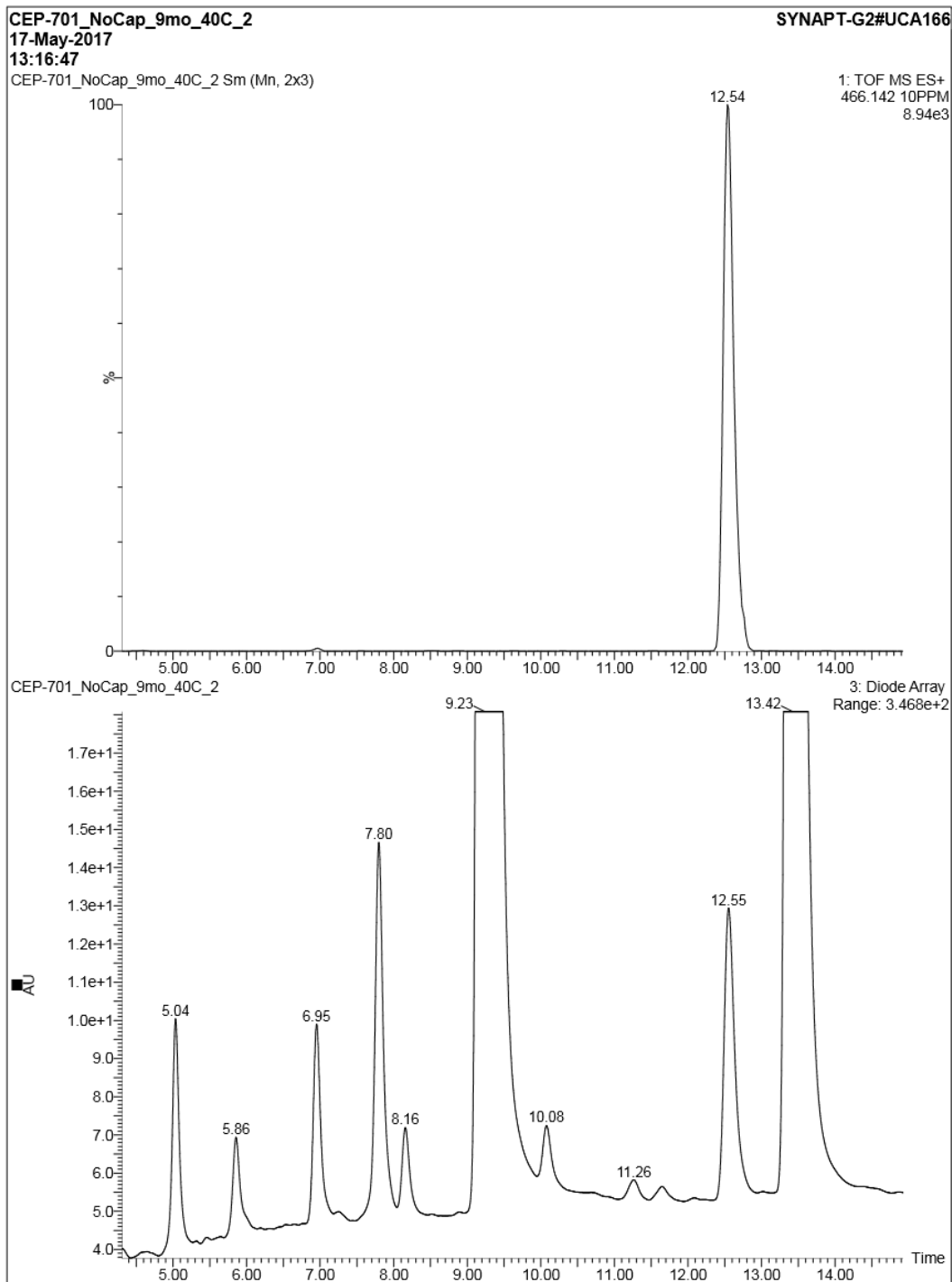
**Figure B.1:** Extracted Ion Chromatograms and Diode Array Chromatogram for the CEP-701 Drug Product Impurity Compounds (Sample: Uncapped Vial Held for 9 Months at 40 °C/75%RH)



**Figure B.2:** Mass Spectrum for the CEP-701 Impurity Peak with  $t_R = 7.80$  min

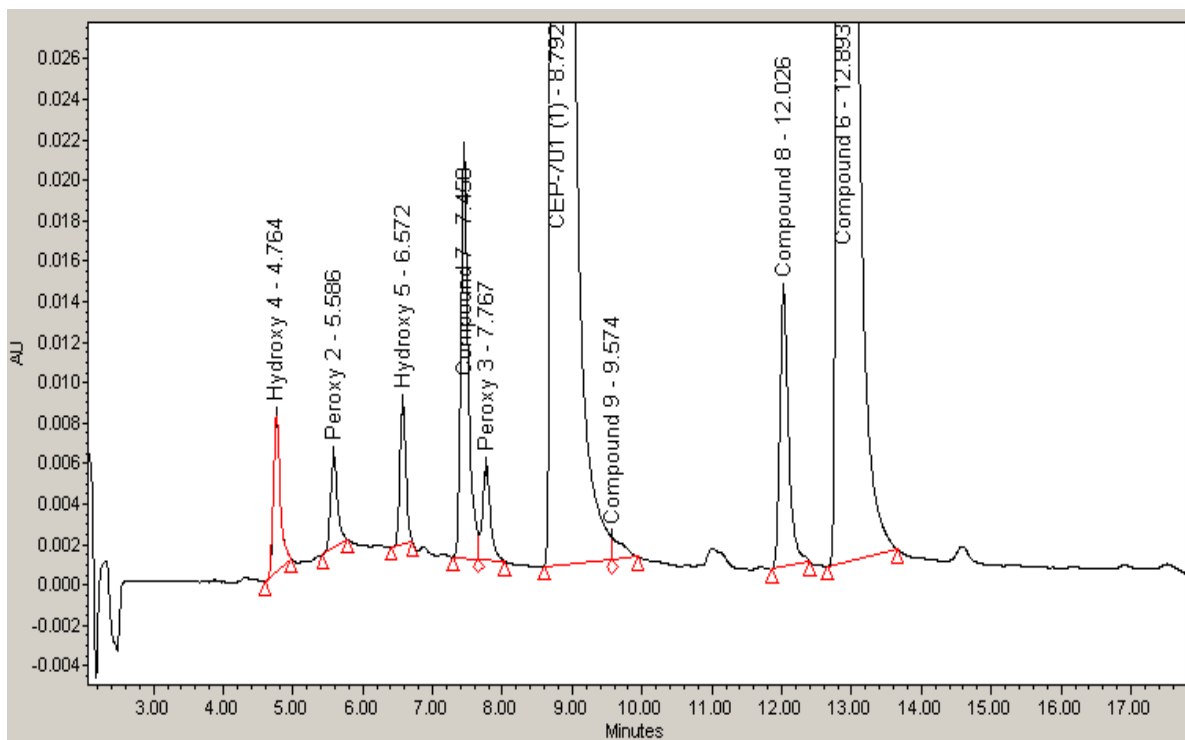


**Figure B.3:** Mass Spectrum for the CEP-701 Impurity Peak with  $t_R = 12.55$  min (\* initially identified as  $[M+H]^+ = 466$ )



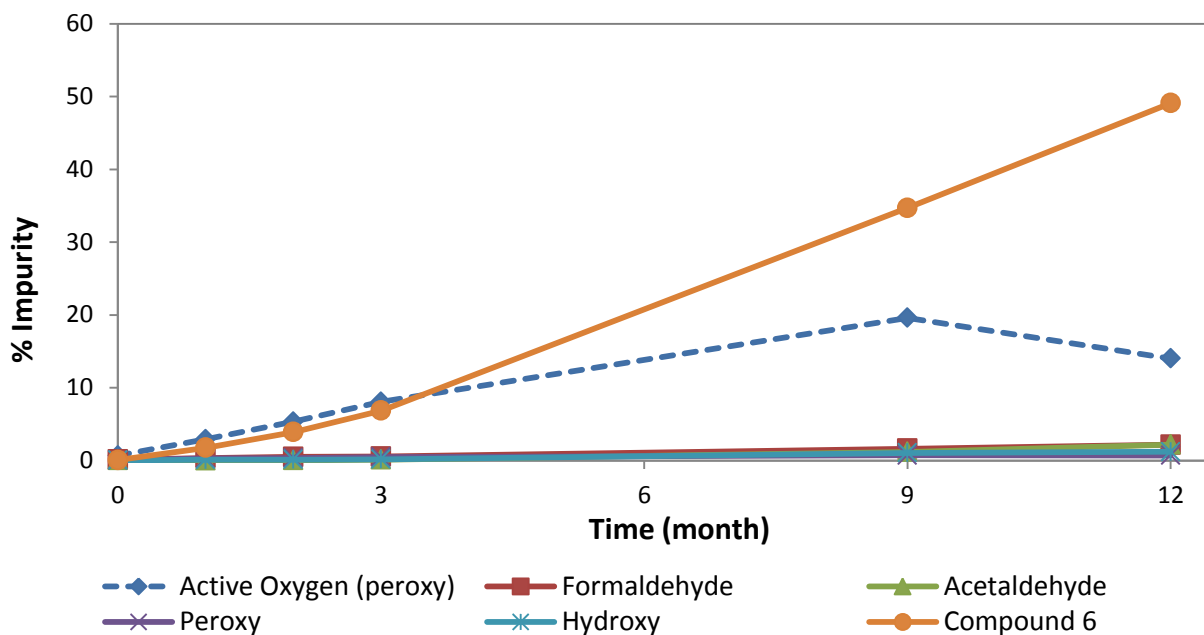
**Figure B.4:** Extracted Ion Chromatogram and Diode Array Chromatogram for the CEP-701 Impurity Peak with  $[M+H]^+ = 466$

## Appendix C.

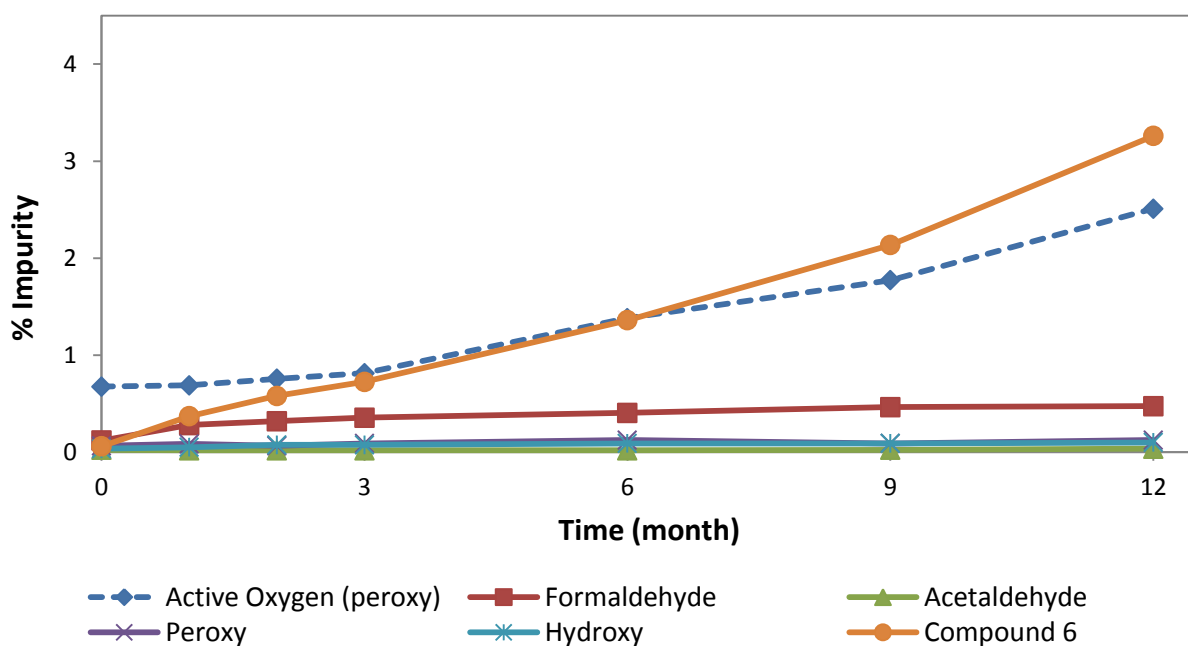


**Figure C.1:** HPLC Chromatogram for the CEP-701 Drug Product Stability Sample: Uncapped Vial Held for 9 Months at 40 °C/75%RH

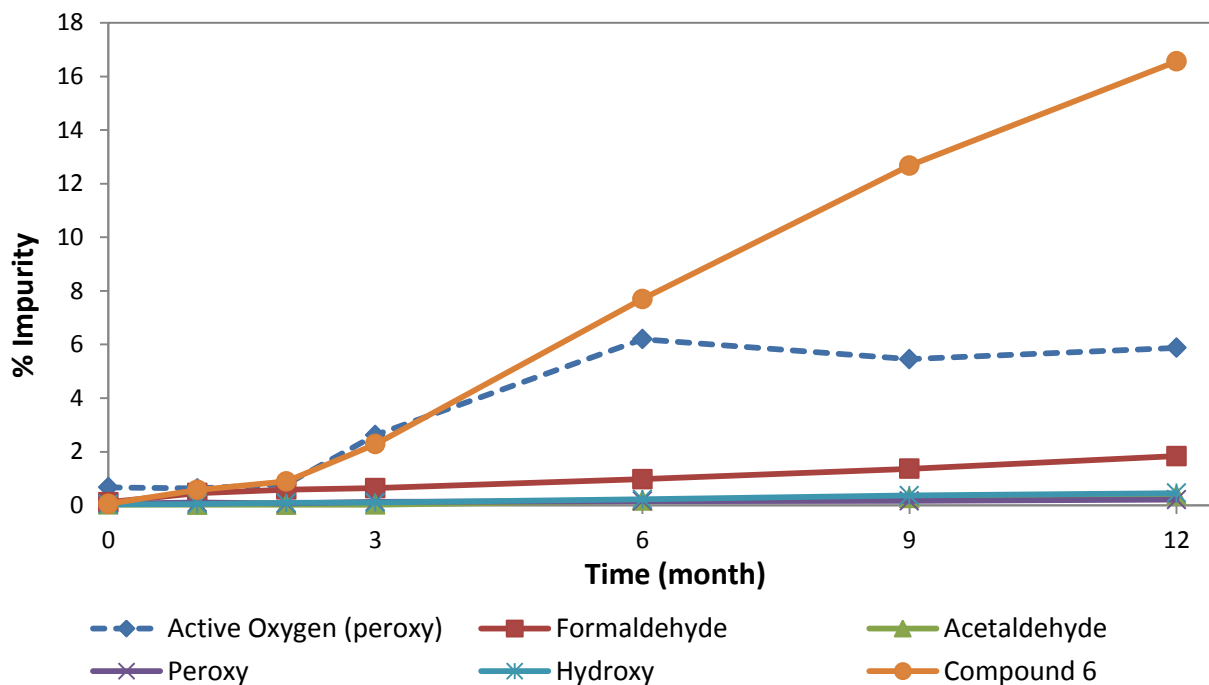
Appendix D.



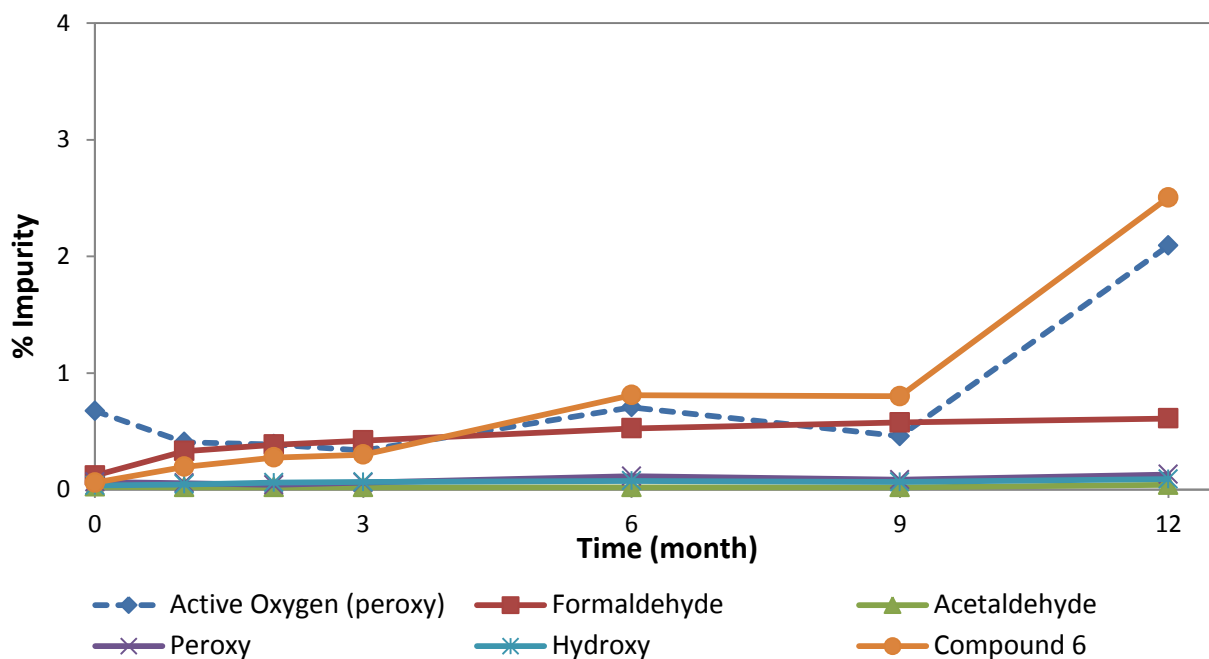
**Figure D.1:** Comparison of CEP-701-Related Active Oxygen (Peroxy), Formaldehyde, Acetaldehyde, Peroxy, Hydroxy, and Compound 6 Impurities in the Uncapped Vial at 40 °C/75% RH Sample



**Figure D.2:** Comparison of CEP-701-Related Active Oxygen (Peroxy), Formaldehyde, Acetaldehyde, Peroxy, Hydroxy, and Compound 6 Impurities in the Uncapped Vial at 30 °C/65% RH Sample



**Figure D.3:** Comparison of CEP-701-Related Active Oxygen (Peroxy), Formaldehyde, Acetaldehyde, Peroxy, Hydroxy, and Compound 6 Impurities in the Nitrogen Overlay Vial at 40 °C/75% RH Sample



**Figure D.4:** Comparison of CEP-701-Related Active Oxygen (Peroxy), Formaldehyde, Acetaldehyde, Peroxy, Hydroxy, and Compound 6 Impurities in the Nitrogen Overlay Vial at 30 °C/65% RH Sample